Masterthesis

Design of hybrid steel bridges resorting to high strength steel by investigating the bending and shear buckling resistance of hybrid steel girders

PROMOTOR :

Prof. dr. ir. Herve DEGEE

PROMOTOR :

prof. dr. Kovesdi BALAZS

Thomas Lenaerts, Aliona Trushenko

Scriptie ingediend tot het behalen van de graad van master in de industriële wetenschappen: bouwkunde

Gezamenlijke opleiding UHasselt en KU Leuven

►► UHASSELT   KU LEUVEN

►► UHASSELT   KU LEUVEN

2021•2022
Faculteit Industriële Ingenieurswetenschappen
master in de industriële wetenschappen: bouwkunde

Masterthesis
Design of hybrid steel bridges resorting to high strength steel by investigating the bending and shear buckling resistance of hybrid steel girders

PROMOTOR :

Prof. dr. ir. Herve DEGEE

PROMOTOR :

prof. dr. Kovesdi BALAZS

Thomas Lenaerts, Aliona Trushenko
Scriptie ingediend tot het behalen van de graad van master in de industriële wetenschappen: bouwkunde

▶▶ UHASSELT   KU LEUVEN

Acknowledgment

Table of content

List of tables

List of figures

Symbol list

Symbol	Explanation
A_i	area of a cross-section
b_f	flange width
c_f	flange width that is used for the classification of the cross-section
χ_w	reduction factor of the contribution of the web for the shear resistance
c_w	web height that is used for the classification of the cross-section
d, d_f	distance between two centers of gravity
ε	material strength
F_c, F_t	compression, tension force
f_y, f_{yw}, f_{yf}	yield strength for homogeneous girder, web, flange
f_u	ultimate strength
$h_{c,eff}$	effective web height of compression part
h_{eff}	effective height
h_w	web height
$h_{w,eff}$	effective web height
I_y	moment of inertia around y-axis
$I_{y,eff}$	effective moment of inertia around y-axis
k_σ	plate buckling factor
L	girder length
$\bar{\lambda}_p$	plate slenderness
$\bar{\lambda}_w$	web slenderness
η	conversion factor
$M_{eff,Rk}$	effective bending resistance for critical cross-section of class 4
$M_{el,Rk}$	elastic bending resistance for critical cross-section of class 3
$M_{pl,Rk}$	plastic bending resistance for critical cross-section of class 1 or 2
ψ	stress ratio
ρ	reduction factor plate buckling
σ_i	stress
s_s	loading length
t_f	flange thickness
t_w	web thickness
$V_{bw,Rk}$	characteristic shear resistance based on web contribution
$W_{eff,min}$	minimum effective bending moduluees
$W_{el,min}$	minimum elastic bending modulus
z_{zi}	distance between neutral axis and center of gravity

Abstract

Nowadays the most common material for bridges is steel, which is a versatile but heavy material. One way to reduce the weight is to use high strength steel (HSS), a steel type with a yield strength higher than 460 MPa. Due to the lack of design rules in Eurocode 3, there is a low demand for HSS resulting in a high cost. An economical solution is the use of hybrid steel girders, in which the flanges are made of HSS. For the web, a lower strength steel type can be used since its contribution to the bending resistance is not vital.

This thesis researches the possibilities of bending and shear resistance in hybrid steel I-girders to determine if the design can be carried out according to Eurocode 3 or if adjustments are required. The first step was to perform a verification in Ansys using an existing study. This model became the base for the bending and shear interaction model. This model was used to perform two kinds of simulations with a variation in steel grades and cross-section classes. The results of the simulations were compared with calculations according to the Eurocode, including bending and shear interaction curves. Finally, a parametric study for hybrid HSS girders took place.

The results of the numerical simulations were used to verify if the current design rules can be used for hybrid HSS girders. The conclusion is that the design rules can be applied for class 3 and 4 cross-sections, however further investigation and adjustments regarding HSS are recommended for Eurocode 3.

Abstract (Nederlands)

Staal is een frequent gebruikt bouwmateriaal voor bruggen. Het is een veelzijdig maar zwaar materiaal. Een manier om het gewicht te reduceren is het gebruik van hoogsterkte staal (HSS), een staalsoort met een vloeigrens van meer dan 460 MPa. Door het ontbreken van ontwerpregels in Eurocode 3, is er weinig vraag naar HSS wat leidt tot een hoge kostprijs. Een economische oplossing is het gebruik van hybride staalprofielen, waarbij de flenzen uit HSS zijn. Voor het lijf kan staal van een lagere sterkte gebruikt worden aangezien zijn bijdrage aan de buigweerstand niet maatgevend is.

Deze masterproef onderzoekt het gedrag van buig- en schuifweerstand in hybride staalprofielen om te zien of Eurocode 3 gebruikt kan worden zonder aanpassingen. De eerste stap was het uitvoeren van een verificatie in Ansys op basis van een bestaande studie. Dit model werd de basis voor het buig- en afschuifinteractiemodel. Hiermee werden twee soorten simulaties uitgevoerd met een variatie in staalsoorten en doorsnedeklassen. De resultaten van de simulaties werden vergeleken met de berekeningen volgens de Eurocode, inclusief buig- en afschuifinteractiekrommen. Tenslotte werd er een parameter studie voor hybride HSS liggers uitgevoerd.

Uit de resultaten van de simulaties werd gekeken of de huidige regels gebruikt konden worden voor hybride HSS liggers. De conclusie is dat de ontwerpregels voor klasse 3 en 4 doorsnedes kunnen worden toegepast, maar verder onderzoek en aanpassingen met betrekking tot HSS worden aanbevolen voor Eurocode 3.

1 Introduction

1.1 Research situation

As master's students of Civil Engineering Technology who are doing their Erasmus in Budapest, the opportunity was offered to conduct the Master's thesis at Budapest University of Technology and Economics (BME). This research investigates the opportunities of the use of steel hybrid girders and whether Eurocode 3 provides sufficient information to design these girders. The whole process is supported by prof. dr. ir. Hervé Degée, Hasselt University, and prof. dr. Balázs Kövesdi, associate professor at BME.

1.2 Problem statement

With today's technology, steel bridges offer an efficient solution to the decay of full concrete bridges, because of the excellent properties and versatility of steel. Nowadays there is the possibility to work with high strength steel (HSS) which has a yield strength starting from 460 MPa and better properties than normal grade steel. And yet, the use of HSS is not widely used up to the present day mainly due to the lack of knowledge. The only official European design rules for higher strength steel are stated in EN 1993-1-12, which summarizes the additional rules for steel grades between S460 and S700. This means there is no specific information about steel grades higher than S700, which makes it difficult to use.

HSS is very interesting for the erection of bridges, especially steel types between S460 and S690, because the stresses can be increased and the thickness of the material can be reduced, which will lead to major weight savings. These savings lead to a reduction in cost for welding, fabrication, erection and transportation. Steel types above S690 are also very interesting, but because there is no specific information, as already mentioned, it is quite complicated to incorporate these in a structure.

As mentioned above, the properties of HSS are better than those of lower grade steel. However, when one property is increased during the fabrication process, another might decrease. Therefore, the perfect combination of good toughness, ductility, strength and weldability is difficult to reach. As a result, there is a variety of HSS grades with variation in the values of the properties. The chosen grade depends on the application of the material, which depends on the material requirements of the project.

To optimize the use of steel elements, hybrid steel has been introduced. The concept of hybrid plate girders is welding steel plates made of different steel grades. The flanges are dimensioned for the strength, using HSS. The web is dimensioned to avoid buckling, using lower steel strength. But again, there are no representative standards

and rules for the design of hybrid plate girders, which complicates the calculation. The limitations are therefore: lack of knowledge, difficult fabrication, cost, lack of guidance by the Eurocode and the lack of developed design methodology.

1.3 Aim of research

It is important to gather more insight on the functionality of hybrid girders. The purpose of this thesis is to develop some numerical prototypes in which the flanges of a hybrid steel girder will be designed with HSS and the body with lower strength steel. Based on the numerical analyses and hand calculations using Eurocode 3, a conclusion is made about the safety of the hybrid steel profiles. This shows if increased safety factors are needed to be implemented in the Eurocode with further investigation in hybrid behavior.

The following paragraphs will include the description of the materials and methods used to develop these numerical simulations. The first step of the simulations is the verification of the model using another scientific study as comparison. After the verification, the ultimate bending moment and shear force resistance is determined for a list of girders using different geometry and classes. Simultaneously, these results of the simulations are compared with theoretical calculations for the bending moment and shear force resistance using Eurocode 3. Both the numerical results as the hand calculations are compared in the bending moment and shear force interaction. Lastly, a parametric study takes place where the ultimate resistances are compared for a hybrid HSS I-girder for different parameters.

All the plotted results are eventually compared in an overview, where it is clear if the stated rules from the Eurocode are sufficient for the design of hybrid girders or not. Finally, every important decision and remark are summarized in the conclusion.

2 Literature review

2.1 Introduction

2.1.1 High strength steel

Today, steel is an indispensable resource in construction, mostly for its excellent properties and versatility. An emerging phenomenon is high strength steel (HSS). This is a steel type with a yield strength higher than 460 MPa with improved properties, including higher strength, better toughness, ductility and weldability. This type of steel can be used in regions with very high static stresses and to avoid brittle failure. However, it is not used very much in Europe due to the lack of official design rules and experience. As the demand for this steel grade is lower due to this, the cost price is very high compared to lower strength steel. This makes it seem that it is not very interesting to use HSS. But continuous testing, more experience and new detailed design codes, would extend the further use of HSS. This leads to promotion of the material, which will result in higher demand and lower prices. However, in Japan and the United States, there is a more frequent use of high strength steel and the market share is way higher, which results in a lower price.

High strength steel is very interesting for the erection of bridges, more specifically steel types between S460 and S690, because the stresses can be increased and the thickness of the material can be reduced, which will lead to major weight savings. These savings lead to a reduction in cost for welding, fabrication, erection and transportation. The named steel types are available in Europe, but they are not widely used. For steel grades up to S700 there are additional design rules and specifications found in Eurocode 3 – Design of steel structures. The biggest problem is the lack of design codes for steel types starting from S700.

2.1.2 Steel grades

There must be noticed that the European standard EN 10025 [1] deals with steel grades up to S960 and EN 1993-1-12 [2] adds specific rules to use steel grades up to S700 when designing a steel bridge according to the Eurocodes. In this paragraph, the advantages and obstacles for using high strength steel will be discussed from the design and economical points of view.

The increase of the steel strength can lead to material savings and the reduction of fabrication costs (time for welding, areas to be painted, etc.) As well the erection costs of the bridge (less material to handle and transport, reduced weight simplifying the erection, less costs for foundations, etc.) The structural elements become lighter and slenderer. This enables special aesthetic and elegant structures. Constructions with less steel are also in good agreement with the sustainability problem and a reduced consumption of the world's natural resources. The material savings also reduce the values of internal forces and moments in the zones surrounding the intermediate supports of the bridge.

It has been shown that HSS can exhibit not only a higher strength, but also an excellent toughness and superior welding properties, so that a high safety both in fabrication and in structural design is ensured. This finally leads to an increase in the competitiveness of a steel or composite bridge using HSS. Generally, the increase of the steel grade will save costs if the strength can be utilized. The limitations of utilizing the strength may be buckling (stability phenomenon), fatigue and deflection limits.

In case of stability, critical loads are independent of the material strength, this means that for slender structures the use of high steel grades becomes uneconomical. A solution is the use of hybrid girders. When using high steel grades, fatigue often becomes decisive because it is almost independent of the base material strength. Therefore, it is reasonable to use high steel grades in cases where the influence of fatigue is small such as large spans and/or small traffic loads as well as for areas e.g., close to interior supports. To increase the fatigue strength of welded structures, post weld treatment methods could be applied. It should be noticed that the fatigue loads will differ from country to country, and from road to road, depending on traffic intensity.

Furthermore, the reduction in girder dimensions also reduces the mechanical properties such as bending stiffness. This leads to higher deflections, which might become a decisive design criterion. The deflection limitations diversify much between different countries. Finally, the useful steel grade for bridges will diversify from country to country due to traffic intensity (fatigue) and due to deflection limitations.

2.1.3 Properties of HSS

As mentioned above, high strength steel has better properties than low grade steel. However, when one property is increased during the fabrication process, another might decrease. Therefore, the perfect combination of good toughness, ductility, strength and weldability is difficult to reach. As a result of this situation, there is a variety of HSS grades with variation in values of the properties. The chosen grade depends on the application of the material, depending on the material requirements of the project. There are two different manners to change the properties of the material, the first one is to change the chemical composition and the second one is to change the production process. The latter depends purely on the supplier. By changing the properties, the HSS grades still need to comply with the specifications provided by the international quality standards, this means EN for Europe, ASTM for US, JIS for Japan, etc. [3, 1.1.1].

The enhanced properties are both mechanical as technological. The most important properties of high strength steel are discussed shortly below. Table 1 shows the nominal values for the tensile properties of high strength steel coming from EN 1993-1-1 [4, 5.2]. The values are given for yield strength f_y and ultimate tensile strength f_u.

Table 1: Nominal values of yield and ultimate tensile strength for structural steel

Steel grade	Nominal thickness of the element $t\,[mm]$			
	$t \leq 40\,mm$		$40\,mm < t \leq 80\,mm$	
	f_y $[N/mm^2]$	f_u $[N/mm^2]$	f_y $[N/mm^2]$	f_u $[N/mm^2]$
S235	235	360	215	360
S275	275	390	245	370
S355	355	490	325	470
S420	420	510	390	490
S460	460	540	410	510
S500	500	580	450	580
S550	550	600	500	600
S600	600	650	550	650
S620	620	700	560	660
S650	650	700	-	-
S690	690	770	630	710
S700	700	750	-	-

The stress-strain curve for HSS differs from the one for mild steels. The curve for mild steels is shown in figure 1a and for HSS in figure 1b. The yield strength is defined by the permanent deformation, more specifically the 0,2% offset and 0,5% total deformation [3, 1.1.4].
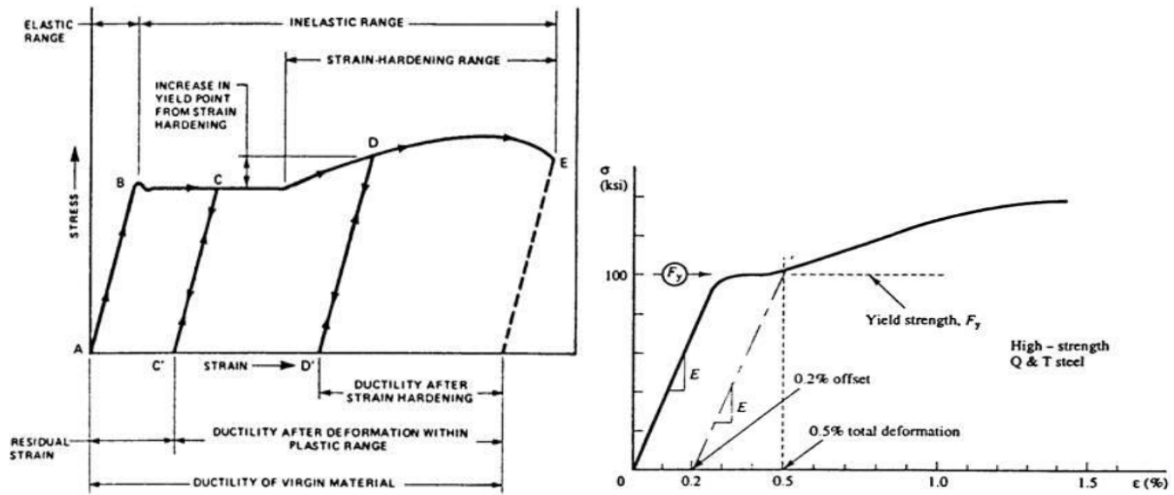
Figure 1: Stress-strain curve (a) for mild steels (b) for Q&T HSS

The improved toughness also reflects in better welding properties. High strength steels have better weldability than regular steel grades. For further instructions on preheating and welding, the Eurocode shall be consulted because it depends on the chemical composition of the steel. In general, the higher the strength of the steel, the more precautions should be performed to ensure the welding process.

In terms of ductility, brittle failure must be prevented. This means that plastic deformations should be sufficiently large. To ensure this, the carbon content should be at very low level, possibly around 0,15%. Figure 2 shows that HSS could be more sensitive to local ductility demands than normal steel grades.
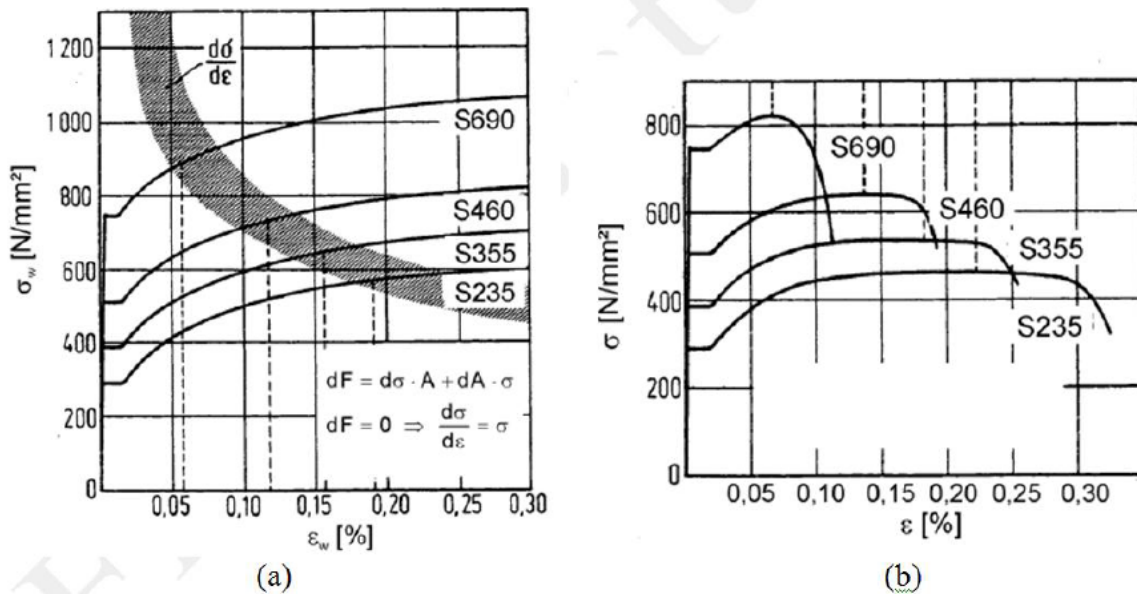
Figure 2: For different grades (a) stress-strain curves (b) load-deflection curves

2.1.4 Hybrid steel girders

An innovation which is more economical than the use of homogenous HSS girders, is the use of hybrid steel girders. Hybrid refers to the use of two different types of steel grade. Such girders are more economical than homogenous girders, because as mentioned before the cost for HSS is very high. Usually, the flanges are made of high strength steel and the web of a lower grade. The web can be made from lower strength steel because the web only contributes 20 to 25 percent to the bending resistance, which makes the use of HSS unnecessary [5, 1].

The design of a hybrid girder can be carried out according to the rules of Eurocode 3 with some minor modifications. The effects of premature yielding of the web affect the resistance of bending and axial forces, but can be ignored. Although some sources might tell otherwise. If there are no stated rules in Eurocode 3, it might mean that it is not allowed to design such structures.

Although, EN1993-1-5 [6] for plated structures mentions hybrid girders in one clause and gives a limitation that the ratio between the yield strengths of flanges and web should not exceed two [6, 6.3]. Therefore, the limitations of hybrid girders are: lack of knowledge, difficult fabrication, cost, lack of guidance of Eurocode and lack of developed design methodology.

Typically, hybrid girders have cross-section type class 4 according to Eurocode 3. The resistance in bending in Ultimate Limit State (ULS) is influenced by the local yielding of the web, which limits the stresses in the web and affects the effective width of the web as well. For Serviceability Limit States (SLS), the local yielding of the web must be accepted, but the requirement of reversible behavior will still be fulfilled. For the limit state of fatigue, Eurocode 3 states a restriction that the stress range should not exceed 1.5 times the yield strength. For hybrid girders, it is shown that this restriction applies to the yield strength of the flanges and that yielding of the web does not influence the fatigue strength [5, 1].

The use of hybrid girders with this difference between the strength of flanges and web, implies that yielding should not occur in SLS and is interpreted in such a way that it applies to the flanges but not to direct stresses in the web. The local yielding in the web is limited by the elastic strains in the flanges and after the first yielding the behavior is reversible. This reasoning is not always accepted and the interpretation may vary from country to country.

The concept of hybrid girders presupposes the use of HSS, the fabrication of which requires a bit stricter procedure than low strength steel [5, 6]. There are no problems related to the mixing of steel grades in hybrid girders. Welding different steel grades is not a practical problem but defining the meaning of matching electrodes is necessary. For the web to flange weld, it is suggested that electrodes matching the web strength are used. The weld should be designed as being of the web steel grade.

2.2 Classification of cross-sections

The role of cross-section classification is to identify the extent to which the resistance and rotation capacity of cross-sections is limited by its local buckling resistance [7, 5.5.1].

2.2.1 Classification

The classification of a cross-section depends on the width to thickness ratio of the parts subject to compression. These compression parts include every part of a cross-section which is either totally or partially in compression under the load combination considered.

Four classes of cross-sections are defined, as follows [7, 5.5.2]:

1) Class 1 cross-sections are those which can form a plastic hinge with the rotation capacity required from plastic analysis without reduction of the resistance.
2) Class 2 cross-sections are those which can develop their plastic moment resistance but have limited rotation capacity because of local buckling.
3) Class 3 cross-sections are those in which the stress in the extreme compression fiber of the steel member, assuming an elastic distribution of stresses, can reach the yield strength, but local buckling is liable to prevent development of the plastic moment resistance.
4) Class 4 cross-sections are those in which local buckling will occur before the attainment of yield stress in one or more parts of the cross-section.

In Class 4 cross-sections, effective widths may be used to make the necessary allowances for reductions in resistance because of local buckling. The various compression parts in a cross-section (such as a web or flange) can, in general, be in different classes. Where the web is considered to resist shear forces only and is assumed not to contribute to the bending resistance of the cross-section, the cross-section may be designed as class 2, 3 or 4, depending only on the flange class.

2.2.2 Rotation capacity

One of the behavior properties that depends on the classification is the rotation capacity. For the rotation capacity of the four classes, the following applies [8, 4.2]:

1) Class 1 cross-sections can develop plastic moment capacity M_{pl} in bending, which means they have enough rotation capacity to distribute the moments.
2) Class 2 cross-sections can also reach the plastic moment capacity, but the rotation capacity is lower than for class 1 cross-sections.

3) Class 3 cross-sections don't reach the plastic moment capacity, because local buckling occurs before reaching it. Therefore, class 3 is limited to a value between the elastic moment capacity M_{el} and plastic moment capacity.
4) Class 4 cross-sections do not even reach the elastic moment capacity, this is also why class 4 will not be used for the flanges in this thesis.

A visualization of the rotation behavior of the different classes is shown in figure 3.
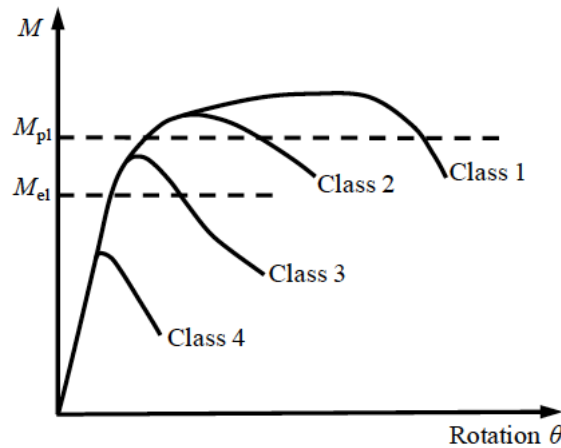
Figure 3: Typical response and cross-section classification of steel sections in bending

Basically, when the plastic moment capacity M_{pl} is reached, the process of plastic rotation can be initiated.

2.2.3 Determination

In general, there are four classes of cross-sections. The purpose of this classification is to check how the resistance and rotation capacity is limited by the local buckling resistance. The cross-section class of the flanges is determined according to Eurocode 3. The cross-section class of the web should however be determined using the yield strength of the compression flange [5, 4.1]. This is slightly conservative because the cross-section class is influenced by both stress and strain.
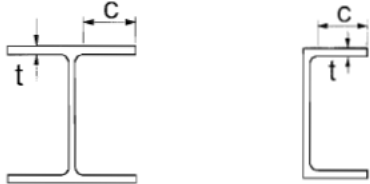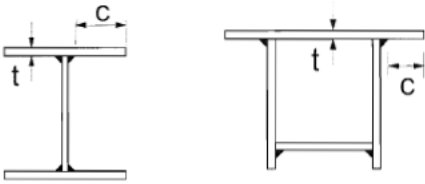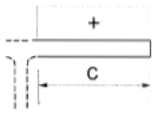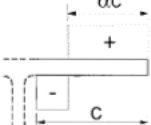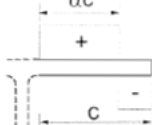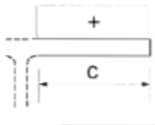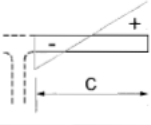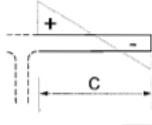
Only the strains, but not the stresses in the web, will correspond to those in the flange. For the classification, a division is made between the internal compression parts and the outstand flanges. Based on this, two parameters can be found and divided, c and t. This ratio is the first thing that is required to know. The second one is epsilon, which is the square root of 235 divided by the yield strength of the steel and thus the material strength. Based on tables 2 and 3 [9, 5.5] below, the determination of the cross-section class can take place. A cross-section should be classified according to the highest, thus least favorable, class of its structure.

Table 2: Maximum width-to-thickness ratios for compression parts (1)

Internal compression parts

Class	Part subject to bending	Part subject to compression	Part subject to bending and compression		
Stress distribution in parts (compression positive)					
1	$c/t \leq 72\varepsilon$	$c/t \leq 33\varepsilon$	when $\alpha > 0,5$: $c/t \leq \dfrac{396\varepsilon}{13\alpha - 1}$ when $\alpha \leq 0,5$: $c/t \leq \dfrac{36\varepsilon}{\alpha}$		
2	$c/t \leq 83\varepsilon$	$c/t \leq 38\varepsilon$	when $\alpha > 0,5$: $c/t \leq \dfrac{456\varepsilon}{13\alpha - 1}$ when $\alpha \leq 0,5$: $c/t \leq \dfrac{41,5\varepsilon}{\alpha}$		
Stress distribution in parts (compression positive)					
3	$c/t \leq 124\varepsilon$	$c/t \leq 42\varepsilon$	when $\psi > -1$: $c/t \leq \dfrac{42\varepsilon}{0,67 + 0,33\psi}$ when $\psi \leq -1^{*)}$: $c/t \leq 62\varepsilon(1 - \psi)\sqrt{(-\psi)}$		
$\varepsilon = \sqrt{235/f_y}$	f_y	235	275	355	420	460
	ε	1,00	0,92	0,81	0,75	0,71

*) $\psi \leq -1$ applies where either the compression stress $\sigma \leq f_y$ or the tensile strain $\varepsilon_y > f_y/E$

Table 3: Maximum width-to-thickness ratios for compression parts (2)

Outstand flanges				
Rolled sections		Welded sections		
Class	Part subject to compression	Part subject to bending and compression		
		Tip in compression	Tip in tension	
Stress distribution in parts (compression positive)	(diagram)	(diagram αc)	(diagram αc)	
1	$c/t \le 9\varepsilon$	$c/t \le \dfrac{9\varepsilon}{\alpha}$	$c/t \le \dfrac{9\varepsilon}{\alpha\sqrt{\alpha}}$	
2	$c/t \le 10\varepsilon$	$c/t \le \dfrac{10\varepsilon}{\alpha}$	$c/t \le \dfrac{10\varepsilon}{\alpha\sqrt{\alpha}}$	
Stress distribution in parts (compression positive)	(diagram)	(diagram)	(diagram)	
3	$c/t \le 14\varepsilon$	$c/t \le 21\varepsilon\sqrt{k_\sigma}$ For k_σ see EN 1993-1-5		
$\varepsilon = \sqrt{235/f_y}$	f_y	235	275	355	420	460
	ε	1,00	0,92	0,81	0,75	0,71

2.3 Design of steel hybrid girders

2.3.1 Bending resistance

The bending resistance of hybrid steel girders are influenced by the different yield strengths in the cross-section. This difference will show differently for every cross-section class. The formulas below give the characteristic resistance, assuming there is no partial safety factor for this analysis, for specifically doubly symmetric I girders for each cross-section class [5, 4.2]. As mentioned above, a cross-section should be classified according to the highest, thus least favorable, class of its structure. This means the calculations below are not specifically for the class of the flange or web.

Cross-section class 1 and 2

The calculation of the bending resistance for cross-sections of class 1 and 2 assumes the cross-section had already fully yielded as shown in figure 4.

$$M_{pl,Rk} = f_{yf} \cdot A_f \cdot (h_w + t_f) + f_{yw} \cdot A_w \cdot \frac{h_w}{4} \qquad (1)$$
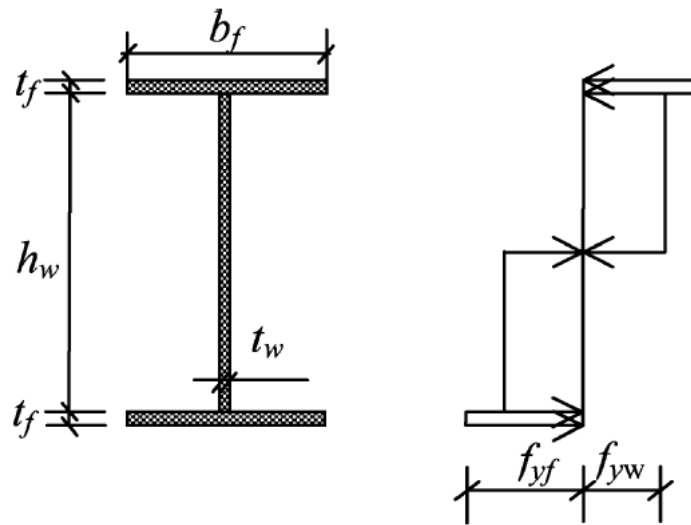
Figure 4: Hybrid I-girder in cross-section class 1

Cross-section class 3

For the calculation of the bending resistance of a cross-section class 3 it is assumed that the elastic moment can be reached, but the plastic not. This means that the elastic bending modulus should match with the fiber with the greatest stress, thus the outer fiber. For both the flange and the web the elastic bending resistances are calculated and then the minimum is taken.

$$M_{el,Rk} = min[W_{f,el,min} \cdot f_{yf}; W_{w,el,min} \cdot f_{yw}] \qquad (2)$$

Cross-section class 4

The calculation of the bending resistance for cross-sections of class 4 is more complicated. The assumption is made that flanges should not be in class 4 because the local buckling should not be considered [5, 4.2.2]. The web however can be class 4, this makes the whole cross-section class 4, because it is the least favorable. The loss in effectiveness will make sure that the neutral axis will move. This means the overall cross-section will be asymmetric and the resistance calculation does not happen in one small step.

First, the effective height of the compressed part of the web needs to be calculated. Using the overall effective height, the moment of inertia is calculated. Then the method is just the same as for class 3. Figure 5 shows a representation of a cross-section of class 4 where a part of the web height is lost due to local buckling.

$$M_{eff,Rk} = min[W_{f,eff} \cdot f_{yf}; W_{w,eff} \cdot f_{yw}]$$
(3)
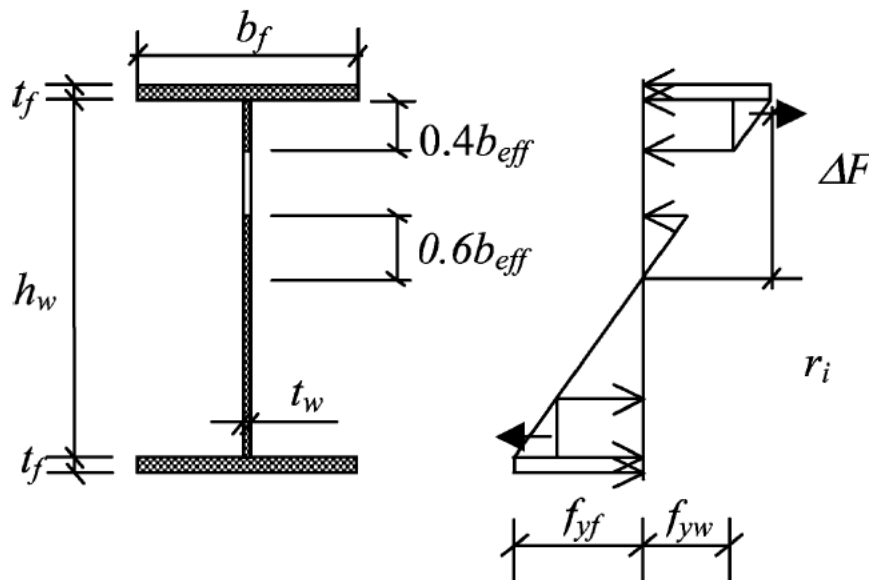
Figure 5: Hybrid I-girder in cross-section class 4

2.3.2 Shear resistance

The shear resistance is calculated using the rules in Eurocode 3-1-5. The formulas for the resistance already considers different yield strength in flanges and web. First, shear buckling should be taken in consideration. For unstiffened webs:

$$\frac{h_w}{t_w} > \frac{72 \cdot \varepsilon}{\eta}$$
(4)

Where η is considered 1.20 for steel types under S460 and 1.20 for HSS. If this is the case the girder needs transverse stiffeners at the supports, which makes the girder considered rigid for the following formulas.

The design resistance for shear is based on the contribution of the web, first the modified slenderness $\bar{\lambda}_w$ is determined:

$$\bar{\lambda}_w = \frac{h_w}{86.4 \cdot t_w \cdot \varepsilon} \tag{5}$$

Depending on the value of the slenderness, the reduction factor χ_w that is needed for the contribution of the web becomes depended on the rigid value and can be found in table 4.

Table 4: Contribution from the web for the shear buckling resistance

	End panels with non-rigid end post	All the other cases (intermediate panels and end panels with rigid end post)
$\bar{\lambda}_w < 0{,}83 / \eta$	η	η
$0{,}83 / \eta \leq \bar{\lambda}_w < 1{,}08$	$\dfrac{0{,}83}{\bar{\lambda}_w}$	$\dfrac{0{,}83}{\bar{\lambda}_w}$
$\bar{\lambda}_w \geq 1{,}08$	$\dfrac{0{,}83}{\bar{\lambda}_w}$	$\dfrac{1{,}37}{0{,}7 + \bar{\lambda}_w}$

For the shear resistance this means that, for this thesis, there is assumed that only the contribution of the web is crucial for the shear resistance.

$$V_{b,Rk} = V_{bw,Rk} = \frac{\chi_w \cdot f_{yw} \cdot h_{w,eff} \cdot t_w}{\sqrt{3}} \tag{6}$$

2.3.3 Bending and shear resistance interaction

Besides the pure bending moment and pure shear force, which already have been discussed, the interaction of these two is also very important for the designing process. The combined effect is a very important issue of the bearing capacity of the plate [10, 2.1.1] and its ignorance can lead to catastrophic designs.

The interaction can be explained as follows: when a girder is under the influence of combined loading, such as bending and shear, there is generally assumed that the shear force resistance is carried by only the web, and not the flanges.

The ultimate shear force resistance is only reached when the web is yielded uniformly and the tension is fully formed. Bending is negligible if the bending moment is smaller than the bending capacity of only the flanges. In case these bending moments cease to become larger, the web should also contribute to the bending moment resistance. This results in a reduction of the shear force resistance of the girder [11, 2.2]. Therefore, bending moment and shear force interaction should always be considered.

Furthermore, the interaction is only defined when the bending moment exceeds the bending moment resistance of the flanges. To define this interaction, an interaction formula can be used. The current interaction formula from 2006 [12, 7.1], does not

follow the numerically obtained results for unstiffened girders that F. Sinur obtained in his research about bending moment – shear force interaction [13].

Using Sinur's numerical results, a new interaction curve was proposed, which is shown in figure 6.
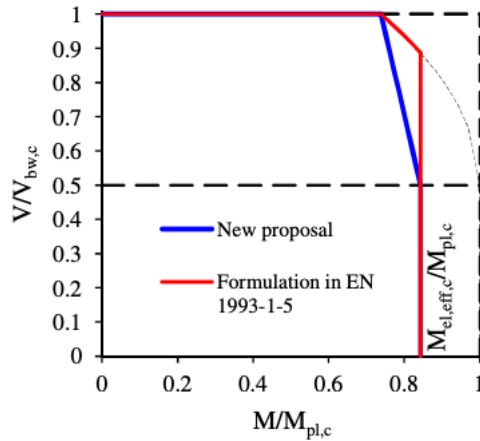
Figure 6: Sinur's proposal for new M-V interaction curve

Figure 6 shows that the current interaction curve is more quadratic, but the proposal shows more linear behavior. Another comparison of an old interaction curve is shown in figure 7.
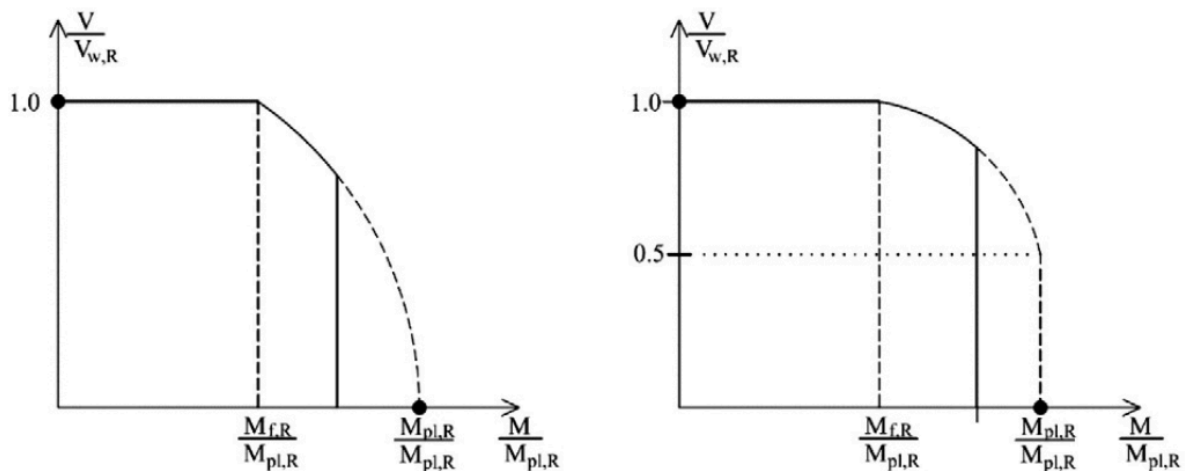
Figure 7: M-V interaction (a) for old curve (b) for new curve

Figure 7a shows the old bending moment – shear force interaction curve. The shape of the interaction curve depends on the slenderness of the web. The numerical results that lie above the curve are in a safe zone, the ones below are not. As figure 7b shows, the new curve gives a larger safety than the old one [13, 4.1]. The proposal for the new interaction formula is given below [13, 4.2]:

$$\eta_1 + \left(1 - \frac{M_{f,Rd}}{M_{el,eff,Rd}}\right)(2\eta_3 - 1)^\kappa \leq 1,0 \tag{7}$$

Where:

$$\eta_1 = \frac{M_{Ed}}{M_{el,eff,Rd}} \text{ and } \eta_3 = \frac{V_{Ed}}{V_{bw,Rd}}$$

This new interaction formula gives the same resistance as the one which is currently used when the bending moment is equal to the bending capacity of the flanges. If it exceeds the bending capacity of the flanges, it shows lower resistances, which makes the design safer. Regarding the bending moment and shear force interaction, figure 8 shows four interesting failure types of a girder [11, 4.4].
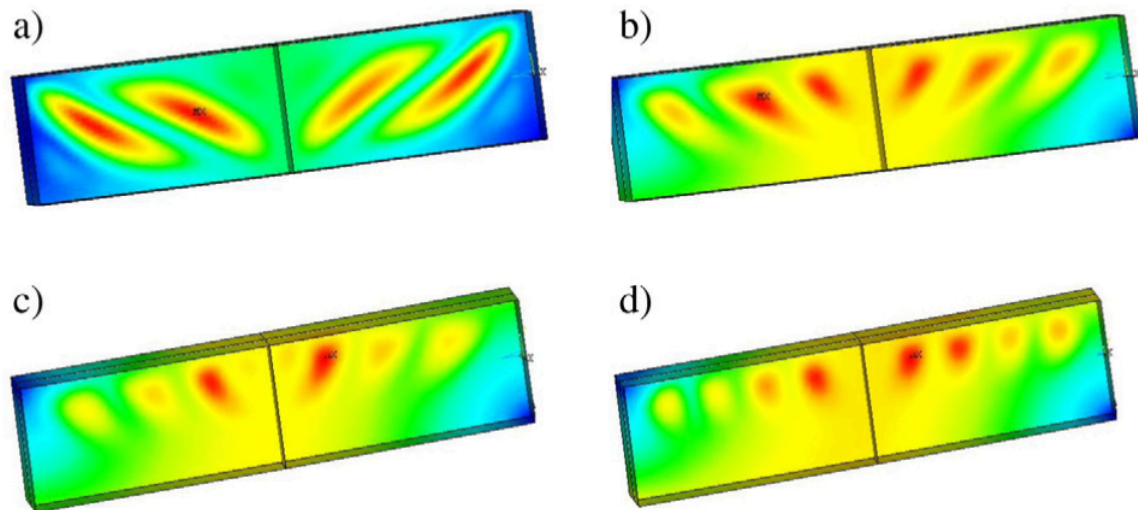
Figure 8: Failure types of girder

Figure 8 shows pure shear force buckling of the web panels in (a), typical bending moment failure in (d) and a combination of both in (b) and (c). The last two demonstrate the interaction between bending and shear. All failure modes also demonstrate that the transition between the failure modes happens very smoothly.

For hybrid girders however, it may seem that the bending moment – shear force interaction is greater than homogeneous girders, especially when the web is already partially yielded before the flanges reach their yield strength [14]. The sequence of the yielding depends on the ratio of flange yield strength to the web yield strength. As mentioned before, this ratio can not exceed two.

2.3.4 Flanges

Flanges play the most important role in the bending resistance of I-girders. They usually have stocky flanges so that they can be fully utilized [4, 4]. Generally, flanges are chosen to be class 3 or lower. If lateral torsional buckling is dominating, a wider flange might be more favorable. The normal solution is to choose the slenderness b/t close to the limit for class 3 and adjust the distance between cross braces such that lateral torsional buckling does not reduce the resistance.

For aesthetical reasons, the visible bottom flange should be made with a constant width. It does not matter if the bottom flange in the sagging region is more slender than the limit for class 3 because it is in tension. The top flange can have a variable width because it does not disturb the appearance. In the sagging region, the size of the top flange will be small and governed by lateral torsional buckling during casting.

The common practice for design of longitudinal stiffened bottom plates is still quite diversified in different European countries and is influenced by the specific construction techniques and traditions [4, 4.3.5]. General recommendations concerning number and size of stiffeners are hard to give as they are dependent on many factors, e.g. the distance between the diaphragms.

2.3.5 Web

Webs are equally important, their main concern is the shear force resistance. Besides, they also have the task to interconnect the flanges [4, 5.1]. The webs thickness is mainly chosen based on the required shear force resistance. For steel plated structures, large heights and plate slenderness occur so the stability behavior of the web usually needs to be considered.

For the stiffening of the web, both longitudinal and transverse stiffeners can be used. A transverse stiffener has mainly influence on the shear force resistance of the web. This is however only the case if the distance between the transverse stiffeners is small, otherwise the influence is low and it does not justify the costs. Longitudinal stiffeners increase not only the bending moment resistance but also the shear force resistance of the web.

Transverse stiffeners

Transverse stiffeners are usually placed at the locations of cross bracings or diaphragms [4, 5.2]. This gives the stiffeners a double purpose of stiffening the web and to serve as brackets for cross bracings. The cross bracings are needed to prevent lateral torsional buckling during erection and in the pier regions also during service. The effect of the transverse stiffeners on the resistance of the girders is limited to an increase of the shear buckling resistance if the web does not have longitudinal stiffeners. The increase in shear resistance makes it possible to reduce the web thickness, which saves costs. This is however counteracted by an increase of the cost of stiffeners and the comparisons between these two show that there is no net saving. The first conclusion is that it does not pay to add stiffeners between the cross bracings. Therefore the second conclusion is to take away redundant vertical stiffeners completely and use small brackets for fixing the cross bracings. This may be suitable in the sagging region of small and medium span bridges. For large spans it may be advisable to add a horizontal beam at the top as well.

Intermediate stiffeners that act as rigid supports at the boundary of inner web panels shall be checked for strength and stiffness. Further minimum stiffness requirements are also given by EN 1993-1-5 for the intermediate transverse stiffeners to be considered as rigid. If the relevant requirements are not met, transverse stiffeners are considered flexible and their actual stiffness may be considered in the calculation of the shear buckling coefficient k_τ. However, no information is given in EN 1993-1-5.

2.4 Finite element method of analysis

Annex C of EN 1993-1-5 [12] gives guidance on the use of finite element methods (FEM) for ultimate limit state, serviceability limit state or fatigue verifications of plated structures.

2.4.1 Use

In using FE methods for design, special care should be taken to the following points:

- The modelling of the structural component and its boundary conditions;
- The choice of software and documentation;
- The use of imperfections;
- The modelling of material properties;
- The modelling of loads;
- The modelling of limit state criteria;
- The partial factors to be applied.

2.4.2 Modelling

The choice of FE-models (shell models or volume models) and the size of mesh determine the accuracy of results. For validation sensitivity, checks with successive refinement may be carried out. The FE-modelling may be carried out either for the component as a whole or a substructure as part of the whole structure. The boundary conditions for supports, interfaces and applied loads should be chosen such that results obtained are conservative. Geometric properties should be taken as nominal. All imperfections should be based on the shapes and amplitudes as given in paragraph 2.4.4 and the material properties should be conform to paragraph 2.4.5.

2.4.3 Choice of software and documentation

The software should be suitable for the task and be proven reliable. Also, the mesh size, loading, boundary conditions and other input data as well as the output should be documented in a way that they can be reproduced by third parties.

2.4.4 Use of imperfections

Where imperfections need to be included in the FE-model, these imperfections should include both geometric and structural imperfections. Unless a more refined analysis of the geometric imperfections and the structural imperfections is carried out, equivalent geometric imperfections may be used.

The geometric imperfections may be based on the shape of the critical plate buckling modes with amplitudes given in the National Annex. 80 % of the geometric fabrication tolerances is recommended. The structural imperfections in terms of residual stresses may be represented by a stress pattern from the fabrication process with amplitude equivalent to the mean (expected) values. The direction of the applied imperfection should be such that the lowest resistance is obtained. For applying equivalent geometric imperfection, table 5 and figure 9 are used.

Table 5: Equivalent geometric imperfections

Type of imperfection	Component	Shape	Magnitude
global	member with length l	bow	see EN 1993-1-1, Table 5.1
global	longitudinal stiffener with length a	bow	min (a/400, b/400)
local	panel or subpanel with short span a or b	buckling shape	min (a/200, b/200)
local	stiffener or flange subject to twist	bow twist	1/50
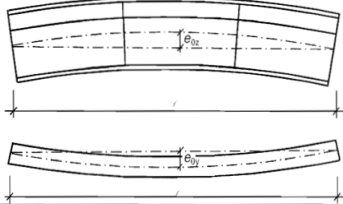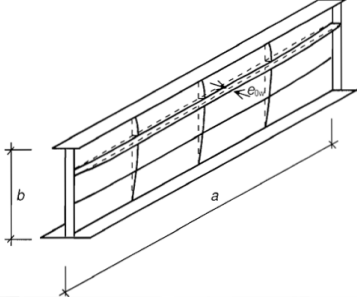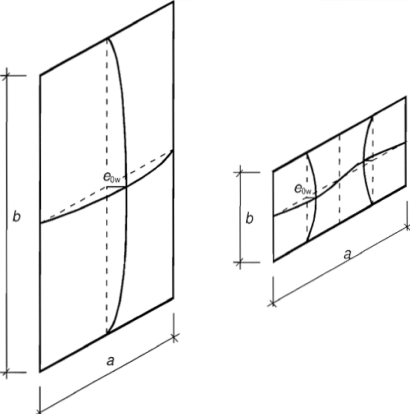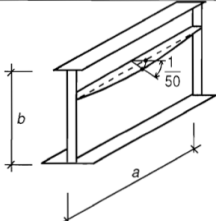
Type of imperfection	Component
global member with length ℓ	
global longitudinal stiffener with length a	
local panel or subpanel	
local stiffener or flange subject to twist	

Figure 9: Modelling of equivalent geometric imperfections

2.4.5 Material properties

Material properties should be taken as characteristic values. Depending on the accuracy and the allowable strain required for the analysis the following assumptions for the material behavior may be used, see figure 10.

a) Elastic-plastic without strain hardening;
b) Elastic-plastic with a nominal plateau slope;
c) Elastic-plastic with linear-strain hardening;
d) True stress-strain curve modified from the test results as follows:

$$\sigma_{true} = \sigma * (1 + \varepsilon) \tag{8}$$

$$\varepsilon_{true} = ln(1 + \varepsilon) \tag{9}$$

Model		
with yielding plateau	a) σ f_y $\tan^{-1}(E)$ ϵ	b) σ f_y $\tan^{-1}(E)$ 1 ϵ *1 tan⁻¹(E/10000)* *(or similarly small value)*
with strain-hardening	c) σ f_y $\tan^{-1}(E/100)$ $\tan^{-1}(E)$ ϵ	d) σ 1 f_y 2 $\tan^{-1}(E)$ ϵ *1 true stress-strain curve* *2 stress-strain curve from tests*
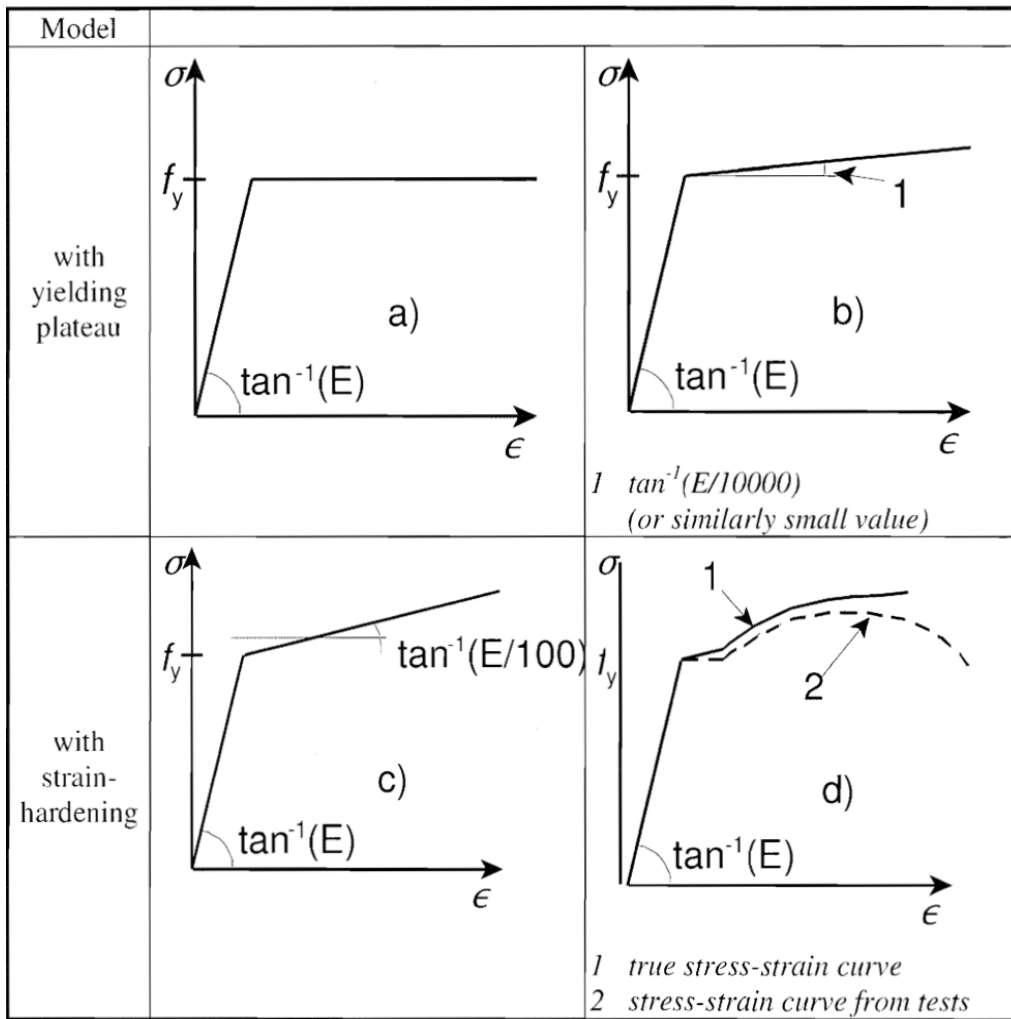
Figure 10: Modelling of material behavior

3 Numerical model development

3.1 General

For the practical part of the thesis, the student version of the software program *Ansys Mechanical APDL 2022* was used. This is a finite element analysis software which is code driven.

In this chapter, the verification of the model was achieved to make sure the results are accurate. The dimensions and parameters for this verification were obtained from the test report [15] that is linked to a research project that is called *"Competitive Steel and Composite Bridges by Improved Steel Plated Structures".* The test report is focused on the interaction between combined shear and patch loading.

3.2 Geometry of verified model

For the verification, two regular welded girders with a steel grade of S355 were modeled using transverse stiffeners. For the verification, the web and flanges were the same steel grade, therefore homogeneous girders. The only difference between the two was the height of the web. The dimensions of both models are displayed in table 6.

Table 6: Geometry of verified model

Girder	Length	Web		Flange		Loading
	$a \ [mm]$	$h_w \ [mm]$	$t_w \ [mm]$	$b_f \ [mm]$	$t_f \ [mm]$	$s_s \ [mm]$
SP 600	2390	600	6	450	20	200
SP 1200	2390	1200	6	450	20	200

Throughout this research, these two models are referred to as the SP 600 and SP 1200 girders.

The applied forces were a shear force V, applied in the center of the girder at span length a, and an additional eccentric patch load F to create a moment. The patch load F was applied over a loading length s_s. A schematic visualization of the model is shown in figures 11 and 12.
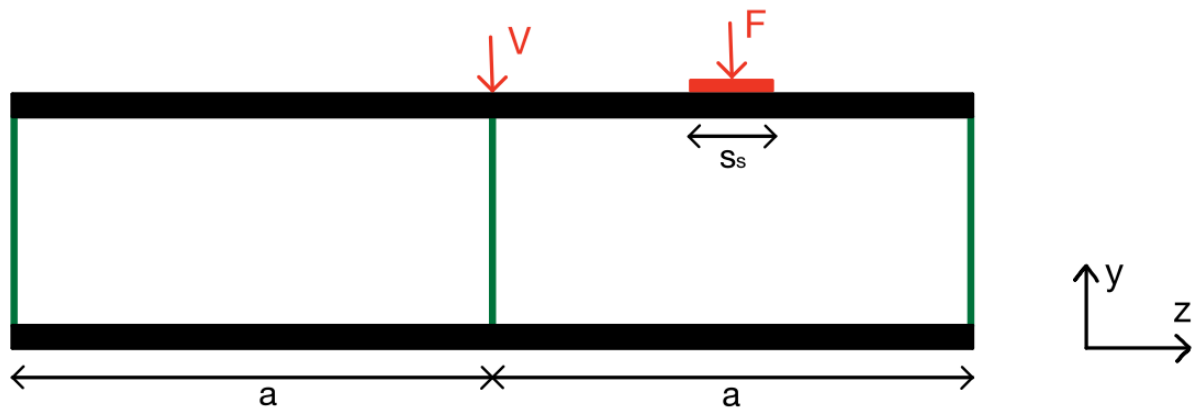
Figure 11: Side view of the tested girder
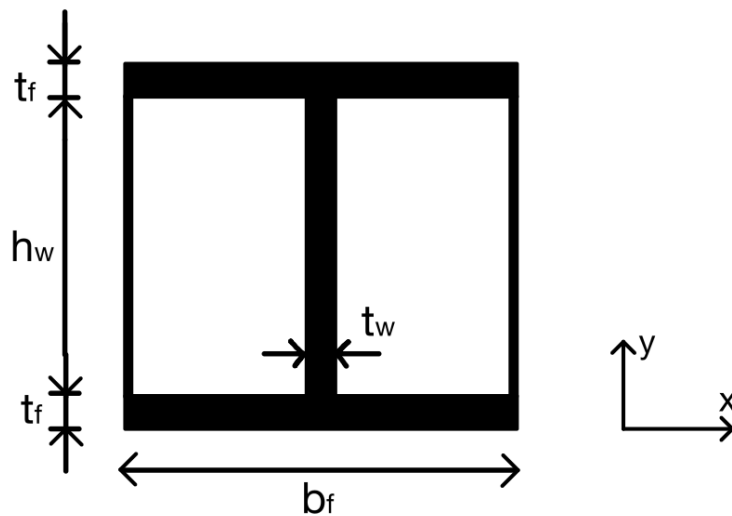
Figure 12: Front and back view of the tested girder

A special remark about the used structure is the presence of transverse stiffeners, these have the same thickness as the flanges, being 20 mm. Figure 11 shows that there were three transverse stiffeners applied on the I-girder, two end posts and one stiffener in the center of the girder. Despite the presence of the stiffeners, the girder was considered non-rigid for the verification only. The transverse stiffeners are indicated in green in figure 11. These did not have an influence on the results of the thesis, they were implemented to avoid buckling of the web.

3.3 Verification numerical model

The numerical model was conducted through the student version of the software *Ansys Mechanical APDL.* Figure 13 shows a 3D representation of the SP 600 girder, using the geometry given above.
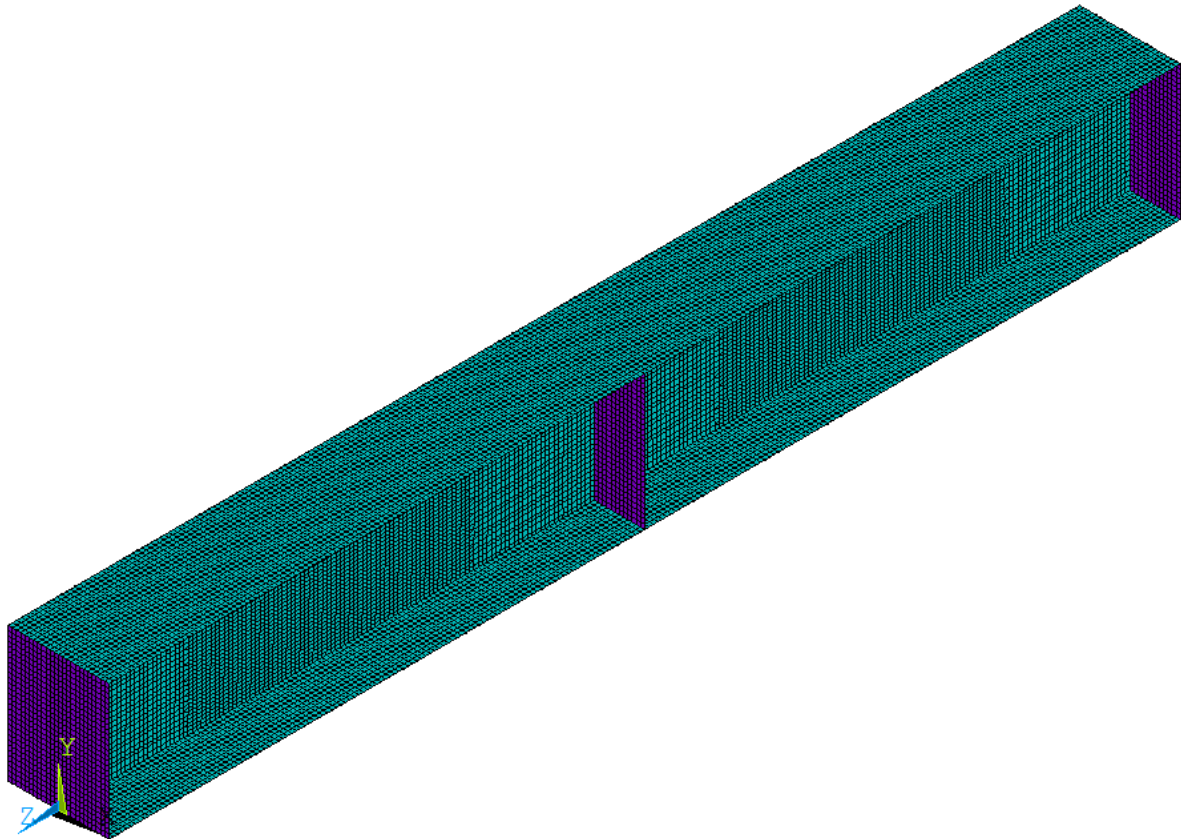
Figure 13: 3D view of the SP 600 girder in Ansys Mechanical APDL

3.3.1 General information

For the model itself, the choice was made to use a shell structure. The shell structure was made of shell181 elements. These kinds of elements consist of four nodes. Each node has six degrees of freedom, these degrees of freedom are: translations in the x, y and z direction as well as rotation around the x, y and z axes. The elements are suitable for analyzing thin to moderately-thick shell structures for linear, large rotation and/or large strain nonlinear applications.

The geometry is the same as described in paragraph 3.2. The verification was carried out for the SP 600 and the SP 1200 girder. The used Young's modulus for the verification was $E = 210\,000\ MPa$. The yield strength and ultimate strength for S355

were obtained from the research project [15, 1.2]. They are the same for the SP 600 and SP 1200 girder and can be found in table 7.

Table 7: Yield strength and ultimate strength for verification of the S355 model

Section	Yield strength f_y [N/mm^2]	Ultimate strength f_u [N/mm^2]
Web	383	543
Flanges / Stiffeners	354	519

In Ansys, the code shown in figure 14 was used to determine the strain – stress curves of the steel. The curves are based on the yield strength and ultimate strength.

```
*DO,i,1,1
      TB,MISO,i,1,4,
      TBTEMP,0
      TBPT,,0,0
      TBPT,,FYw/EX,FYw
      TBPT,,0.01,FYw+5
      TBPT,,0.15,Fuw
*ENDDO


*DO,i,2,2
      TB,MISO,i,1,4,
      TBTEMP,0
      TBPT,,0,0
      TBPT,,FYf/EX,FYf
      TBPT,,0.01,FYf+5
      TBPT,,0.15,Fuf
*ENDDO
```

```
*DO,i,3,4
      TB,MISO,i,1,4,
      TBTEMP,0
      TBPT,,0,0
      TBPT,,FYb/EX,FYb
      TBPT,,0.01,FYb+5
      TBPT,,0.15,Fub
*ENDDO
```

Figure 14: Code for the strain-stress graphs

In the code above, the two alineas on the left are used for the web and the flanges. The one on the right was used for the transversal stiffeners. The strain–stress curves were created through three points. The graphs all start from the origin, the first point is where the strain is equal to the yield strength divided by the elastic modulus (EX in the code) and where the stress is equal to the yield strength. The second point is where the strain is equal to 0.01 and the stress is equal to the yield strength plus five. The third and last point is where the strain is equal to 0.15 and the stress is equal to the ultimate strength.

The results of this code are shown in figures 15a and 15b.

	T1	0			T1	0
	STRAIN	STRESS			STRAIN	STRESS
1	0.0018238	383		1	0.0016857	354
2	0.01	388		2	0.01	359
3	0.15	543		3	0.15	519

Figure 15: Strain - stress values (a) for the web (b) for the flanges and the stiffeners

These values can be automatically turned into a graph to verify the progress. The strain - stress graphs are shown in figures 16 and 17.
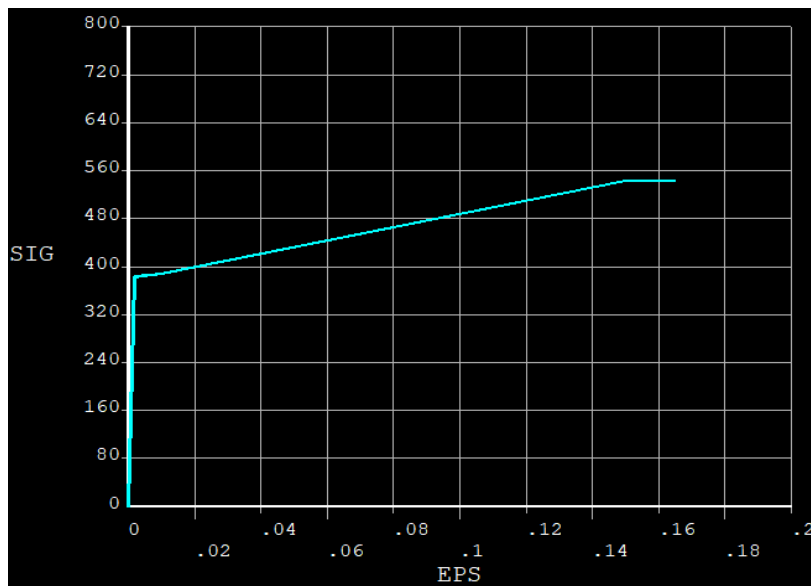
Figure 16: Strain - stress graph for the web in Ansys Mechanical APDL
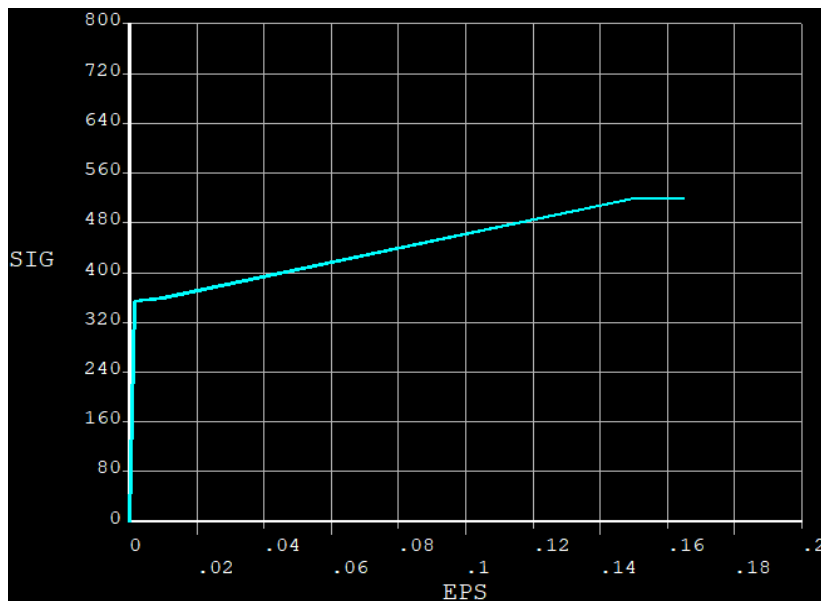
Figure 17: Strain - stress graph for the flanges and stiffeners in Ansys Mechanical APDL

When comparing figures 16 and 17, to figures 1 and 2 from the literature review, as well as paragraph 2.4.5, a reasonable approximation of the actual course is obtained.

The applied forces, V and F, had the same value throughout the verification. This means that if the shear force V is 500 kN, the patch loading F was also 500 kN. The model with the boundary conditions and applied loads is shown in figure 18.
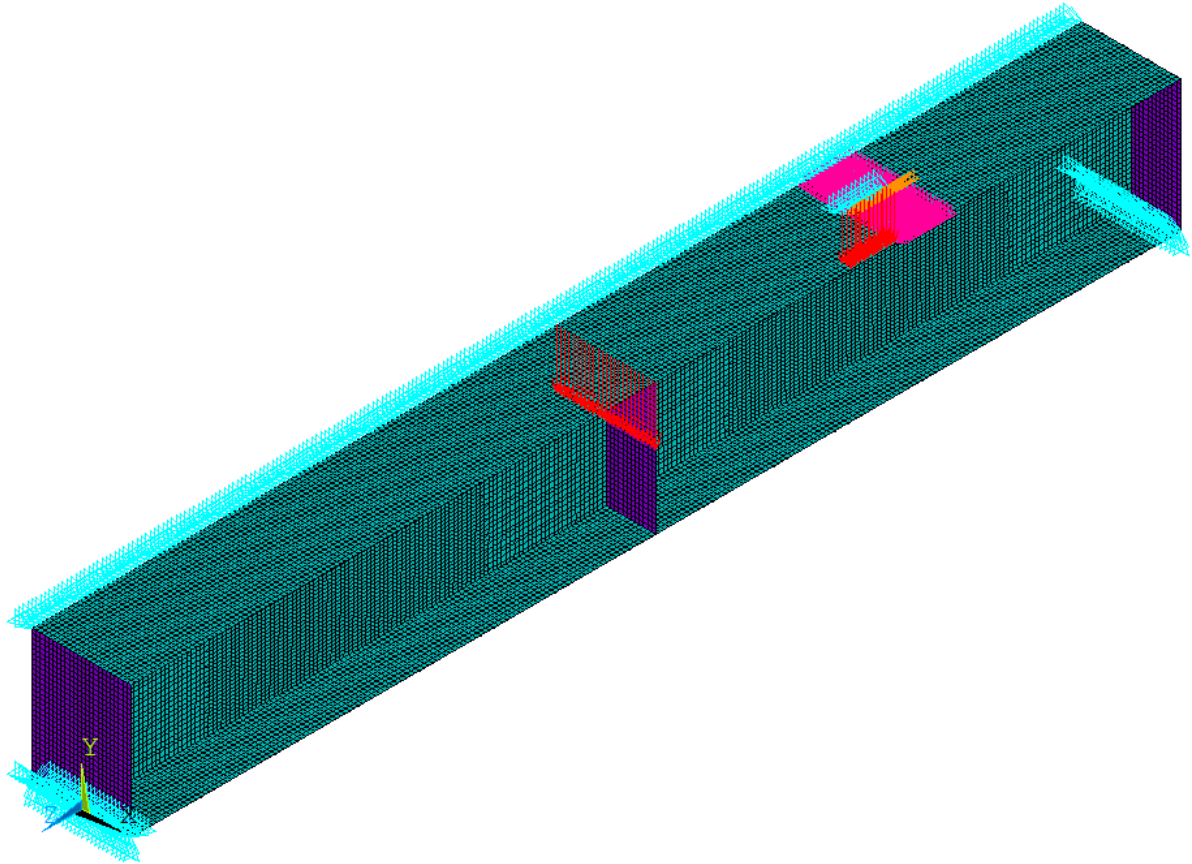
Figure 18: SP 600 model with applied loads and shown boundary conditions in Ansys Mechanical APDL

As shown in figure 18, the beginning and the end of the girder are both fixed at the bottom of the flange. Over the whole length on the top flange, a support was applied to ensure the correct failure mode. Figure 18 also visually shows the mesh size. For all the simulations, a mesh size of 20 mm was used. Increasing the mesh size would lead to less accurate results. The chosen mesh size is good for the combination of both accuracy as running time.

3.3.2 Applied imperfections for the verification

Correct imperfections need to be added in the structural analysis to represent the variance in the dimensions of the members, or even lack of verticality or straightness of a structural member. In the aim of this research, buckling influences the structural behavior of the girder. To include this in the model, imperfections were applied. The imperfection which had the best results for this research, was the hand defined method. These imperfections display the imperfection shapes of the structural members after

fabrication. This imperfection was used following the recommendations as discussed in paragraph 2.4.4 in the literature review for all the performed simulations. The imperfection itself is considered as the height of the web divided by 200. Figures 19 and 20 shows the applied hand defined imperfection for the SP 600 model.
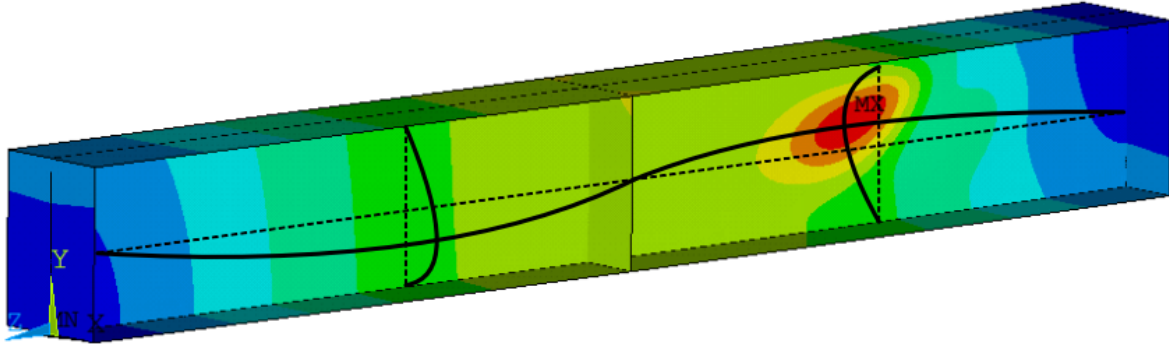
Figure 19: Applied local imperfection for the SP 600 model

The imperfection of the web, which is shown in figure 19 was manually drawn for an easy visualization on the failure mode of the SP 600 model. The imperfection was applied to the model in the code, which can be found in the annex A, by the hand defined method as mentioned above. The visualization of the imperfection of the web in Ansys is shown in figure 20, this figure was obtained by amplifying the imperfection by 100 times and increasing the mesh size by 20 times.

Figure 20: Amplified imperfection for the SP 600 model in Ansys Mechanical APDL

As mentioned in the literature review in paragraph 2.4.4, the imperfection is based on the definition of plate buckling for panels and subpanels considering the buckling

shape. The stiffener in the middle of the girder ensures that there are two waves. This imperfection was also mentioned in the test report [15, 4.2.2].

3.3.3 Verification of the SP 600 and SP 1200 model

As shown in figure 19, the failure occurred at the position where the patch load F was applied. Therefore, after the completion of the model, the displacement was analyzed in the middle node of where the eccentric patch load F was applied. This is shown in figure 21 and was obtained through an additional macro function which can be found in the annex B. This macro function was provided by prof. dr. Kövesdi Balázs Géza.
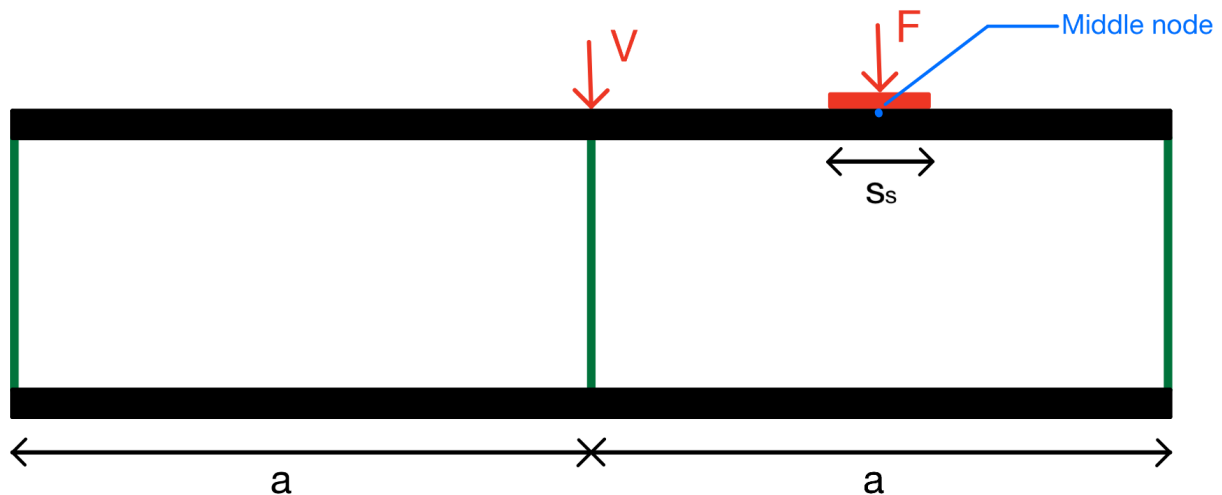
Figure 21: Middle node used for determining displacement

The verification of the model was performed by running the following line of code in Ansys Mechanical APDL:

$$verification,' Sp600', 2390 * 2, 600, 6, 450, 20, 200, 430, 430$$

The parameters of this piece of code consist of:

- The name of the macro function which creates the model;
- The name of the simulation;
- The length of the model, being 2*a;
- The height of the web h_w in mm;
- The thickness of the web t_w in mm;
- The width of the flanges b_f in mm;
- The thickness of the flanges t_f in mm;
- The loading length s_s in mm;
- The patch load F in kN;
- The shear force V in kN.

By running the simulation, the displacements on each given time $(0.00 - 1.00)$ were obtained at the middle node. By multiplying the total force $(V + F)$ with the time, the force was determined and then compared with the results of the performed research.

The results of the verification can be found in the Annex C for both the SP 600 and the SP 1200 model. For the SP 600 model, a total force of 860 kN was applied (430 kN for V and 430 kN for F). For the SP 1200 model, a total force of 1040 kN was applied.

To obtain the effective total force, the total force applied on the model was multiplied by the time. These results were compared with the results mentioned in the same test report, which are shown in table 8.

Table 8: Comparison Ansys and tests

Specimen	Ansys result	Test result	Ratio [%]
SP 600	851.4	846	101
SP 1200	977.6	1030	95

As shown in table 8, the model for the SP 600 is a bit more resistant than the performed tests, while the SP 1200 model is less resistant. This needs to be considered for the upcoming simulations. The failure modes of both the SP 600 and the SP 1200 model are shown in figures 22 and 23.
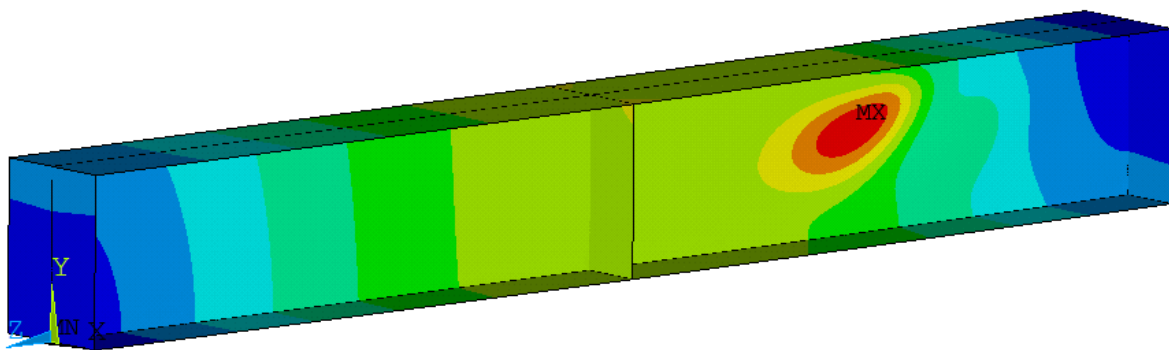
Figure 22: Failure mode SP 600 in Ansys Mechanical APDL
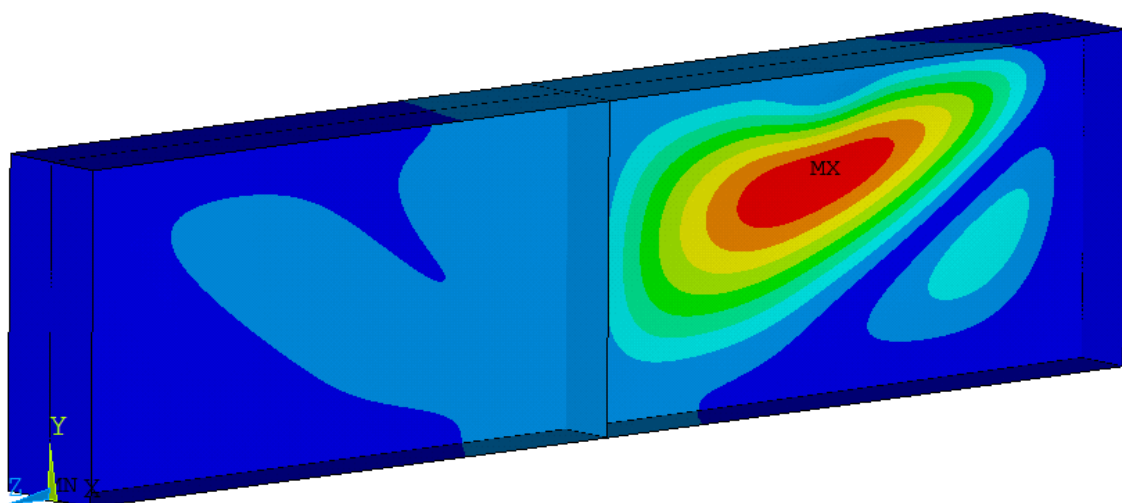
Figure 23: Failure mode SP 1200 in Ansys Mechanical APDL

As shown in figures 22 and 23, both models fail where the patch load F is applied. Due to the increase of the height of the web for the SP 1200 model, the failure mode is more severe than for the SP 600 model.

4 Parametric simulations

4.1 Numerical test design

For the further simulations different parameters were used. These parameters decide the class of the cross-section. The classification of the cross-sections was done by using the material strength ε and the ratio of width-thickness c/t using table 2 and 3, from paragraph 2.2.3.

For both the web and the flanges, a list of possible dimensions was obtained. The dimensions vary from 250 to 800 mm for the web height, 200 to 450 mm for the flange width and from 4 to 22 mm for the thickness of the flange and web. A clarification on the determination of the dimensions is shown in figure 24.
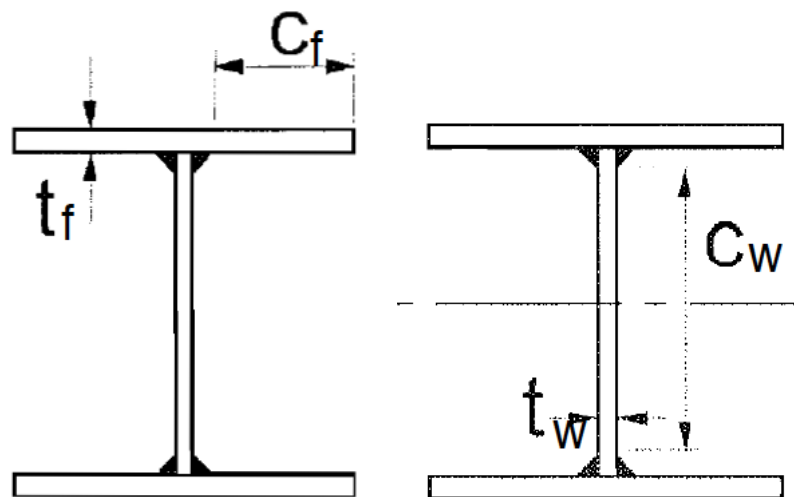
Figure 24: Clarification of dimensioning of test set-ups

The size of the welding of the plates is assumed to be the same as the web thickness, therefore the following formulas are used:

$$c_f = \frac{b_f - 3t_w}{2} \tag{8}$$

$$c_w = h - 2t_f - 2t_w \tag{9}$$

All these dimensions were cross-referenced and for every option, the class was calculated for both, the bending of the web and the compression of the flange. Based on this list, a few possibilities were chosen to conduct the numerical tests, each based on the minimum amount of material, thus smallest material area. For each combination of steel strengths two types of simulations took place: the first one had class 3 flanges and class 3 – 4 web, the second one had class 1 flanges and class 1 – 4 web. A visualization is shown in figure 25.
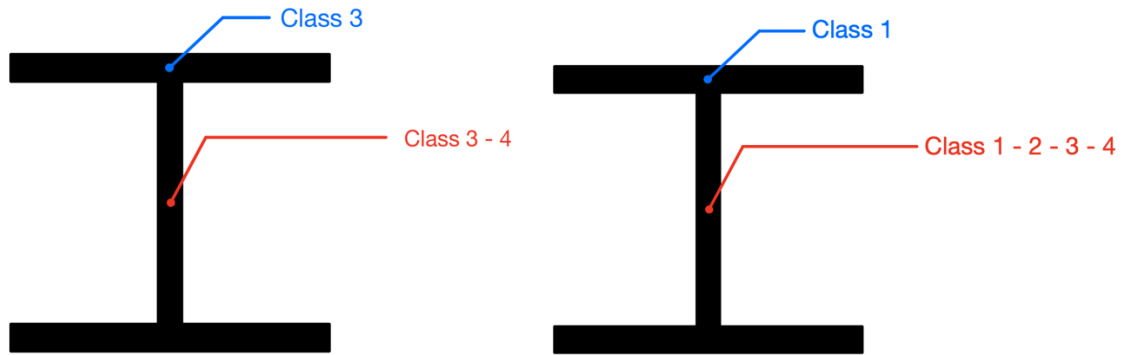
Figure 25: Two types of simulations, (a) First type (b) Second type

An overview of the possibilities for each web strength is given in tables 9, 10 and 11.

Table 9: Geometry and properties of chosen test set-ups for web S355

| test | flange | | | | web | | | |
	f_y [N/mm^2]	b_f [mm]	t_f [mm]	class	f_y [N/mm^2]	h_w [mm]	t_w [mm]	class
1	355	200	7	3	355	300	4	3
2	355	200	7	3	355	500	4	4
3	355	200	10	1	355	250	5	1
4	355	200	10	1	355	250	4	2
5	355	200	10	1	355	300	4	3
6	355	200	10	1	355	500	4	4
7	460	200	7	3	355	300	4	3
8	460	200	7	3	355	500	4	4
9	460	200	12	1	355	250	5	1
10	460	200	12	1	355	250	4	2
11	460	200	12	1	355	300	4	3
12	460	200	12	1	355	500	4	4
13	690	200	9	3	355	300	4	3
14	690	200	9	3	355	500	4	4
15	690	200	14	1	355	250	5	1
16	690	200	14	1	355	250	4	2
17	690	200	14	1	355	300	4	3
18	690	200	14	1	355	500	4	4
19	960	200	10	3	355	300	4	3
20	960	200	10	3	355	500	4	4
21	960	200	16	1	355	250	5	1
22	960	200	16	1	355	250	4	2
23	960	200	16	1	355	300	4	3
24	960	200	16	1	355	500	4	4

Table 10: Geometry and properties of chosen test set-ups for web S460

test	flange				web			
	f_y $[N/mm^2]$	b_f $[mm]$	t_f $[mm]$	class	f_y $[N/mm^2]$	b_w $[mm]$	t_w $[mm]$	class
25	460	200	7	3	460	250	4	3
26	460	200	7	3	460	400	4	4
27	460	200	12	1	460	250	5	1
28	460	200	12	1	460	300	5	2
29	460	200	12	1	460	250	4	3
30	460	200	12	1	460	400	4	4
31	690	200	9	3	460	250	4	3
32	690	200	9	3	460	400	4	4
33	690	200	14	1	460	250	5	1
34	690	200	14	1	460	300	5	2
35	690	200	14	1	460	250	4	3
36	690	200	14	1	460	400	4	4
37	960	200	10	3	460	250	4	3
38	960	200	10	3	460	400	4	4
39	960	200	16	1	460	250	5	1
40	960	200	16	1	460	300	5	2
41	960	200	16	1	460	250	4	3
42	960	200	16	1	460	400	4	4

Table 11: Geometry and properties of chosen test set-ups for web S690

test	flange				web			
	f_y $[N/mm^2]$	b_f $[mm]$	t_f $[mm]$	class	f_y $[N/mm^2]$	b_w $[mm]$	t_w $[mm]$	class
43	690	200	9	3	690	250	4	3
44	690	200	9	3	690	300	4	4
45	690	200	14	1	690	250	6	1
46	690	200	14	1	690	300	7	2
47	690	200	14	1	690	250	4	3
48	690	200	14	1	690	300	4	4
49	960	200	10	3	690	250	4	3
50	960	200	10	3	690	300	4	4
51	960	200	16	1	690	250	6	1
52	960	200	16	1	690	300	7	2
53	960	200	16	1	690	250	4	3
54	960	200	16	1	690	300	4	4

Regarding these steel grades, the yield strength and ultimate strength values were used from paragraph 2.4.5 in the literature review, for the simulations in Ansys. All the elements are thinner than 40 mm which results in the use of the associated values, which are shown in table 12.

Table 12: Strain - stress values for the used steel grades

Steel grade	f_y $[N/mm^2]$	f_u $[N/mm^2]$	Element
S355	355	490	For web, flanges and stiffeners
S460	460	540	For web, flanges and stiffeners
S690	690	770	For web, flanges and stiffeners
S960	960	1056	For web, flanges and stiffeners

The ultimate strength for S960 in table 12, was chosen to be equal to the yield strength multiplied by a factor 1.1 due to insufficient information in the Eurocode.

4.2 M-V interaction model

After the verification, the hand calculations (see chapter 5) and deciding which simulations to perform, a second model was created based on the verified numerical model to perform the bending moment and shear force interaction simulations.

4.2.1 General information

The parameters of this model are the same as the verified model, except the following:

- The length of the model becomes $2h_w$;
- Loading on the girder;
- Boundary conditions;
- Adjusted local imperfection.

In figure 26, a sketch is shown of the model with the mentioned changes.
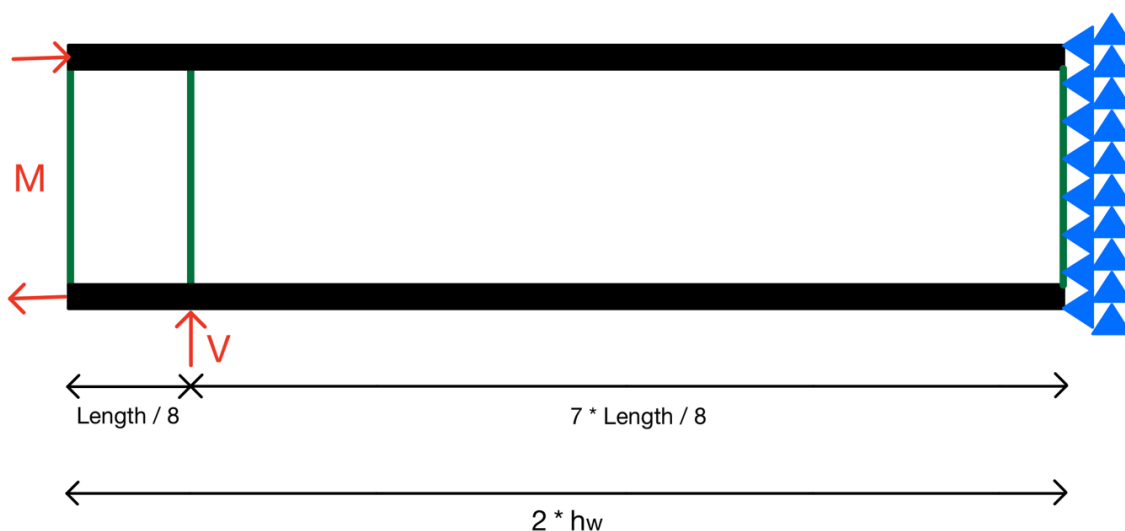
Figure 26: Sketch M-V interaction model

As shown in figure 26, two rows of forces were applied on the left flange in opposite directions to create the bending moment. The bending moment was applied in the software as a force in kN. The bending moment is determined as follows:

$$Bending\ moment = applied\ force\ on\ one\ side \cdot height\ of\ the\ web$$

In the model, the applied force was divided by the number of nodes along the top and along the bottom of the left flange. This means that the force was applied on both the top and the bottom of the left flange. For example, when a force of 2000 kN was applied for the bending moment, a force of 2000 kN was divided on the top flange, and a force of 2000 kN was divided on the bottom flange. For example, the bending moment that is created with a force of 2000 kN on the SP 600 model, is:

$$M = 2000 \, kN \cdot 0.6 \, m = 1200 \, kNm$$

The shear force was applied over the full width of the extra stiffener, placed over a distance $L/8$ away from the first stiffener.

This extra stiffener and the supports along the full length of the top and bottom flange, which is shown in figure 27, were added to the model to obtain the correct failure mode. The specifications of the stiffeners are the same as for the verification of the model. On the right side of the model, a fixed support was created along the right flange to restrain the rotations in all directions. The SP 600 model with the boundary conditions and applied loads is shown in figure 27.
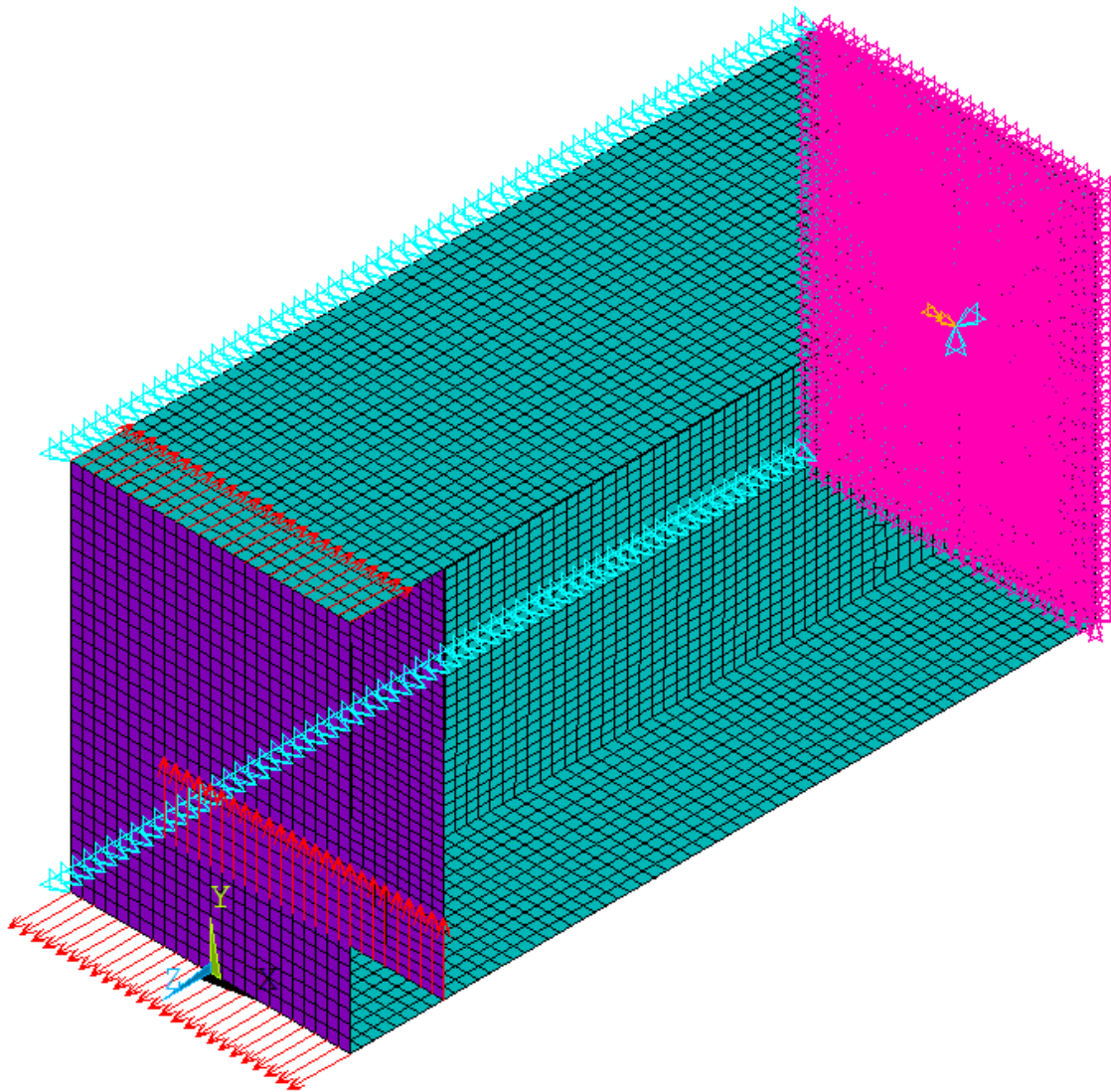
Figure 27: SP 600 M-V interaction model with applied loads and shown boundary conditions in Ansys Mechanical APDL

4.2.2 Applied imperfection for the M-V interaction model

The local imperfection was adjusted so it is applicable for this model. The imperfection needed to match with the imperfection which is explained in figure 7 for a local panel or subpanel, resulting in a buckling shape. The visualization of the imperfection of the web in Ansys is shown in figure 28, this figure was obtained by amplifying the imperfection by 100 times and increasing the mesh size by 20 times.
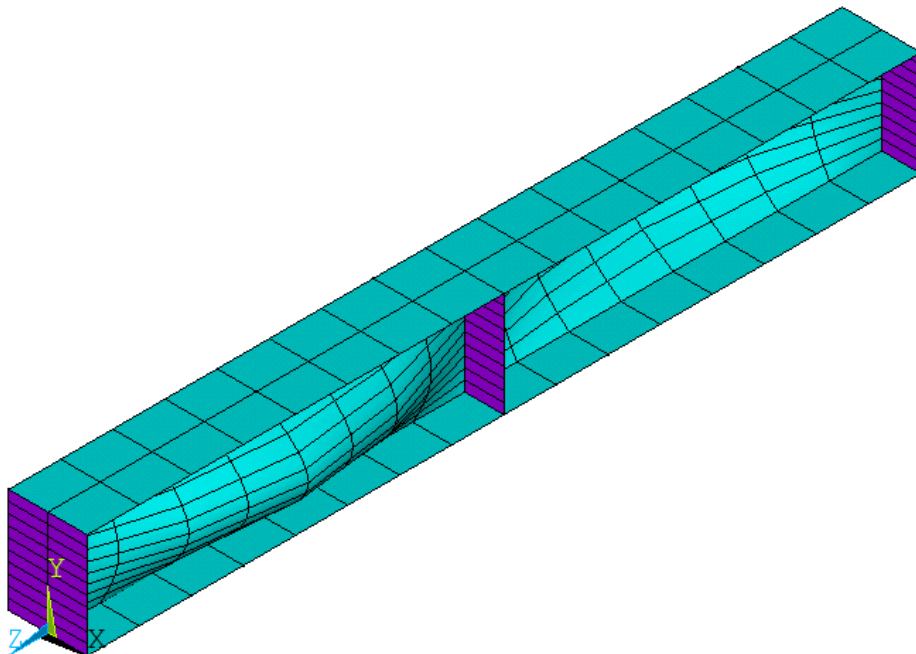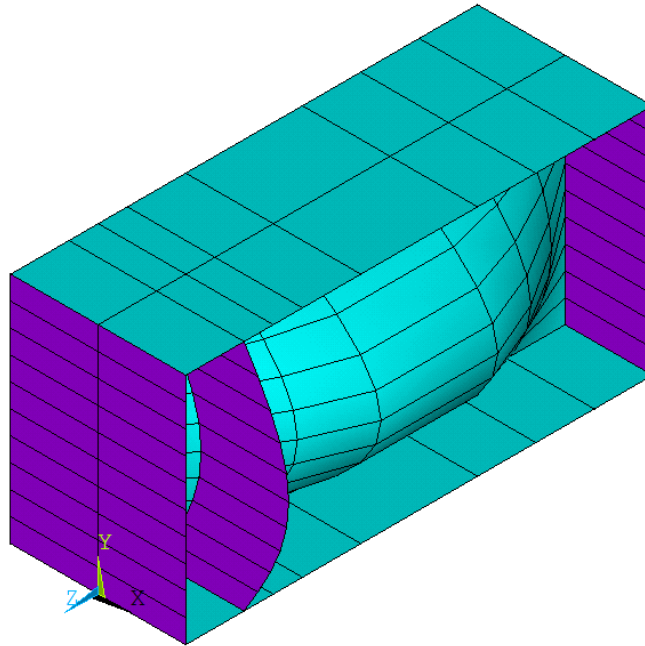

Figure 28: Amplified imperfection for the SP 600 model in Ansys Mechanical APDL

4.2.3 Bending moment and shear force interaction for the simulations

For all the simulations listed in chapter 4, a bending moment and shear force interaction was performed. In paragraph 2.3.3 of the literature review, this interaction is explained. For all the 54 simulations, five points were calculated with a different shear force and bending moment value. For clarification, the five investigated points of the shear and bending interaction graph are shown in figure 29.
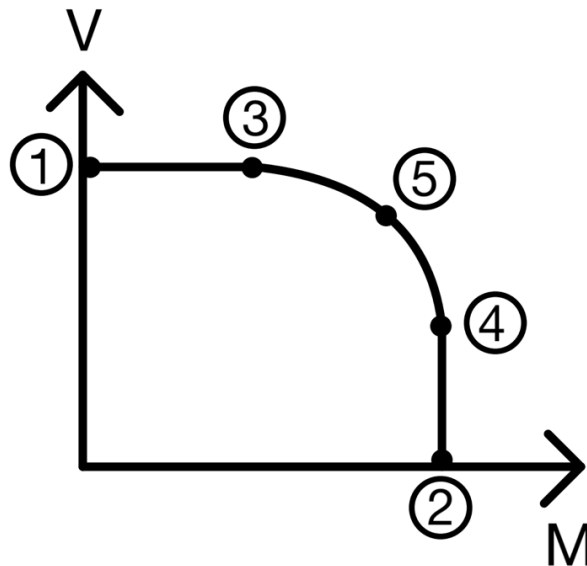
Figure 29: Order of simulations for the bending moment and shear force interaction

The first and second point are respectively the pure bending and pure shear analysis. These simulations are compared with the hand calculated values from chapter 5. The third point is performed with the maximum bending moment and half of the maximum shear force value.

The fourth point is performed with the maximum shear force and half of the maximum bending moment value. The fifth and final point, is performed with 0.8 of both the maximum shear force and maximum bending moment.

To be able to consider the interaction, the bending moment and shear force values are determined at a length h_w from the right flange. This means at half of the length of the model, due to the total length of the model being $2h_w$. These values were obtained through coding parameters that determine these values on this specific location for the linear analysis.

The code for these bending moment and shear force interactions can be found in the Annex D, the code used for the bending moment and shear force at a length of h_w can be found at the end of the code. To perform these interactions in *Ansys Mechanical APDL* the following line of code is used:

$$Interaction,' Sp1200', 2400, 1200, 6, 450, 20, 200, M, V$$

The parameters of this piece of code consist of:

- The name of the macro function which creates the model;
- The name of the simulation;
- The length of the model, being $2h_w$;
- The height of the web h_w in mm;
- The thickness of the web t_w in mm;
- The width of the flanges b_f in mm;
- The thickness of the flanges t_f in mm;
- The loading length s_s in mm;

- The force which creates the bending moment in kN;
- The shear force V in kN.

The failure modes of both the pure bending moment and the pure shear force are shown in figures 30 and 31 for the SP 600 model.
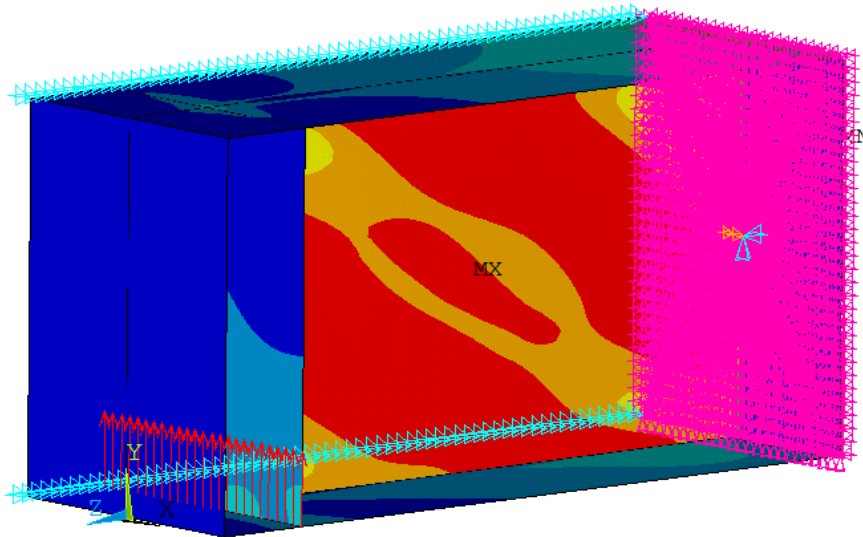
Figure 30: Failure pure shear force - SP 600 in Ansys Mechanical APDL
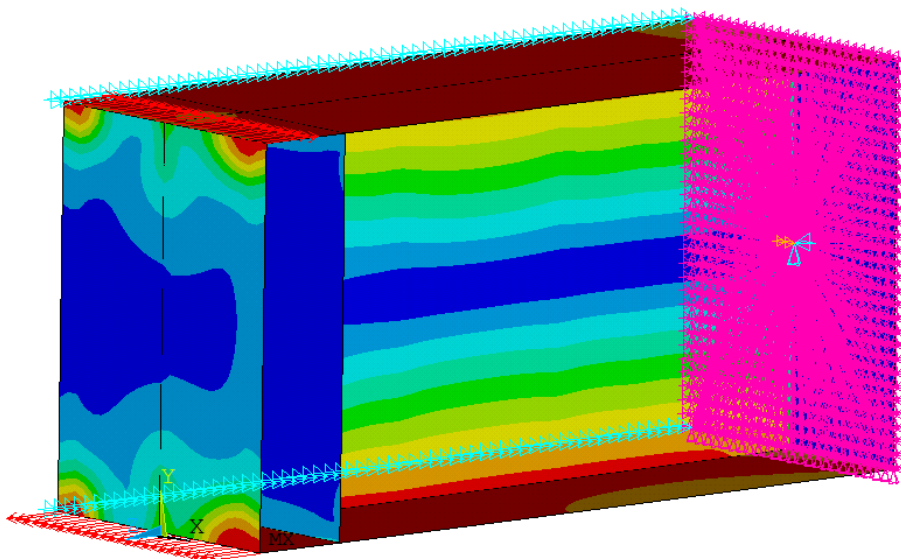
Figure 31: Failure pure bending moment - SP 600 in Ansys Mechanical APDL

As shown in figure 30, when applying only a shear force, it results in the failure of the web. The stress is distributed along the full web. Figure 31 shows that the failure will occur in the flanges when only applying a bending moment.

5 Bending and shear resistance based on Eurocode 3

5.1 General

For the Eurocode analysis the geometry and properties of the girder are analyzed first. Next, the material strengths and moments of inertia are calculated. Afterwards, a classification of web and flanges takes place, if not already decided. The bending resistance is calculated using the formulas from EN 1993-1-1 [9, 6.2.5] and the shear resistance, taking shear buckling into consideration, is calculated using the formulas from EN 1993-1-5 for plated materials [12, 7]. Both are calculated for the characteristic value, so without safety factors. These values are needed to compare with the resistances determined with Ansys. An important remark for the values determined with Eurocode is that the patch loading is neglected in these calculations. The SP 600 and SP 1200 models are first calculated as examples.

5.2 Bending and shear resistance for SP 600

5.2.1 Geometry

For the geometry of the SP 600 model, the dimensions are used from the COMBRI Test Report [15, 1.2], which is shown in figure 32. The total height of this girder is $h = 640\ mm$.
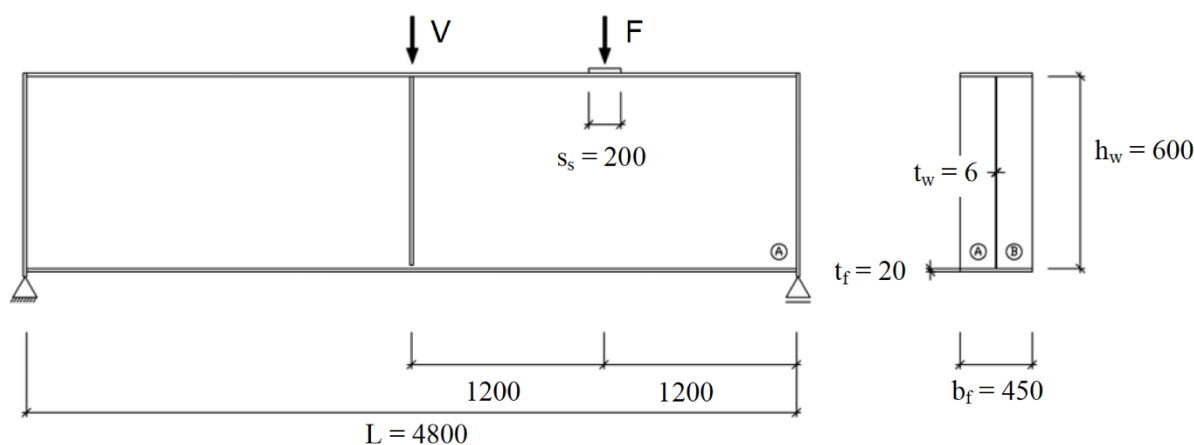
Figure 32: Geometry of verified model SP 600

5.2.2 Properties

The steel type used for the verification of the model is S355, for the yield and material strength this means:

$$f_y = 355 \, MPa \text{ and } \varepsilon = \sqrt{235/f_y} = \sqrt{235/355} = 0.81$$

The moment of inertia around the strong axis becomes:

$$I_y = \frac{b_f \cdot h^3}{12} - 2 \cdot \frac{c_f \cdot h_w^3}{12} = \frac{450 \cdot 640^3}{12} - 2 \cdot \frac{222 \cdot 600^3}{12} = 1.84 \cdot 10^9 \, mm^4$$

5.2.3 Classification

For the classification [9, 5.5] of the welded girder, the assumption is made that the welding itself has the dimensions of t_w x t_w, thus in this case: 6 mm x 6 mm. For the compression on the flange this means:

$$c_f = \frac{b_f - 3 \cdot t_w}{2} = \frac{450 - 3 \cdot 6}{2} = 216 \, mm$$

$$\frac{c_f}{t_f} = \frac{216}{20} = 10.8 \leq 14 \cdot \varepsilon = 11.3 \rightarrow \text{class 3}$$

For the bending of the web this means:

$$c_w = h_w - 2 \cdot t_w = 600 - 2 \cdot 6 = 588 \, mm$$

$$\frac{c_w}{t_w} = \frac{588}{6} = 98.0 \leq 124 \cdot \varepsilon = 100.4 \rightarrow \text{class 3}$$

This means that both the flange and the web belong to class 3. This is important for the calculation of the bending resistance.

5.2.4 Bending resistance

For the bending resistance, formulas from part 1 of Eurocode 3 are used. Because the cross-section belongs to class 3, the calculation of the bending resistance must take place using the elastic bending modulus, which corresponds to the fiber with the maximum elastic stress, thus the outer fiber.

$$W_{el,min} = \frac{I_y}{h/2} = \frac{1.84 \cdot 10^9}{640/2} = 5.75 \cdot 10^6 \, mm^3$$

For the characteristic value of the elastic bending resistance this means:

$$M_{el,Rk} = W_{el,min} \cdot f_y = 5.75 \cdot 10^6 \cdot 355 = 2.04 \cdot 10^9 \, Nmm = 2041 \, kNm$$

5.2.5 Shear resistance

Shear buckling verification

Before the shear resistance is calculated, shear buckling should be taken in consideration. For unstiffened webs this means:

$$\frac{h_w}{t_w} = \frac{600}{6} = 100 > \frac{72 \cdot \varepsilon}{\eta} = \frac{72 \cdot 0.81}{1.20} = 48.6$$

Where η is considered 1.20 for steel types under S460 and 1.00 for higher steel types. In this case the shear buckling is relevant because the ratio of web height and thickness is bigger than the reference value. This means the girder needs transverse stiffeners at the supports and needs to be considered rigid.

Shear resistance

The design resistance for shear is based on only the contribution of the web, first the modified slenderness $\bar{\lambda}_w$ is considered for rigid end posts.

$$\bar{\lambda}_w = \frac{h_w}{86.4 \cdot t_w \cdot \varepsilon} = \frac{600}{86.4 \cdot 6 \cdot 0.81} = 1.43$$

If the modified slenderness is higher than 1.08, the reduction factor χ_w that is needed for the contribution of the web becomes depended on the rigid value.

$$\chi_w = \frac{1.37}{0.7 + \bar{\lambda}_w} = \frac{1.37}{0.7 + 1.43} = 0.64$$

For the characteristic value of the shear resistance this means:

$$V_{bw,Rk} = \frac{\chi_w \cdot f_{yw} \cdot h_w \cdot t_w}{\sqrt{3}} = \frac{0.64 \cdot 355 \cdot 600 \cdot 6}{\sqrt{3}} = 472\,226\ N = 472\ kN$$

An overview of the bending and shear resistance for the verified model SP 600 are given in table 13.

Table 13: Bending and shear resistance for homogeneous SP 600 girder

test	f_y [MPa]	b_f [mm]	t_f [mm]	h_w [mm]	t_w [mm]	h [mm]	$M_{el,Rk}$ [kNm]	$V_{bw,Rk}$ [kN]
SP 600	355	450	20	600	6	640	2041	472

5.3 Bending and shear resistance for SP 1200

5.3.1 Geometry

For the geometry of the verified model with reference SP 1200 the dimensions are used from the COMBRI Test Report [15, 1.2], which is shown in figure 33.
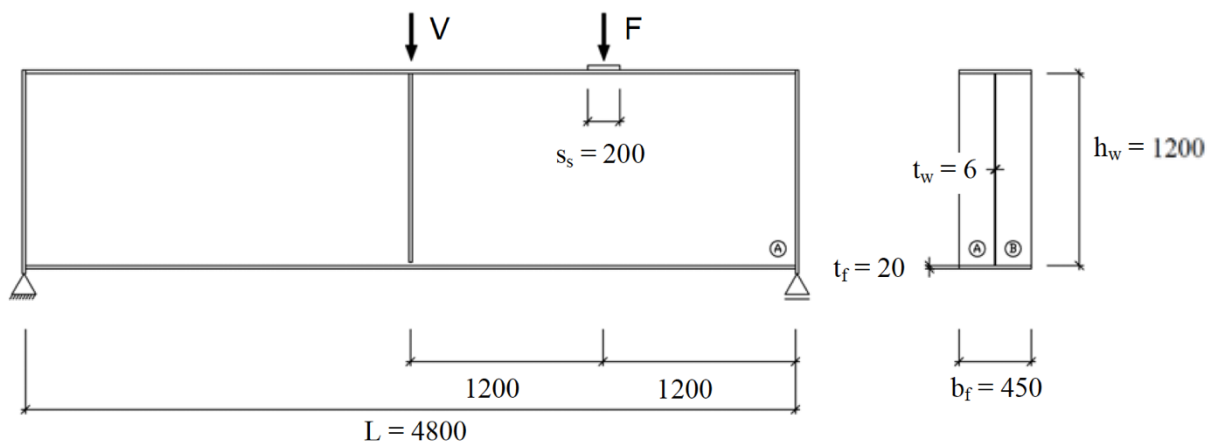
Figure 33: Geometry of verified model SP 1200

5.3.2 Properties

The steel type used for the verification of the model is S355, this means:

$f_y = 355\ MPa$ and $\varepsilon = \sqrt{235/f_y} = \sqrt{235/355} = 0.81$

5.3.3 Classification

For the compression on the flange this means:

$$c_f = \frac{b_f - 3 \cdot t_w}{2} = \frac{450 - 3 \cdot 6}{2} = 216\ mm$$

$\frac{c_f}{t_f} = \frac{216}{20} = 10.8 \le 14 \cdot \varepsilon = 11.3 \rightarrow$ class 3

For the bending of the web this means:

$$c_w = h_w - 2 \cdot t_w = 1200 - 2 \cdot 6 = 1188\ mm$$

$\frac{c_w}{t_w} = \frac{1188}{6} = 198.0 > 124 \cdot \varepsilon = 100.4 \rightarrow$ class 4

This determines that the flange belongs to class 3 and the web to class 4. This is important for the calculation of the bending resistance since, the highest and thus least favorable, class is crucial for this calculation.

5.3.4 Effective height

Because the web belongs to class 4, a calculation is required to obtain the effective height of the web because a part of the effectiveness is lost due to local buckling. It is assumed that the stress on the upper side of the web is the same as the lower part, thus $\sigma_1 = \sigma_2$, this means that $\psi = -\frac{\sigma_1}{\sigma_2} = -1$. Which indicates that the buckling factor is $k_\sigma = 23,9$, according to EN1993-1-5 [12, 4.4].

First the slenderness is calculated.

$$\overline{\lambda_p} = \frac{h_w/t_w}{28.4\varepsilon\sqrt{k_\sigma}} = \frac{1200/6}{28.4 \cdot 0.81 \cdot \sqrt{23.9}} = 1.78$$

For internal compression parts, EN 1993-1-5 mentions following formulas for the determination of the reduction factor. For the slenderness:

$$\text{If } \overline{\lambda_p} = 1.78 > 0.5 + \sqrt{0.085 - 0.055\psi} = 0.5 + \sqrt{0.085 + 0.055} = 0.87$$

$$\text{then } \rho = \frac{\overline{\lambda_p} - 0.055(3+\psi)}{\overline{\lambda_p}^2} = \frac{1.78 - 0.055(3+1)}{4.35^2} = 0.94$$

Which means that for the effective height of the web, because $\psi = -1$, only the part that is under compression is considered, which is $h_w/2$. The reduction factor ρ is therefore multiplied by the compression part and this will symbolize the loss of effectiveness due to local buckling.

$$h_{c,eff} = \rho \cdot \frac{h_w}{2} = 0.94 \cdot \frac{1200}{2} = 564 \ mm$$

This means the total effective height of the web is the tension part added to the effective compression height.

$$h_{w,eff} = h_{c,eff} + \frac{h_w}{2} = 564 + \frac{1200}{2} = 1164 \ mm$$

Therefore, the total effective height will become:

$$h_{eff} = h_{w,eff} + 2 \cdot t_f = 1164 + 2 \cdot 20 = 1204 \ mm$$

5.3.5 Bending resistance

Because the cross-section belongs to class 4 due to the web, the calculation of the bending resistance must take place using the effective bending modulus, which corresponds to the fiber with the maximum elastic stress, thus the outer fiber. Knowing the effective width, the effective moment of inertia can be calculated first.

$$I_{y,eff} = \frac{b_f \cdot h_{eff}^3}{12} - 2 \cdot \frac{c_f \cdot h_{w,eff}^3}{12} = \frac{450 \cdot 1204^3}{12} - 2 \cdot \frac{222 \cdot 1164^3}{12} = 7.09 \cdot 10^9 \; mm^4$$

When working with cross sections of class 4, it is important to consider the change of the position of the neutral axis. The neutral axis divides the amount of material equally, but because of the loss in height, the neutral axis moves. In this case the neutral axis moves 18 mm down. This influences the bending modulus.

$$W_{eff,min} = \frac{I_y}{z} = \frac{7.09 \cdot 10^9}{\frac{h_w}{2} - 18} = 1.18 \cdot 10^7 \; mm^3$$

For the elastic bending resistance this means:

$$M_{eff,Rk} = W_{eff,min} \cdot f_y = 1.18 \cdot 10^7 \cdot 355 = 4.19 \cdot 10^9 \; Nmm = 4185 \; kNm$$

5.3.6 Shear resistance

Shear buckling

First, shear buckling should be taken in consideration. For unstiffened webs:

$$\frac{h_{w,eff}}{t_w} = \frac{1164}{6} = 194 > \frac{72 \cdot \varepsilon}{\eta} = \frac{72 \cdot 0.81}{1.20} = 48.6$$

Where η is considered 1.20 for steel types under S460. In this case the girder needs transverse stiffeners at the supports, which makes the girder considered rigid.

Shear resistance

The design resistance for shear is based on the contribution of the web, first the modified slenderness $\bar{\lambda}_w$ is determined:

$$\bar{\lambda}_w = \frac{h_{w,eff}}{86.4 \cdot t_w \cdot \varepsilon} = \frac{1164}{86.4 \cdot 6 \cdot 0.81} = 2.77$$

If the modified slenderness is a value bigger than 1.08, the reduction factor χ_w that is needed for the contribution of the web becomes depended on the rigid value:

$$\chi_w = \frac{1.37}{0{,}7 + \bar{\lambda}_w} = \frac{1.37}{0.7 + 2.77} = 0.40$$

For the shear resistance this means:

$$V_{b,Rk} = V_{bw,Rk} = \frac{\chi_w \cdot f_{yw} \cdot h_{w,eff} \cdot t_w}{\sqrt{3}} = \frac{0.40 \cdot 355 \cdot 1164 \cdot 6}{\sqrt{3}} = 572\,574\,N = 573\,kN$$

An overview of the bending and shear resistance for the verified model SP 1200 are given in table 14.

Table 14: Bending and shear resistance for homogeneous SP 1200 girder

test	f_y [MPa]	b_f [mm]	t_f [mm]	h_w [mm]	t_w [mm]	h [mm]	$M_{el,Rk}$ [kNm]	$V_{bw,Rk}$ [kN]
SP 600	355	450	20	600	6	640	2041	472

5.4 Bending and shear resistance for cross-section of class 1 or 2

In this paragraph, an example calculation is written down for a cross-section of which the highest class, thus the least favorable, is either a class 1 or 2. The plastic modulus is used for the calculation of the bending resistance. For the homogeneous girder test case 3 is used as example and for the hybrid girder test case 9.

5.4.1 Bending resistance of homogeneous girder

The first step is to determine the location of the neutral axis. The neutral axis divides the girder in two equal areas. Because the girders in this thesis are symmetrical and there is no loss in effectiveness (see class 4), the neutral axis is located at $h_w/2$. This is the case for all girder except class 4. A simple clarification of the figure is shown in figure 34.

The properties of test case 3 are:

- $f_{yw} = f_{yf} = 355\ MPa$
- $b_f = 200\ mm$
- $t_f = 10\ mm$
- $h_w = 250\ mm$
- $t_w = 5\ mm$
- $h = 270\ mm$
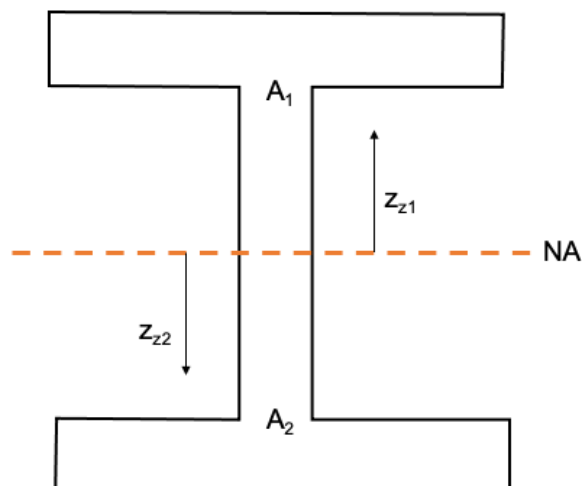
Figure 34: Homogeneous girder of class 1 or 2

The next step is to calculate the areas A_1 and A_2. Because of symmetry they are equal.

$$A_1 = A_2 = b_f \cdot t_f + \frac{h_w}{2} \cdot t_w = 200 \cdot 10 + \frac{250}{2} \cdot 5 = 2625\ mm^2$$

These areas are needed to determine the compression force in the upper part and the tension force in the lower part. Again, because of symmetry they are equal but opposite.

$$F_t = F_c = A_1 \cdot f_y = A_2 \cdot f_y = 2625 \cdot 355 \cdot 10^{-3} = 932\ kN$$

Next, the center of gravity in each area is determined. The distance from the neutral axis to this point, is the same for both areas because of the symmetrical girder. This means:

$$z_{z1} = z_{z2} = \frac{\sum z_{zi} A_i}{A_1} = \frac{\left(\frac{h_w}{2} + \frac{t_f}{2}\right) b_f t_f + \frac{h_w}{8} t_w}{b_f t_f + \frac{h_w}{2} t_w} = \frac{\left(\frac{250}{2} + \frac{10}{2}\right) 200 \cdot 10 + \frac{250}{8} \cdot 5}{200 \cdot 10 + \frac{250}{2} \cdot 5} = 99\ mm$$

This means for distance d, which is needed for the bending resistance:

$$d = z_{z1} + z_{z2} = 99 + 99 = 198\ mm$$

For the characteristic value of the plastic bending resistance this results in:

$$M_{pl,Rk} = F_c \cdot d = F_t \cdot d = 932 \cdot 198 \cdot 10^{-3} = 185\ kNm$$

The other plastic bending resistances of the homogeneous girders cross-section class 1 or 2 are given in table 15.

Table 15: Plastic bending resistances for homogeneous girders of class 1 or 2

test	f_{yf} [MPa]	b_f [mm]	t_f [mm]	f_{yw} [MPa]	h_w [mm]	t_w [mm]	h [mm]	$M_{pl,Rk}$ [kNm]
3	355	200	10	355	250	5	270	185
4	355	200	10	355	250	4	270	185
27	460	200	12	460	250	5	274	289
28	460	200	12	460	300	5	324	345
45	690	200	14	690	250	6	278	510
46	690	200	14	690	300	7	328	607

5.4.2 Bending resistance of hybrid girder

The properties of hybrid test case 9 are:

- $f_{yf} = 460\ MPa$
- $b_f = 200\ mm$
- $t_f = 12\ mm$
- $f_{yw} = 355\ MPa$
- $h_w = 250\ mm$
- $t_w = 5\ mm$
- $h = 274\ mm$

A clarification of the parameters to use in the calculation of a hybrid cross-section of class 1 or 2 is shown in figure 35.
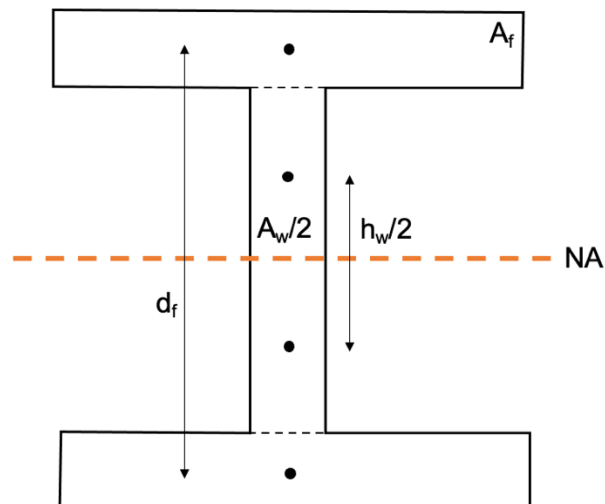
Figure 35: Hybrid girder of class 1 or 2

For the hybrid girder, the areas of the upper flange and upper part of the web are calculated.

$$A_f = b_f \cdot t_f = 200 \cdot 12 = 2400\ mm^2$$

$$\frac{A_w}{2} = \frac{t_w \cdot h_w}{2} = \frac{5 \cdot 250}{2} = 625\ mm^2$$

To calculate the plastic bending resistance, the distance between the centers of gravity is needed, for both the flanges d_f and the web $h_f/2$.

$$d_f = h_w + t_f = 250 + 12 = 262\ mm$$

$$\frac{h_w}{2} = \frac{250}{2} = 125\ mm$$

For the characteristic value of the plastic bending resistance this means:

$$M_{pl,Rk} = \frac{A_w}{2} f_{yw} \frac{h_w}{2} + A_f f_{yf} d_f = [625 \cdot 355 \cdot 125 + 2400 \cdot 460 \cdot 262] \cdot 10^{-6} = 317\ kNm$$

The other plastic bending resistances of the homogeneous girders cross-section class 1 or 2 are given in table 16.

Table 16: Plastic bending resistances for hybrid girders of class 1 or 2

test	f_{yf} [MPa]	b_f [mm]	t_f [mm]	f_{yw} [MPa]	h_w [mm]	t_w [mm]	h [mm]	$M_{pl,Rk}$ [kNm]
9	460	200	12	355	250	5	274	317
10	460	200	12	355	250	4	274	311
15	690	200	14	355	250	5	278	538
16	690	200	14	355	250	4	278	532
21	960	200	16	355	250	5	282	845
22	960	200	16	355	250	4	282	839
33	690	200	14	460	250	5	278	546
34	690	200	14	460	300	5	328	658
39	960	200	16	460	250	5	282	853
40	960	200	16	460	300	5	332	1023
51	960	200	16	690	250	6	282	882
52	960	200	16	690	300	7	332	1079

5.4.3 Shear resistance

The shear resistance calculations are identical to the calculation used in SP 600 girder, which can be found in paragraph 5.2.5. The overview of these values is given in table 17.

Table 17: Shear resistances of girder of class 1 or 2

test	f_{yf} [MPa]	b_f [mm]	t_f [mm]	f_{yw} [MPa]	h_w [mm]	t_w [mm]	h [mm]	$V_{bw,Rk}$ [kN]
3	355	200	10	355	250	5	270	299
4	355	200	10	355	250	4	270	191
9	460	200	12	355	250	5	274	299
10	460	200	12	355	250	4	274	191
15	690	200	14	355	250	5	278	299
16	690	200	14	355	250	4	278	191
21	960	200	16	355	250	5	282	299
22	960	200	16	355	250	4	282	191
27	460	200	12	460	250	5	274	299
28	460	200	12	460	300	5	324	191
33	690	200	14	460	250	5	278	340
34	690	200	14	460	300	5	328	340
39	960	200	16	460	250	5	282	340
40	960	200	16	460	300	5	332	340
45	690	200	14	690	250	6	278	600
46	690	200	14	690	300	7	328	817
51	960	200	16	690	250	6	282	600
52	960	200	16	690	300	7	332	817

5.5 Bending and shear resistance for cross-section of class 3

In this paragraph, an example calculation is written down for a cross-section of which the highest class, thus the least favorable, is a class 3. The elastic modulus is used for the calculation of the bending resistance. For the homogeneous girder, test case 25 is used as example and for the hybrid girder test case 13.

5.5.1 Bending resistance of homogeneous girder

The properties of test case 25 are:

- $f_{yf} = f_{yw} = 460\ MPa$
- $b_f = 200\ mm$
- $t_f = 7\ mm$
- $h_w = 250\ mm$
- $t_w = 4\ mm$
- $h = 264\ mm$

First, the moment of inertia needs to be calculated around the strong axis y.

$$I_y = \frac{b_f \cdot h^3}{12} - 2 \cdot \frac{c_f \cdot h_w^3}{12} = \frac{200 \cdot 264^3}{12} - 2 \cdot \frac{98 \cdot 250^3}{12} = 5.15 \cdot 10^7\ mm^4$$

The next step is to determine the elastic bending modulus, which corresponds to the fiber with the highest elastic stress, thus the outer fiber. Since the girder is symmetrical, the neutral axis lies in the middle of the girder, thus the distance from the neutral axis to the outer fiber is $h/2$.

$$W_{el,min} = \frac{I_y}{h/2} = \frac{5.15 \cdot 10^7}{264/2} = 3.90 \cdot 10^5\ mm^3$$

For the characteristic value of the elastic bending resistance this means:

$$M_{el,Rk} = W_{el,min} \cdot f_y = 3.90 \cdot 10^5 \cdot 460 \cdot 10^{-6} = 179\ kNm$$

The other elastic bending resistances of homogeneous girders cross-section class 3 are given in table 18.

Table 18: Elastic bending resistances of homogeneous girders of class 3

test	f_{yf} [MPa]	b_f [mm]	t_f [mm]	f_{yw} [MPa]	h_w [mm]	t_w [mm]	h [mm]	$M_{el,Rk}$ [kNm]
1	355	200	7	355	300	4	314	170
5	355	200	10	355	300	4	320	233
25	460	200	7	460	250	4	264	179
29	460	200	12	460	250	4	274	294
43	690	200	9	690	250	4	268	338
47	690	200	14	690	250	4	278	511

5.5.2 Bending resistance of hybrid girder

The properties of test case 13 are:

- $f_{yf} = 690\ MPa$
- $b_f = 200\ mm$
- $t_f = 9\ mm$
- $f_{yw} = 355\ MPa$
- $h_w = 300\ mm$
- $t_w = 4\ mm$
- $h = 318\ mm$

First, the moment of inertia needs to be calculated around the strong axis y.

$$I_y = \frac{b_f \cdot h^3}{12} - 2 \cdot \frac{c_f \cdot h_w^3}{12} = \frac{200 \cdot 318^3}{12} - 2 \cdot \frac{98 \cdot 300^3}{12} = 9.50 \cdot 10^7\ mm^4$$

The next step is to determine the elastic bending modulus for the flange and web separately. The bending resistance is also calculated separately. So, for the flange it means that the distance from the neutral axis to the outer fiber is the whole height of the girder divided by two.

$$W_{f,el,min} = \frac{I_y}{h/2} = \frac{9.50 \cdot 10^7}{318/2} = 5.97 \cdot 10^5\ mm^3$$

For the characteristic value of the elastic bending resistance of the flange this means:

$$M_{f,el,Rk} = W_{f,el,min} \cdot f_{yf} = 5.98 \cdot 10^5 \cdot 690 \cdot 10^{-6} = 412\ kNm$$

For the web, the distance between the neutral axis and the outer fiber is the height of the web divided by two.

$$W_{w,el,min} = \frac{I_y}{h_w/2} = \frac{9.50 \cdot 10^7}{300/2} = 6.33 \cdot 10^5\ mm^3$$

For the characteristic value of the elastic bending resistance of the web this means:

$$M_{w,el,Rk} = W_{w,el,min} \cdot f_{yw} = 6.33 \cdot 10^5 \cdot 355 \cdot 10^{-6} = 225\ kNm$$

To obtain the elastic bending moment of the whole girder the minimum of both values needs to be chosen, because the girder fails when it reaches the first value of bending resistance.

$$M_{el,min} = min[M_{f,el,Rk}; M_{w,el,Rk}] = min[412; 225] = 225\ kNm$$

The other elastic bending resistances of hybrid girders cross-section class 3 are given in table 19.

Table 19: Elastic bending resistances of hybrid girders of class 3

test	f_{yf} [MPa]	b_f [mm]	t_f [mm]	f_{yw} [MPa]	h_w [mm]	t_w [mm]	h [mm]	$M_{el,Rk}$ [kNm]
7	460	200	7	355	300	4	314	177
11	460	200	12	355	300	4	324	298
13	690	200	9	355	300	4	318	225
17	690	200	14	355	300	4	328	348
19	960	200	10	355	300	4	320	249
23	960	200	16	355	300	4	332	400
31	690	200	9	460	250	4	268	241
35	690	200	14	460	250	4	278	379
37	960	200	10	460	250	4	270	268
41	960	200	16	460	250	4	282	436
49	960	200	10	690	250	4	270	402
53	960	200	16	690	250	4	282	654

5.5.3 Shear resistance

The shear resistance calculations are identical to the calculation used in SP 600 girder, which can be found in paragraph 5.2.5. The overview of these values is given in table 20.

Table 20: Shear resistances of girders of class 3

test	f_{yf} [MPa]	b_f [mm]	t_f [mm]	f_{yw} [MPa]	h_w [mm]	t_w [mm]	h [mm]	$V_{bw,Rk}$ [kN]
1	355	200	7	355	300	4	314	191
5	355	200	10	355	300	4	320	191
7	460	200	7	355	300	4	314	191
11	460	200	12	355	300	4	324	191
13	690	200	9	355	300	4	318	191
17	690	200	14	355	300	4	328	191
19	960	200	10	355	300	4	320	191
23	960	200	16	355	300	4	332	191
25	460	200	7	460	250	4	264	218
29	460	200	12	460	250	4	274	218
31	690	200	9	460	250	4	268	218
35	690	200	14	460	250	4	278	218
37	960	200	10	460	250	4	270	218
41	960	200	16	460	250	4	282	218
43	690	200	9	690	250	4	268	281
47	690	200	14	690	250	4	278	281
49	960	200	10	690	250	4	270	281
53	960	200	16	690	250	4	282	281

5.6 Bending and shear resistance for cross-section of class 4

In this paragraph, an example calculation is written down for a cross-section of which the highest class, thus the least favorable, is a class 4. For the calculation of the bending resistance the effective height is used, due to loss of effectiveness. For the homogeneous girder, test case 44 is used as example and for the hybrid girder test case 18.

5.6.1 Bending resistance of homogeneous girder

The properties of test case 44 are:

- $f_{yf} = f_{yw} = 690 \ MPa$
- $b_f = 200 \ mm$
- $t_f = 9 \ mm$
- $h_w = 300 \ mm$
- $t_w = 4 \ mm$
- $h = 318 \ mm$

Effective height

First, a calculation needs to happen to obtain the effective height of the web because a part of the effectiveness is lost due to local buckling. It is assumed that the stress on the upper side of the web is the same as the lower part, this means that $\psi = -1$. Which indicates that the buckling factor is $k_\sigma = 23{,}9$.

First the slenderness is calculated.

$$\overline{\lambda_p} = \frac{h_w/t_w}{28.4\varepsilon\sqrt{k_\sigma}} = \frac{300/4}{28.4 \cdot \sqrt{\frac{235}{690}} \cdot \sqrt{23.9}} = 0.93$$

For the slenderness:

$$\text{If } \overline{\lambda_p} = 0.93 > 0.5 + \sqrt{0.085 - 0.055\psi} = 0.5 + \sqrt{0.085 + 0.055} = 0.87$$

$$\text{then } \rho = \frac{\overline{\lambda_p} - 0.055(3+\psi)}{\overline{\lambda_p}^2} = \frac{0.93 - 0.055(3-1)}{0.93^2} = 0.95$$

The reduction factor ρ is multiplied by the compression part and this will symbolize the loss of effectiveness due to local buckling.

$$h_{c,eff} = \rho \cdot \frac{h_w}{2} = 0.95 \cdot \frac{300}{2} = 143 \ mm$$

This means the total effective height of the web is the tension part added to the effective compression height.

$$h_{w,eff} = h_{c,eff} + \frac{h_w}{2} = 143 + \frac{300}{2} = 293 \ mm$$

Therefore, the total effective height will become:

$$h_{eff} = h_{w,eff} + 2 \cdot t_f = 293 + 2 \cdot 9 = 311 \ mm$$

Bending resistance

The calculation of the bending resistance must take place using the effective bending modulus, which corresponds to the fiber with the maximum elastic stress, thus the outer fiber. Knowing the effective width, the effective moment of inertia can be calculated first.

$$I_{y,eff} = \frac{b_f \cdot h_{eff}^3}{12} - 2 \cdot \frac{c_f \cdot h_{w,eff}^3}{12} = \frac{200 \cdot 311^3}{12} - 2 \cdot \frac{98 \cdot 293^3}{12} = 9.05 \cdot 10^7 \ mm^4$$

It is important to consider the change of the position of the neutral axis. The neutral axis divides the amount of material equally, but because of the loss in height, the neutral axis moves. In this case the neutral axis moves 4 mm down. This influences the bending modulus.

$$W_{eff,min} = \frac{I_y}{z} = \frac{9.05 \cdot 10^7}{\frac{h}{2} - 4} = 6.20 \cdot 10^5 \ mm^3$$

For the elastic bending resistance this means:

$$M_{eff,Rk} = W_{eff,min} \cdot f_y = 6.20 \cdot 10^5 \cdot 690 \cdot 10^{-6} = 424 \ kNm$$

The other effective bending resistances of homogeneous girders of class 4 are given in table 21.

Table 21: Effective bending resistances of homogeneous girders of class 4

test	f_{yf} [MPa]	b_f [mm]	t_f [mm]	f_{yw} [MPa]	h_w [mm]	t_w [mm]	h [mm]	$M_{eff,Rk}$ [kNm]
2	355	200	7	355	500	4	514	260
6	355	200	10	355	500	4	520	352
26	460	200	7	460	400	4	414	285
30	460	200	12	460	400	4	424	458
44	690	200	9	690	300	4	318	424
48	690	200	14	690	300	4	328	637

5.6.2 Bending resistance of hybrid girder

The properties of test case 18 are:

- $f_{yf} = 690 \; MPa$
- $b_f = 200 \; mm$
- $t_f = 14 \; mm$
- $f_{yw} = 355 \; MPa$
- $h_w = 500 \; mm$
- $t_w = 4 \; mm$
- $h = 528 \; mm$

The effective height of the girder is determined the same as for a homogeneous girder, see paragraph 5.6.1. For test case 18 this gives: $h_{w,eff} = 453 \; mm$ and $h_{eff} = 481 \; mm$.

For the moment of inertia this means:

$$I_{y,eff} = \frac{b_f \cdot h_{eff}^3}{12} - 2 \cdot \frac{c_f \cdot h_{w,eff}^3}{12} = \frac{200 \cdot 481^3}{12} - 2 \cdot \frac{98 \cdot 453^3}{12} = 3.36 \cdot 10^8 \; mm^4$$

Like for the cross-sections of class 3 the purpose here is the same; determine the effective bending modulus and bending resistance for flange and web separately and then choose the minimum. The neutral axis drops 24 mm in this case.

$$W_{f,eff,min} = \frac{I_y}{z} = \frac{3.36 \cdot 10^8}{\dfrac{h}{2} - 24} = 1.44 \cdot 10^6 \; mm^3$$

For the elastic bending resistance of the flange this means:

$$M_{f,eff,Rk} = W_{f,eff,min} \cdot f_{yf} = 1.44 \cdot 10^6 \cdot 690 \cdot 10^{-6} = 994 \; kNm$$

For the web:

$$W_{f,eff,min} = \frac{I_y}{z} = \frac{3.36 \cdot 10^8}{\dfrac{h_w}{2} - 24} = 1.49 \cdot 10^6 \; mm^3$$

For the elastic bending resistance of the flange this means:

$$M_{w,eff,Rk} = W_{w,eff,min} \cdot f_{yw} = 1.49 \cdot 10^6 \cdot 355 \cdot 10^{-6} = 528 \; kNm$$

The bending resistance of the whole cross-section is then:

$$M_{el,min} = min\left[M_{f,el,Rk}; M_{w,el,Rk}\right] = min[994; 528] = 528 \; kNm$$

The other effective bending resistances of hybrid girders of class 4 are given in table 22.

Table 22: Effective bending resistances of hybrid girders of class 4

test	f_{yf} $[MPa]$	b_f $[mm]$	t_f $[mm]$	f_{yw} $[MPa]$	h_w $[mm]$	t_w $[mm]$	h $[mm]$	$M_{eff,,Rk}$ $[kNm]$
8	460	200	7	355	500	4	514	281
12	460	200	12	355	500	4	524	456
14	690	200	9	355	500	4	518	350
18	690	200	14	355	500	4	528	528
20	960	200	10	355	500	4	520	385
24	960	200	16	355	500	4	532	601
32	690	200	9	460	400	4	418	371
36	690	200	14	460	400	4	428	566
38	960	200	10	460	400	4	420	409
42	960	200	16	460	400	4	432	647
50	960	200	10	690	300	4	320	472
54	960	200	16	690	300	4	332	759

5.6.3 Shear resistance

The shear force resistance calculations are identical to the calculation used in SP 1200 girder, which can be found in paragraph 5.3.6. The overview of these values is given in table 23.

Table 23: Shear resistances of girders of class 4

test	f_{yf} [MPa]	b_f [mm]	t_f [mm]	f_{yw} [MPa]	h_w [mm]	t_w [mm]	h [mm]	$V_{bw,Rk}$ [kN]
2	355	200	7	355	500	4	514	227
6	355	200	10	355	500	4	520	227
8	460	200	7	355	500	4	514	227
12	460	200	12	355	500	4	524	227
14	690	200	9	355	500	4	518	227
18	690	200	14	355	500	4	528	227
20	960	200	10	355	500	4	520	227
24	960	200	16	355	500	4	532	227
26	460	200	7	460	400	4	414	251
30	460	200	12	460	400	4	424	251
32	690	200	9	460	400	4	418	251
36	690	200	14	460	400	4	428	251
38	960	200	10	460	400	4	420	251
42	960	200	16	460	400	4	432	251
44	690	200	9	690	300	4	318	299
48	690	200	14	690	300	4	328	299
50	960	200	10	690	300	4	320	299
54	960	200	16	690	300	4	332	299

6 Bending and shear interaction

6.1 Aim of interaction

A comparison can be made using the ultimate bending moment and shear force resistances that are obtained by the numerical analyses with Ansys and the hand calculations with Eurocode 3. The goal is to determine the ratio of numerical resistance and hand calculated resistance. These points are the outer points of the curve, which means that they are either subjected to pure bending (x-axis) or pure shear (y-axis). After these points are determined, Ansys is used to obtain the values corresponding to bending and shear interaction, meaning where both bending and shear is applied on the girder.

The curve that is obtained for each type, class and steel strength is compared to a reference curve that shows the expected interaction. The reference curve is shown in figure 36. The orange lines represent the new interaction formula, referencing to F. Sinur [13, 4.2] and the grey lines the one that is currently used by the Eurocode. If the interaction points in the further paragraphs are situated above the curve, they can be found as safe. This means that the reference curve gives a lower bound for the bending moment and shear force interaction.
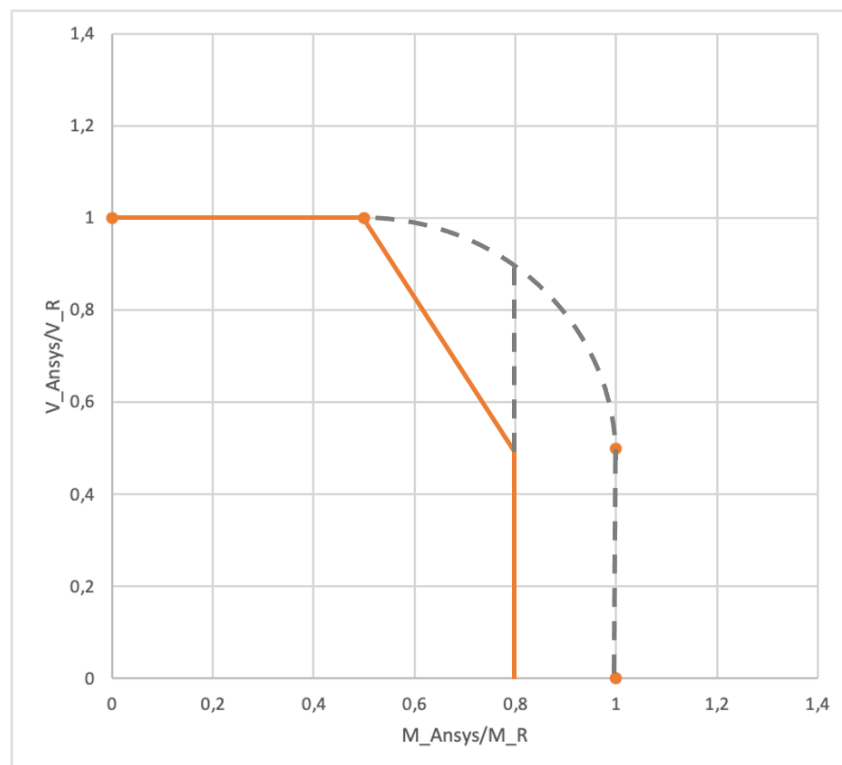
Figure 36: Bending moment and shear force interaction curve as reference

Based on whether the calculated points are above or below the curve, a conclusion is made on the use of the Eurocode 3 and its formulas, the different types and classes,

and the used steel grades. The total list of results of the numerical simulations and hand calculations can be found in annex E.

6.2 M-V interaction results per type and cross-section class

6.2.1 Cross-section class 1 or class 2

An overview of the pure bending moment and pure shear force resistances for the simulations and hand calculations are given in table 24.

Table 24: Bending and shear resistance comparison for Ansys and Eurocode for class 1 or 2

test	f_{yf} [MPa]	f_{yw} [MPa]	$M_{pl,Rk}$ [kNm]	M_{Ansys} [kNm]	$\dfrac{M_{Ansys}}{M_{pl,Rk}}$	$V_{bw,Rk}$ [kN]	V_{Ansys} [kN]	$\dfrac{V_{Ansys}}{V_{bw,Rk}}$
3	355	355	185	195	1,06	299	266	0,89
4	355	355	185	191	1,03	191	208	1,09
9	460	355	317	291	0,92	299	284	0,95
10	460	355	311	283	0,91	191	194	1,01
15	690	355	538	387	0,72	299	294	0,98
16	690	355	532	357	0,67	191	215	1,12
21	960	355	845	437	0,52	299	355	1,19
22	960	355	839	390	0,46	191	350	1,83
27	460	460	289	292	1,01	340	343	1,01
28	460	460	345	353	1,02	340	400	1,18
33	690	460	546	372	0,68	340	362	1,06
34	690	460	658	451	0,68	340	408	1,20
39	960	460	853	432	0,51	340	360	1,06
40	960	460	1023	503	0,49	340	405	1,19
45	690	690	510	403	0,79	600	623	1,04
46	690	690	607	506	0,83	817	850	1,04
51	960	690	882	517	0,59	600	642	1,07
52	960	690	1079	630	0,58	817	860	1,05

A general conclusion about the shear resistance of class 1 or 2 girders is that the ratio is good, except for 2 or 3 values. This means that the numerical values match very well with the hand calculations that consider only the contribution of the web. This also means that for class 1 and 2, the flanges do not contribute to the shear resistance.

The values of the bending ratio differ from 1,06 to 0,49. To explain this large difference, a distinction was made between the test results of the homogeneous girders and the hybrid girders. The difference in bending resistances is clarified through figures 37 and 38.

It is also important to note that tests 21, 22, 39 and 40 are actually not a qualified combination of yield strengths for a hybrid girder. Eurocode 3 part 5 states that the ratio of flange yield strength over web yield strength should not exceed two [6, 6.3]. They have been tested anyway, but as shown in table 24 the values are inconsistent and the ratio rather low.
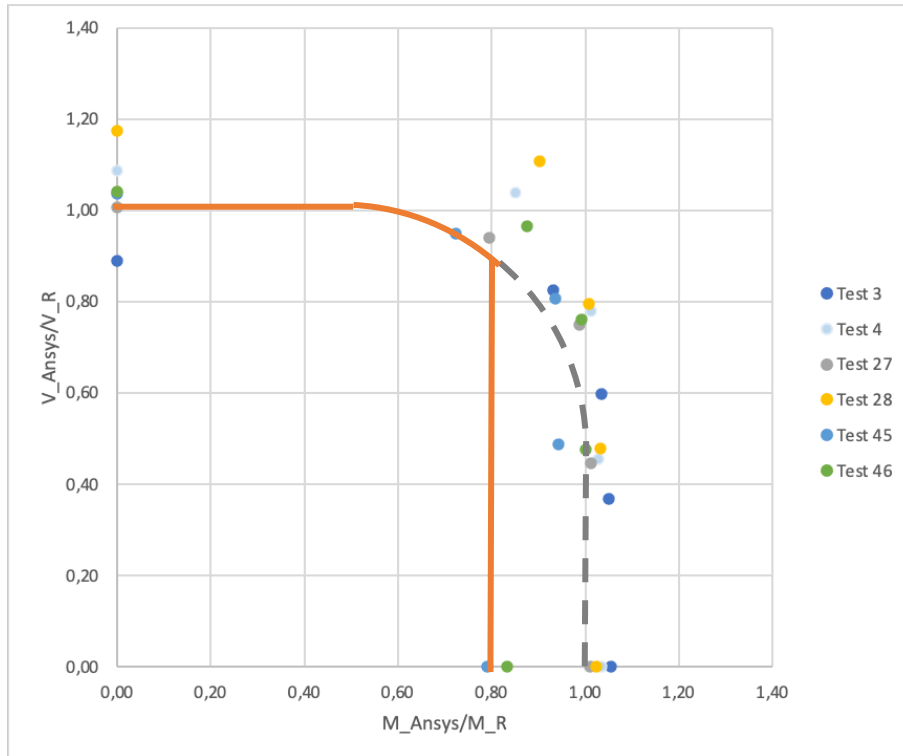
Figure 37: Bending and shear interaction for homogeneous girders of class 1 or 2

Figure 37 shows that the interaction points for the homogeneous test cases of class 1 or 2 are laying closely around the reference curve. Which means that the values obtained by the Eurocode resemble the values from the models. Most of the numerical points are also located above the curve, which means they are safe.
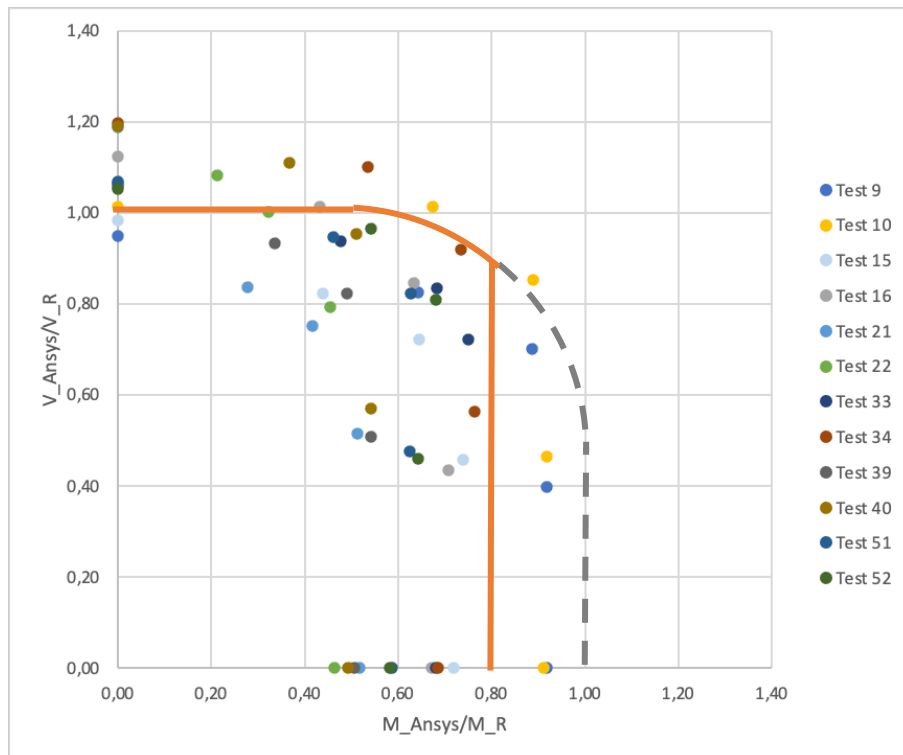
Figure 38: Bending and shear interaction for hybrid girders of class 1 or 2

Figure 38 shows that the dispersion of the interaction points is rather broad. This is mostly due to the bending moment ratio. Once the steel grade starts to raise, reaching high strength steel, thus 690 MPa, the ratio of Ansys value and Eurocode value starts to drop. When looking at the highest strength, 960 MPa, the ratio is dropped to approximately 0,50. This is further discussed in the comparison of steel grades, see paragraph 6.3. The numerical points in this comparison are located below the curve, therefore they are not safely designed.

6.2.2 Cross-section class 3

An overview of the pure bending moment and pure shear force resistances for the simulations and hand calculations are given in table 25.

Table 25: Bending and shear resistance comparison for Ansys and Eurocode for class 3

test	f_{yf} [MPa]	f_{yw} [MPa]	$M_{el,Rk}$ [kNm]	M_{Ansys} [kNm]	$\dfrac{M_{Ansys}}{M_{el,Rk}}$	$V_{bw,Rk}$ [kN]	V_{Ansys} [kN]	$\dfrac{V_{Ansys}}{V_{bw,Rk}}$
1	355	355	170	170	1,00	191	241	1,26
5	355	355	233	232	0,99	191	244	1,28
7	460	355	177	214	1,21	191	241	1,26
11	460	355	298	364	1,22	191	245	1,28
13	690	355	225	307	1,37	191	243	1,27
17	690	355	348	420	1,21	191	246	1,29
19	960	355	249	337	1,35	191	244	1,28
23	960	355	400	466	1,17	191	248	1,30
25	460	460	179	177	0,99	218	264	1,21
29	460	460	294	285	0,97	218	268	1,23
31	690	460	241	263	1,09	218	265	1,22
35	690	460	379	360	0,95	218	272	1,25
37	960	460	268	296	1,10	218	267	1,23
41	960	460	436	415	0,95	218	275	1,26
43	690	690	338	263	0,78	281	385	1,37
47	690	690	511	360	0,70	281	392	1,39
49	960	690	402	296	0,74	281	388	1,38
53	960	690	654	438	0,67	281	394	1,40

For class 3, the shear force values obtained from the simulations are significantly larger than the calculated values with a maximum raise of 40%. This shows that for a class 3 girder, the contribution of the flanges should not be neglected. The difference is due to the limitation in the calculation method which only assumes the contribution of the web.

It is also important to note that test designs 19, 23, 37 and 41 are not a qualified combination of yield strengths for a hybrid girder as explained above. They have been tested anyway, but as shown in table 25, the values are inconsistent.

The difference in bending resistances is clarified through figures 39 and 40.
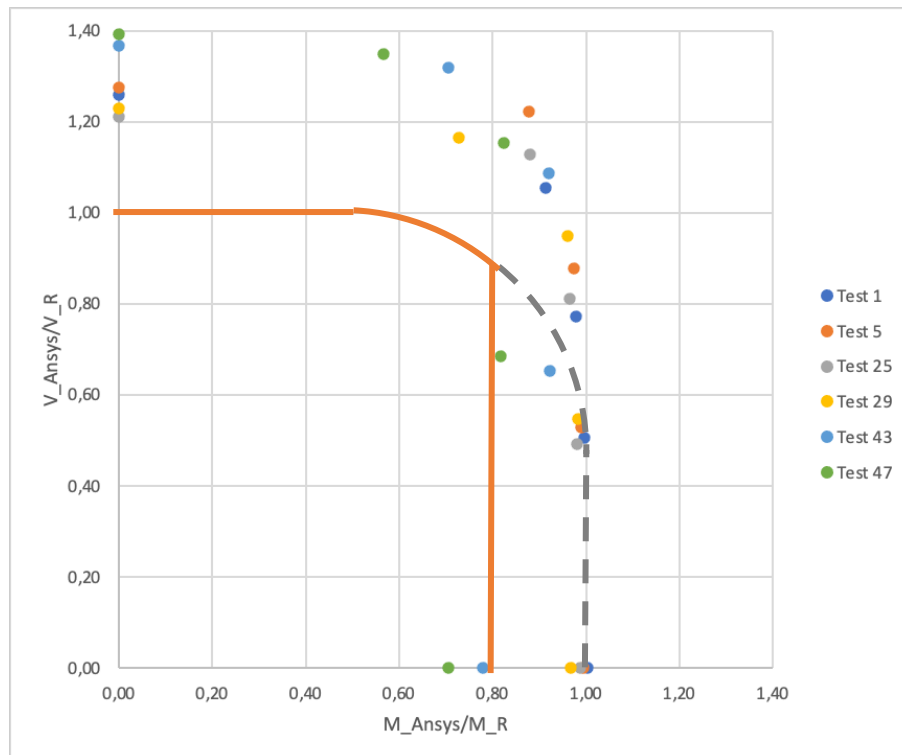
Figure 39: Bending and shear interaction for homogeneous girders of class 3

Figure 39 shows that the interaction points for the homogeneous test cases of class 3 are laying closely around the reference curve for the bending moment, but outside the reference curve for the shear force. As mentioned before, this is due to the neglection in the hand calculations of the contribution of the flanges.
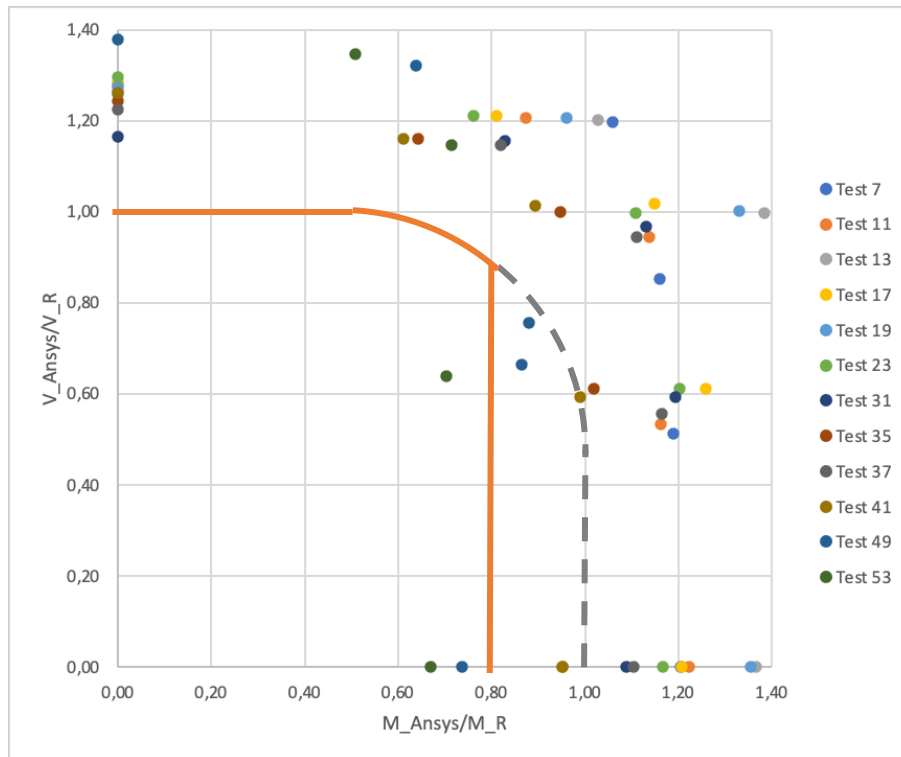
Figure 40: Bending and shear interaction for hybrid girders of class 3

Figure 40 shows that the interaction points for the hybrid test cases of class 3, are in general, laying outside the reference curve for both the shear force and the bending moment. This means that the resistance values are on the safe side, but it also means that the Eurocode rules are too safe for the design of hybrid girders.

6.2.3 Cross-section class 4

An overview of the pure bending moment and pure shear force resistances for the simulations and hand calculations are given in table 26.

Table 26: Bending and shear resistance comparison for Ansys and Eurocode for class 4

test	f_{yf} [MPa]	f_{yw} [MPa]	$M_{eff,Rk}$ [kNm]	M_{Ansys} [kNm]	$\dfrac{M_{Ansys}}{M_{eff,Rk}}$	$V_{bw,Rk}$ [kN]	V_{Ansys} [kN]	$\dfrac{V_{Ansys}}{V_{bw,Rk}}$
2	355	355	260	299	1,15	227	298	1,32
6	355	355	352	403	1,14	227	307	1,35
8	460	355	281	352	1,25	227	298	1,32
12	460	355	456	534	1,17	227	309	1,36
14	690	355	350	453	1,29	227	306	1,35
18	690	355	528	630	1,19	227	312	1,38
20	960	355	385	491	1,28	227	307	1,35
24	960	355	601	656	1,09	227	314	1,39
26	460	460	285	296	1,04	251	334	1,33
30	460	460	458	451	0,98	251	346	1,38
32	690	460	371	385	1,04	251	340	1,35
36	690	460	566	548	0,97	251	348	1,39

38	960	460	409	429	1,05	251	343	1,37
42	960	460	647	664	1,03	251	350	1,39
44	690	690	424	312	0,74	299	415	1,39
48	690	690	637	427	0,67	299	424	1,42
50	960	690	472	349	0,74	299	418	1,40
54	960	690	759	515	0,68	299	427	1,43

For class 4, the shear force values obtained from the simulations are again significantly larger than the calculated values with a maximum raise of 43%. This shows that for a class 4 girder, the contribution of the flanges should not be neglected. The difference is again due to the limitation in the calculation method which only assumes the contribution of the web.

It is also important to note that test designs 20, 24, 38 and 42 are actually not a qualified combination of yield strengths for a hybrid girder as explained above. They have been tested anyway, but as shown in table 26 the values are inconsistent.

The difference in bending resistances is clarified through figures 41 and 42.
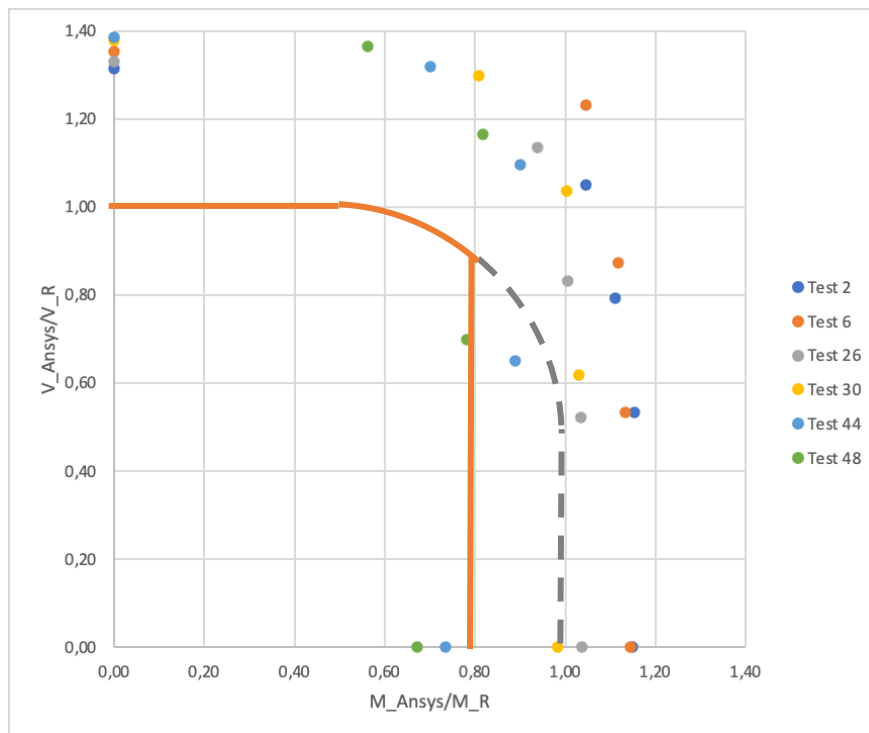
Figure 41: Bending and shear interaction for homogeneous girders of class 4

Figure 41 shows that the interaction points for the homogeneous test cases of class 4 are laying closely around the reference curve for the bending moment, but outside the reference curve for the shear force. As mentioned before, this is due to the neglection in the Eurocode of the contribution of the flanges. Most points are above the curve and therefore safely designed. Even for homogeneous girders, the Eurocode resistance values are quite safe in comparison with the numerical values. This is because of to the use of effective height in the formulas instead the whole girder height.
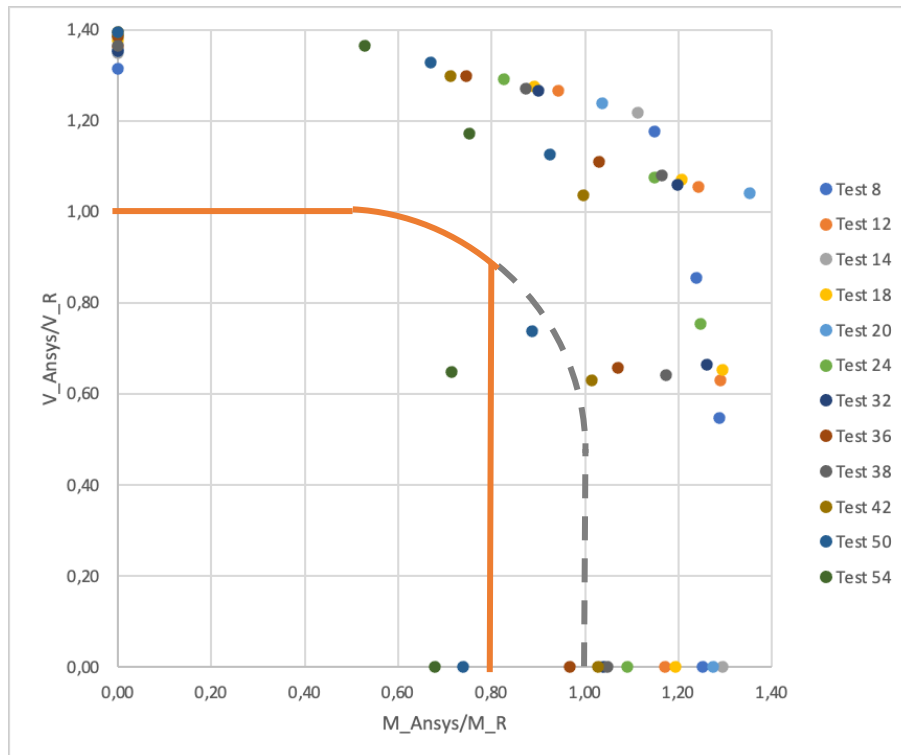
Figure 42: Bending and shear interaction for hybrid girders of class 4

Figure 42 shows that the interaction points for the hybrid test cases of class 4, are in general, laying outside the reference curve for both the shear force and the bending moment. Most points are located above the reference curve and therefore on the safe side of the design. Because the points are located quite far from the curve, it can be said that the girders are designed too safely using Eurocode 3. The numerical resistances are significantly larger than the calculated ones.

6.3 M-V interaction results per steel grade of the flanges

6.3.1 S355

The test results for the girders of which the flange is of steel grade S355, are shown in table 27. Note that the class mentioned in this table is the least favorable class for the whole girder. This is repeated for the next comparisons.

Table 27: Bending and shear resistance comparison for Ansys and Eurocode 3 for flange S355

test	f_{yf} [MPa]	f_{yw} [MPa]	class	M_{Rk} [kNm]	M_{Ansys} [kNm]	$\dfrac{M_{Ansys}}{M_{Rk}}$	$V_{bw,Rk}$ [kN]	V_{Ansys} [kN]	$\dfrac{V_{Ansys}}{V_{bw,Rk}}$
1	355	355	3	170	170	1,00	191	241	1,26
2	355	355	4	260	299	1,15	227	298	1,32
3	355	355	1	185	195	1,06	299	266	0,89
4	355	355	2	185	191	1,03	191	208	1,09
5	355	355	3	233	232	0,99	191	244	1,28
6	355	355	4	352	403	1,14	227	307	1,35

Table 27 shows that the girders where the flanges have a steel grade of 355 MPa, are chosen as homogeneous girders for this thesis. The interaction is visualized in figure 43.
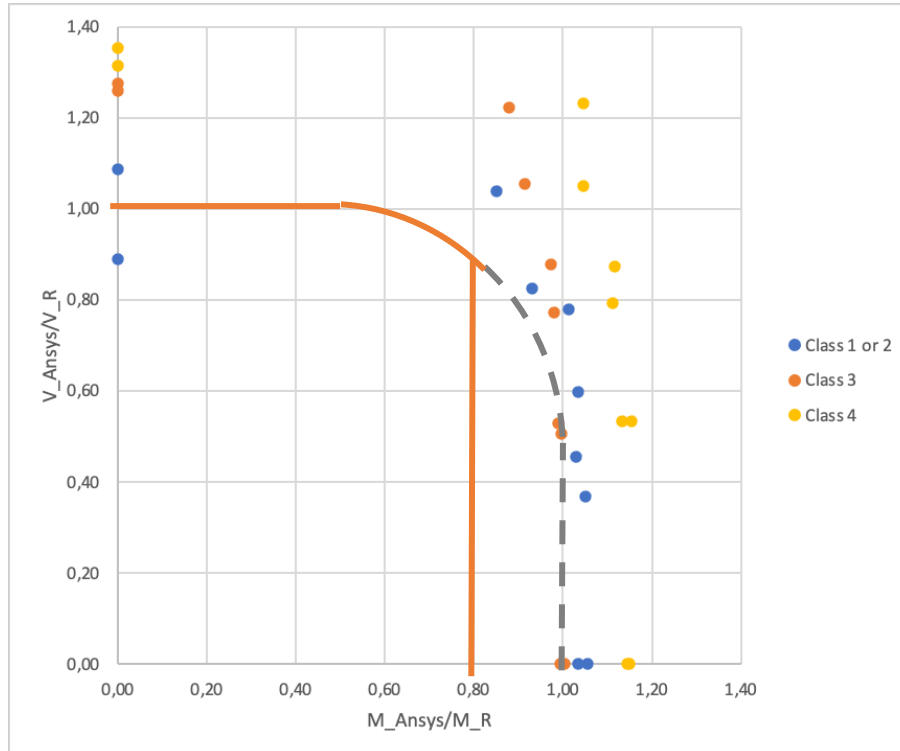
Figure 43: Bending and shear interaction for girders with flange S355 per cross-section class

Overall, a difference is seen in shear resistance between girders of class 1 or 2 and girders of class 3 or 4. For the class 1 or 2 girders, it is assumed that only the

contribution of the web is enough. For class 3 or class 4 girders on the other hand, the shear resistance is too safely designed because the lack of contribution of the flange.

6.3.2 S460

The test results for the girders of which the flange is of steel grade S460 are shown in table 28.

Table 28: Bending and shear resistance comparison for Ansys and Eurocode 3 for flange S460

test	f_{yf} [MPa]	f_{yw} [MPa]	class	M_{Rk} [kNm]	M_{Ansys} [kNm]	$\dfrac{M_{Ansys}}{M_{Rk}}$	$V_{bw,Rk}$ [kN]	V_{Ansys} [kN]	$\dfrac{V_{Ansys}}{V_{bw,Rk}}$
7	460	355	3	177	214	1,21	191	241	1,26
8	460	355	4	281	352	1,25	227	298	1,32
9	460	355	1	317	291	0,92	299	284	0,95
10	460	355	2	311	283	0,91	191	194	1,01
11	460	355	3	298	364	1,22	191	245	1,28
12	460	355	4	456	534	1,17	227	309	1,36
25	460	460	3	179	177	0,99	218	264	1,21
26	460	460	4	285	296	1,04	251	334	1,33
27	460	460	1	289	292	1,01	340	343	1,01
28	460	460	2	345	353	1,02	340	400	1,18
29	460	460	3	294	285	0,97	218	268	1,23
30	460	460	4	458	451	0,98	251	346	1,38

Table 28 shows that there are two types of girders where the flanges have a steel grade of 460 MPa: hybrid girders with a web steel grade of S355 and homogeneous S460 girders. The interaction per cross-section class is visualized in figure 44 and the interaction per type is visualized in figure 45.
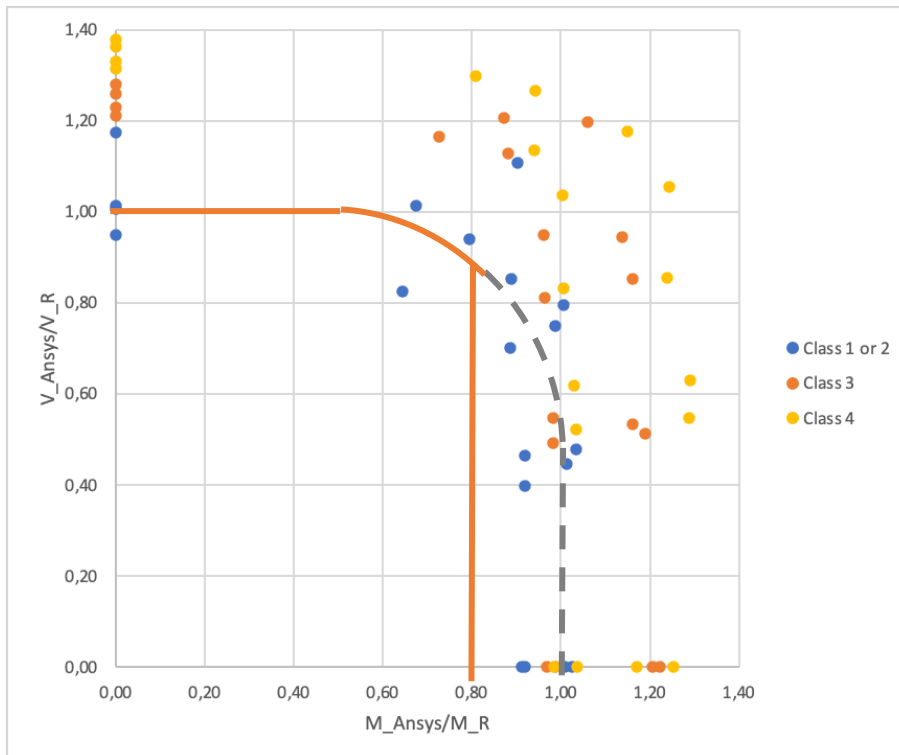
Figure 44: Bending and shear interaction for girders with flange S460 per cross-section class

Overall, most points are above the interaction curve, which means they are safe. However, for a few points of cross-section class 1 or 2 it is risky because they are hovering around the limits of the lower bound of the resistance. The higher the class, the safer the Eurocode rules state the resistance. For class 4 this means the numerical values of the shear resistance are maximum 40% greater than the hand calculated values.
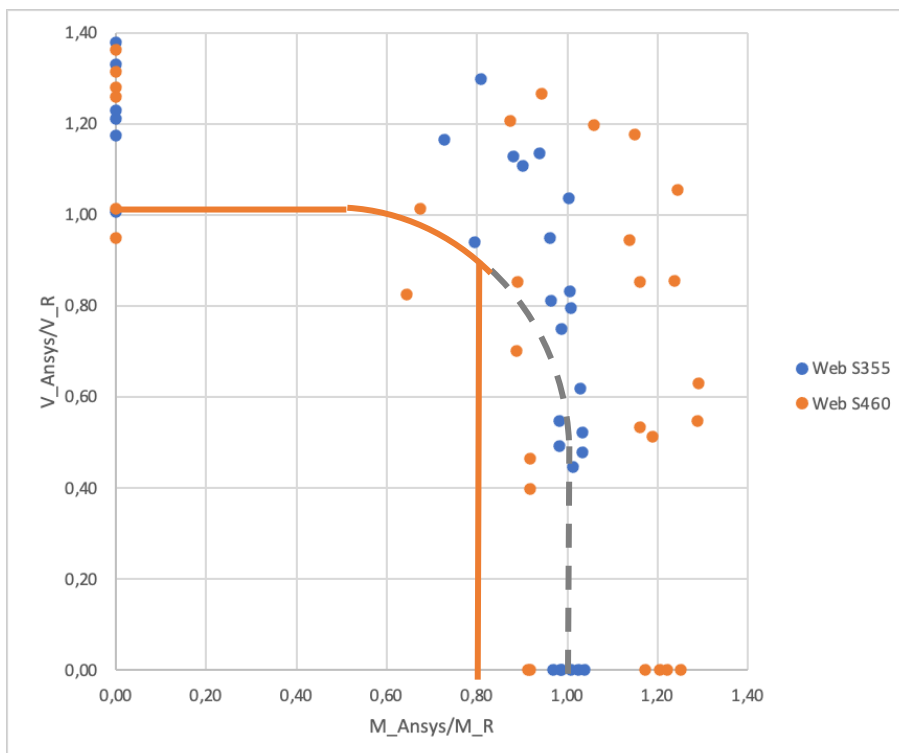
Figure 45: Bending and shear interaction for girders with flange S460 per web yield strength

At first sight, the cloud of points is difficult to read. To analyze this pattern, first the combination of the flange with the web with steel grade S355 will be analyzed. These points follow the shape of the reference curve and elevate more in the vertical direction, which means the numerical shear resistance value is bigger than the Eurocode. Again, due to the contribution of the flanges.

When analyzing the combination of the flange with the web with steel grade S460, which makes the girder homogeneous, it can be concluded that the points closer to the curve are the ones that belong to cross-section 1 or 2, as mentioned in paragraph 6.3.2 for flange steel grade S355. The further points belong to cross-section classes 3 and 4.

6.3.3 S690

The test results for the girders of which the flange is of steel grade S690 are shown in table 29. Important to notice, is that these girders are the ones that work with high strength steel flanges.

Table 29: Bending and shear resistance comparison for Ansys and Eurocode 3 for flange S690

test	f_{yf} [MPa]	f_{yw} [MPa]	class	M_{Rk} [kNm]	M_{Ansys} [kNm]	$\dfrac{M_{Ansys}}{M_{Rk}}$	$V_{bw,Rk}$ [kN]	V_{Ansys} [kN]	$\dfrac{V_{Ansys}}{V_{bw,Rk}}$
13	690	355	3	225	307	1,37	191	243	1,27
14	690	355	4	369	453	1,23	227	306	1,35
15	690	355	1	538	387	0,72	299	294	0,98
16	690	355	2	532	357	0,67	191	215	1,12
17	690	355	3	348	420	1,21	191	246	1,29
18	690	355	4	554	630	1,14	227	312	1,38
31	690	460	3	241	263	1,09	218	265	1,22
32	690	460	4	372	385	1,03	251	340	1,35
33	690	460	1	546	372	0,68	340	362	1,06
34	690	460	2	658	451	0,68	340	408	1,20
35	690	460	3	379	360	0,95	218	272	1,25
36	690	460	4	568	548	0,96	251	348	1,39
43	690	690	3	338	263	0,78	281	385	1,37
44	690	690	4	393	312	0,79	299	415	1,39
45	690	690	1	510	403	0,79	600	623	1,04
46	690	690	2	607	506	0,83	817	850	1,04
47	690	690	3	511	360	0,70	281	392	1,39
48	690	690	4	592	427	0,72	299	424	1,42

Table 29 shows that the girders where the flanges have a steel grade of 460 MPa, there are two types of girders; hybrid girders with web steel grade S355, steel grade S460 and homogeneous girders. The interaction per cross-section class is visualized in figure 46 and the interaction per type is visualized in figure 47.
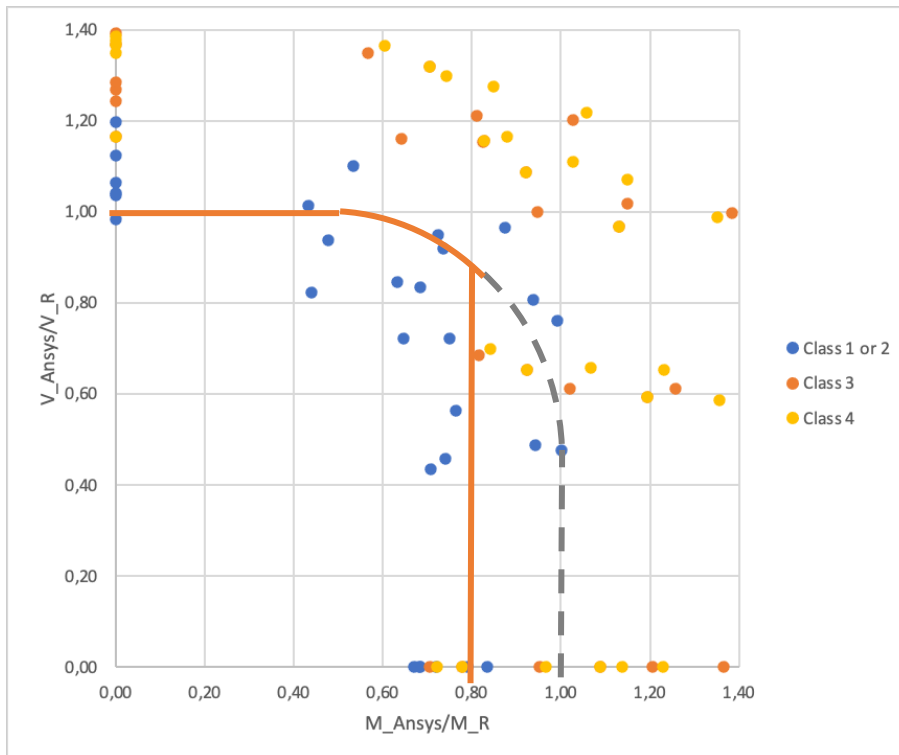
Figure 46: Bending and shear interaction for girders with flange S690 compared for each class

It is obvious that cross-section class 1 or 2 are in the unsafe zone of the curve. These numerical resistances are smaller than the Eurocode calculates ones. This means they fail earlier than the calculated value, which can have catastrophic consequences if not considered in the design of high strength steel hybrid girders.

Cross-section classes 3 and 4 are in the safe zone, but again designed too safely.
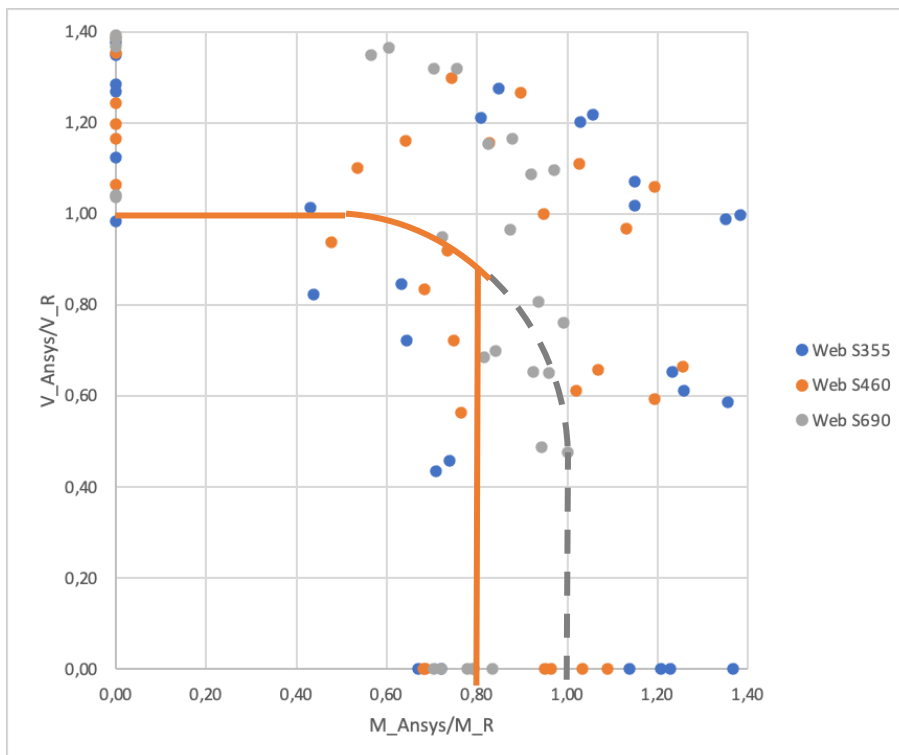
Figure 47: Bending and shear interaction for girders with flange S690 per web yield strength

Figure 47 shows that still some points of every combination are on the unsafe side of the curve. They will fail sooner than the theoretical resistance is reached that is calculated using the Eurocode. These points are mostly cross-section class 1 or 2 and web steel grade S355 or S460.

6.3.4 S960

The test results for the girders of which the flange is of steel grade S960 are shown in table 30.

Table 30: Bending and shear resistance comparison for Ansys and Eurocode 3 for flange S960

test	f_{yf} [MPa]	f_{yw} [MPa]	class	M_{Rk} [kNm]	M_{Ansys} [kNm]	$\dfrac{M_{Ansys}}{M_{Rk}}$	$V_{bw,Rk}$ [kN]	V_{Ansys} [kN]	$\dfrac{V_{Ansys}}{V_{bw,Rk}}$
19	960	355	3	249	337	1,35	191	244	1,28
20	960	355	4	405	491	1,21	227	307	1,35
21	960	355	1	845	437	0,52	299	355	1,19
22	960	355	2	839	390	0,46	191	350	1,83
23	960	355	3	400	466	1,17	191	248	1,30
24	960	355	4	630	656	1,04	227	314	1,39
37	960	460	3	268	296	1,10	218	267	1,23
38	960	460	4	410	429	1,05	251	343	1,37
39	960	460	1	853	432	0,51	340	360	1,06
40	960	460	2	1023	503	0,49	340	405	1,19
41	960	460	3	436	415	0,95	218	275	1,26
42	960	460	4	649	664	1,02	251	350	1,39
49	960	690	3	402	296	0,74	281	388	1,38
50	960	690	4	454	349	0,77	299	418	1,40
51	960	690	1	882	517	0,59	600	642	1,07
52	960	690	2	1079	630	0,58	817	860	1,05
53	960	690	3	654	438	0,67	281	394	1,40
54	960	690	4	733	515	0,70	299	427	1,43

First note to mention is that 12 out of 18 test designs do already not oblige to Eurocode 3 part 5. It is stated that the ratio of the flange yield strength to the web yield strength can not exceed two, which is the case for web steel grades S355 and S460. This means that 67% of the points in the figures below are not suitable for the design of high strength steel hybrid girders. The interaction per cross-section class is visualized in figure 48 and per web steel grade in figure 49.
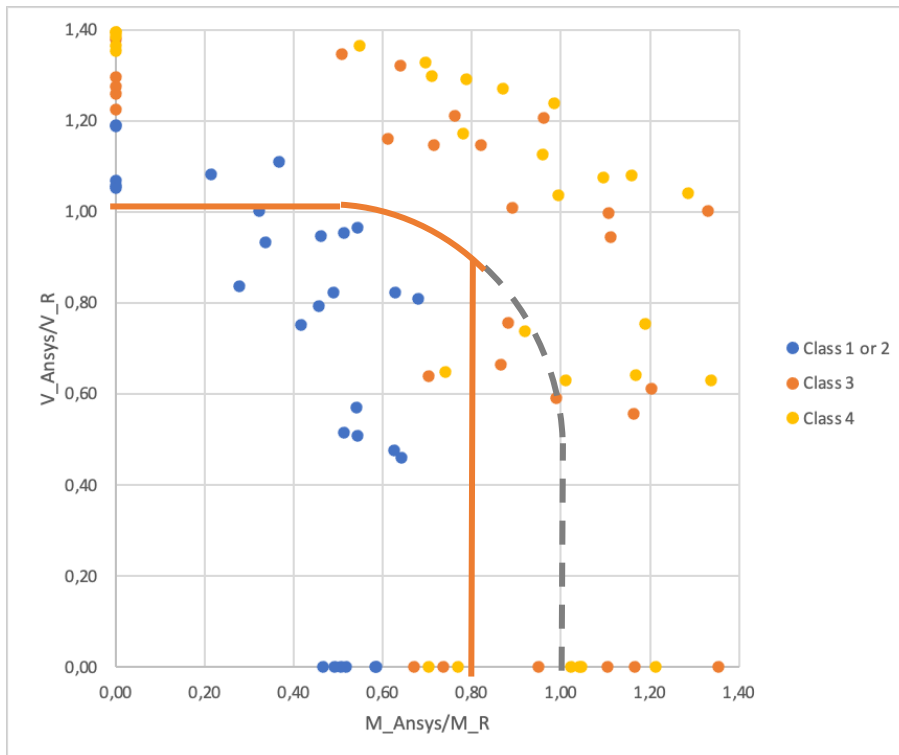
Figure 48: Bending and shear interaction for girders with flange S960 compared for each class

Figure 48 shows that class 1 or 2 Eurocode rules are not sufficient to work with this strength of steel. For classes 3 and 4 are again designed too safely.
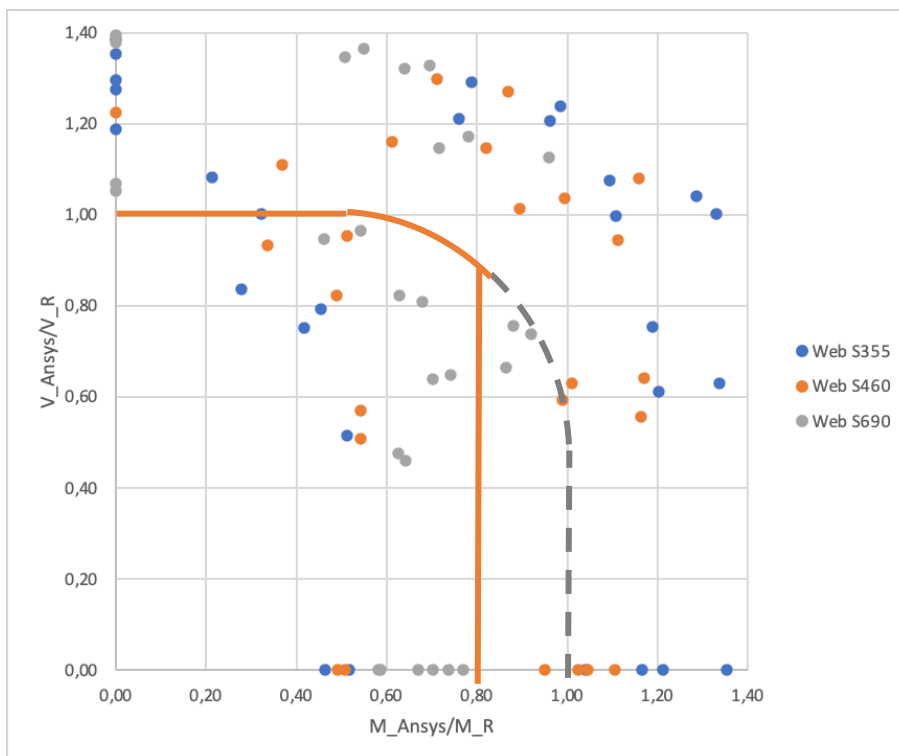
Figure 49: Bending and shear interaction for girders with flange S960 per web yield strength

Although, figure 49 shows a lot of unsafe points for the lower strength steel, there are some combinations that are safe. Even though it is mentioned in Eurocode that it is not

allowed to exceed the ratio of two. For the combination with the web with steel grade S690 there is also some discrepancy. Approximately 50% of the points is located under the curve and 50% above. Which makes the chance of premature failure around 50%.

7 Parametric study

In this chapter, the results of the parametric study in which parameters of the flanges for hybrid high strength steel are discussed. This combination achieved very good results: the hybrid girder with flanges in S690 and web in S460. Due to these results, these tests were used to perform this parametric study (tests 31 to 36). This means that the parametric study was performed for each kind of performed simulation, which were shown in figure 25.

7.1 Effect of changing the width and thickness of the flanges (b_f and t_f)

Due to the different classes of flanges for the different simulations, as well as the different steel grades of the web and the flanges, it had to be ensured that the flanges remained in the same class while adjusting the height and width of the flanges. Also, the ratio of geometry between the flanges and the web was considered. This resulted in the following range of the parameters for each test.

For test 31 and 32 with flanges in class 3, the six simulations shown in table 31 were performed.

Table 31: Geometry of the flanges for tests 31 and 32

Simulation	$b_f\ [mm]$	$t_f\ [mm]$
1	200	9
2	200	10
3	200	12
4	250	12
5	250	14
6	250	16

For tests 33 to 36 with flanges in class 1, the following parameters shown in table 32 were used.

Table 32: Geometry of the flanges for tests 33 to 36

Simulation	$b_f\ [mm]$	$t_f\ [mm]$
1	200	14
2	200	16
3	200	18
4	200	20
5	250	18
6	250	20

The first simulation in each table 31 and 32, was already performed in chapter 7 and is used as reference. As already discussed, the performed simulations for the 54 tests

from chapter 5 were chosen for the most economical use, thus the least amount of material. This parametric study investigated if using more material, thus larger dimensions, justifies the increase in bending moment resistance.

Because flanges are mainly responsible to resist bending moments, the focus was only on the influence of the bending moment and not the shear force. The results of the parametric simulations with increased width and thickness of the flanges are shown in figure 50. The results are plotted for each test and for each simulation with adjusted dimensions.
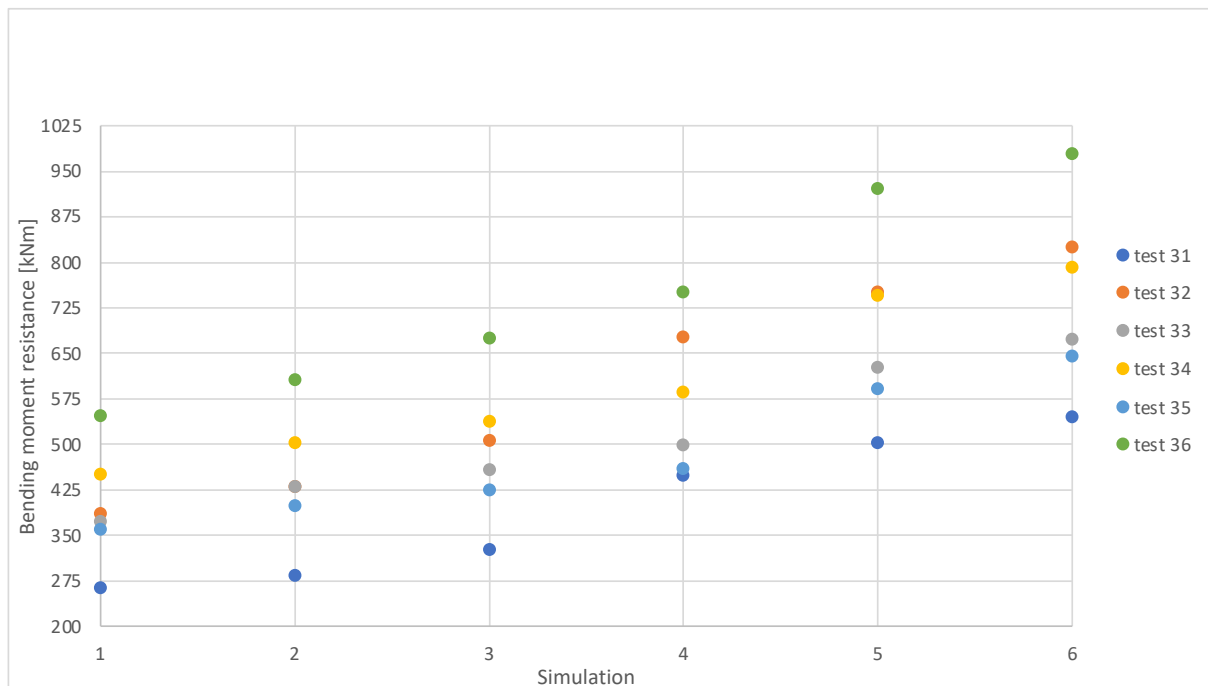
Figure 50: Results of the increase of bending moment resistance when increasing the width and thickness of the flanges for each simulation

Figure 50 shows the increase in bending resistance for the investigated tests for each simulation, as discussed in tables 31 and 32.

The results of tests 31 and 32 can be seen in table 33 and 34:

Table 33: Results parametric study - test 31

First simulation	Second simulation	Δt_f [mm]	Δb_f [mm]	ΔM [%]
1	3	3	0	23.8
3	4	0	50	37.5
4	6	4	0	21.5

Table 34: Results parametric study - test 32

First simulation	Second simulation	Δt_f [mm]	Δb_f [mm]	ΔM [%]
1	4	3	0	31.3
3	4	0	50	33.8
4	6	4	0	21.9

From these tables, the following is concluded: increasing the thickness of the flanges with three millimeters, while keeping the width constant on 200 millimeters (comparing simulation 1 with simulation 3) shows that a relatively big increase of the bending moment resistance is obtained for both tests. Test 32 had the biggest increase with 31.3%, being the test where the flange is class 3 and the web is class 4.

Increasing the width of the flanges from 200 millimeters to 250 millimeters, while keeping the thickness of the flanges the same (comparing simulation 3 with simulation 4), shows a fairly improvement of the bending moment resistance. Test 31 had the biggest increase with 37.5%, being the test where the flange and the web are class 3.

Increasing the thickness of the flange from 12 to 16 millimeters while keeping the width of the flanges constant on 250 millimeters (comparing simulation 4 with simulation 6), results in an increase of the bending moment of 21.5% for test 31, and an increase of the bending moment of 21.9% for test 32.

Very similar results were obtained for tests 33 to 36. A distinction was made for each test. The results for each test are shown in tables 35, 36, 37 and 38:

Table 35: Results parametric study - test 33

First simulation	Second simulation	Δt_f [mm]	Δb_f [mm]	ΔM [%]
1	4	6	0	34
4	5	-2	50	25.7
5	6	2	0	7.5

Table 36: Results parametric study - test 34

First simulation	Second simulation	Δt_f [mm]	Δb_f [mm]	ΔM [%]
1	4	6	0	30
4	5	-2	50	27.4
5	6	2	0	6

Table 37: Results parametric study - test 35

First simulation	Second simulation	Δt_f [mm]	Δb_f [mm]	ΔM [%]
1	4	6	0	27.7
4	5	-2	50	28.6
5	6	2	0	9.2

Table 38: Results parametric study - test 36

First simulation	Second simulation	Δt_f [mm]	Δb_f [mm]	ΔM [%]
1	4	6	0	37
4	5	-2	50	22.8
5	6	2	0	6.3

From these tables, the following is concluded: increasing the thickness of the flanges while keeping the width constant on 200 millimeters (comparing simulation 1 with simulation 4) shows that a relatively big increase of the bending moment resistance is

obtained for each test. Test 36 had the biggest increase with 37%, being the test where the flange is class 1 and the web is class 4.

Increasing the width of the flanges from 200 millimeters to 250 millimeters, while keeping the thickness of the flanges the same (comparing simulation 4 with simulation 5), shows a fairly improvement of the bending moment resistance. Test 35 had the biggest increase with 28.6%, being the test where the flange is class 1 and the web is class 3.

Increasing the thickness of the flange from 18 to 20 millimeters while keeping the width of the flanges constant on 250 millimeters (comparing simulation 5 with simulation 6), results in an increase of the bending moment of 6 to 9.2% for the four tests. The biggest increase is for the class 1 flange and class 3 web girder.

Comparing the results of the parametric study for the six different simulations for the six tests, the following can be concluded.

Increasing the thickness of the flanges, while keeping the width of the flanges constant on 200 millimeters, shows very similar increase of the bending moment resistance for all tests.

Increasing the width of the flanges, while keeping the thickness of the flanges constant, also shows very similar result for all tests. To make a faire comparison for all tests, there must be kept in mind that for test 33 to test 36 simulation 4 needs to be compared with simulation 6.

Finally, increasing the thickness of the flanges, after increasing the width of the flanges, shows a big difference between test 31 and 32 compared with test 33 to test 36. This is because for test 31 and 32, an additional increase of 2 millimeters of the thickness was tested. In general, the results for all the tests are again very similar when looking at the same increase in thickness and the increase of the bending moment resistance.

This shows that increase of the bending moment resistance by increasing the geometry of the flanges, is linear for the different investigated class combinations of the flanges and the web for HSS hybrid girders.

7.2 Comparing increase of bending moment resistance with material cost

As mentioned previously, all the bending and shear interaction simulations were performed with the least material consumption. By analyzing the effect of increasing the bending moment resistance by increasing the width and thickness of the flanges, it was determined if using more material to obtain a higher resistance justifies the use of extra material. The results are shown in figure 51, for tests 31 to 36.
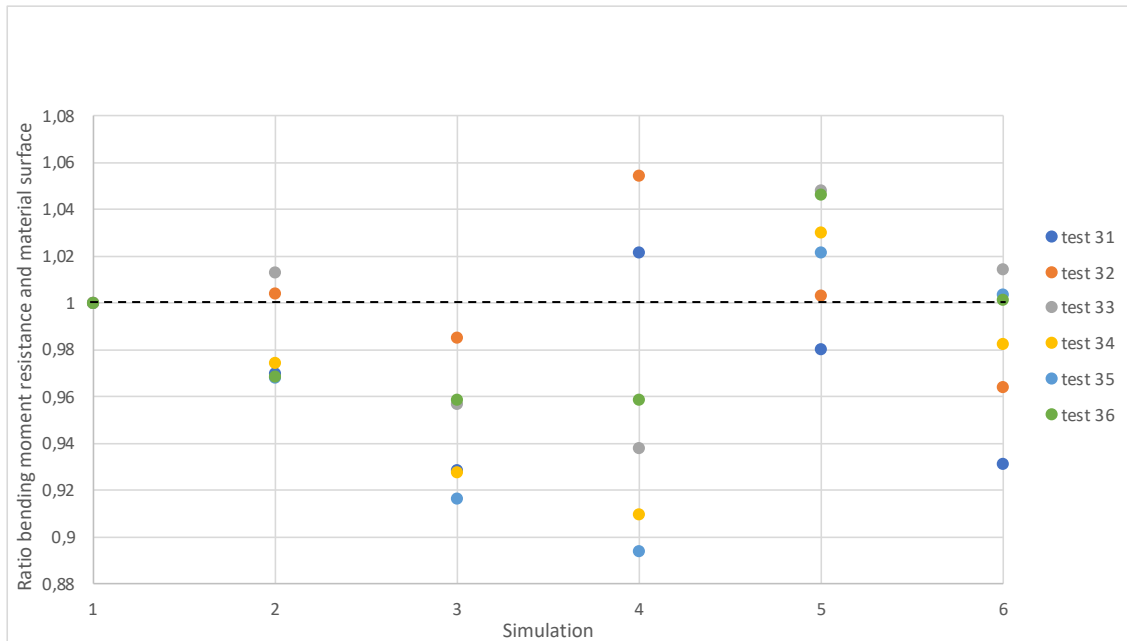
Figure 51: Ratio between the bending moment resistance and the used material for each simulation

Figure 51 shows the ratio of the bending resistance and the used material in function of each simulation. The optimized solution was to achieve the highest possible resistance, while using the least amount of material possible.

The first simulation was used as reference with the least amount of material. All the points above the line that indicates the value of simulation 1, indicate a better bending moment resistance to used material ratio for tests 31 to 36. Figure 51 also shows that there is not one simulation in which all tests have a better bending moment resistance to used material ratio than the reference tests. This shows that the relation between the class of the flanges and the class of the web do not have a linear connection.

For test 31 and 32, simulation 4, it seems that an increase of the width of the flange a positive effect has on the bending resistance (increase of the bending moment resistance and used material ratio of 2 – 5.8%). For test 33 to 36, simulation 5, the increase also has a positive effect on the ratio (2 – 5.5%).

There can be concluded from figure 51, that only the increase of the width of the flanges results in a better bending moment resistance to used material ratio then the minimal material cost flanges. Due to the minimal increase in the bending moment resistance, and an increase of production cost, material, transport, the minimal material

use is still preferred. All the values that were used to create figures 50 and 51, can be found in the Annex F.

8 Conclusion

This thesis was conducted with two main purposes, the first being the verification of the Eurocode 3 design rules regarding the bending moment and shear force resistance calculations in high strength steel hybrid girders. For steel grades up to S700 there are additional design rules and specifications found in Eurocode 3. For high strength steel grades greater than S700 there is no information provided by the Eurocode. This made it interesting to do research about the usability of the design rules for higher strength steel types and to initiate further investigation. The second purpose being the investigation of high strength steel regarding the bending moment and shear force resistance and its economical relevance in material use.

The verification of the Eurocode 3 design rules took place in three segments. There was a comparison made for homogeneous girders as well as for hybrid girders. These girders are divided into different cross-section classes, 1 or 2, 3 and 4. The cross-section class is determined by the highest, thus least favorable, class of the structural elements. Another way to do the comparison is to divide the girders into different steel grades of the flange. Each flange steel grade has one or more web steel grades, this was also investigated.

For the homogeneous girders, the testing results were very similar to the calculated values for classes 1 or 2, as described in the Eurocode. This means that the bending moment resistance and shear force resistance values of the numerical models are equal to the Eurocode values where the contribution of the flange is not considered in the shear resistance. For classes 3 and 4 however, the numerical values of the shear resistance are way higher than the design formulas. This means that in these classes the contribution of the flange should be considered in the calculation.

For the hybrid girders with cross-section class 1 or 2 it was obvious that the ratio of the numerical values to the calculated values was significantly lower than the reference curve values. Because the test points are located below the reference curve, the design of class 1 or 2 cross-sections is unsafe. The structure will fail before the design resistance values are reached. Therefore, it is not recommended to design hybrid girders with cross-section classes 1 or 2. For cross-section classes 3 and 4 however, the ratio was significantly higher than the reference curve values. This means that the test points were on the safe side and the calculated resistance is smaller than the numerical value. Although, the existing design rules can be used for these cross-sections, it is recommended to review them for further application for hybrid girders in class 3 and 4. Therefore, following the current design rules will lead to significant over dimensioning of the girders.

When deciding which steel grades to use for the flanges and the web of a hybrid girder, it was very important to take into account the ratio of the flange yield strength to the web yield strength. Eurocode 3 states that this ratio can not exceed two. Although this

rule was stated, there was chosen to investigate yield strengths of the flanges, which were more than twice the yield strength of the web. For the lower strength steel grades up until S460 and the high strength steel grade S690, the design rules are safe to use for cross-section classes 3 and 4.

However, for high strength steels above 700 MPa, which do not have any design rules in the Eurocode, there is still some discrepancy of whether the design rules are safe to use due to the statistics that show that approximately 50% of the performed tests show premature failure before reaching the design value resistance.

From this master thesis, it can be concluded that the obtained results provide tangible evidence on the usability of Eurocode 3 design rules for hybrid high strength steel girders. The design rules should be reviewed for each cross-section class and corrected accordingly. For the calculated values that differ significantly from the numerical values, further research is recommended to consider safe and economical design for hybrid high strength steel girders. Furthermore, steel strengths higher than 700 MPa should be considered for further investigation as well as being included in Eurocode 3.

References

[1] EN 10025: Hot rolled products of structural steel, 2007.

[2] EN 1993-1-12. Eurocode 3: Design of steel structures – Part 1-12: Additional rules for the extension of EN1993 to steel grades up to S700, 2007.

[3] Baddoo N., Francis P., Pilpilidou A., Sansom M. "Stronger Steels in the Built Environment STROBE" (D7.1 Project Overview), 2017.

[4] EN 1993-1-1: Eurocode 3: Design of steel structures. Part 1.1 General rules and rules for buildings, 2019.

[5] Veljkovic, B.J.M. "Design of hybrid steel girders", Division of Steel Structures, Lulea University of Technology, Lulea, SE-971 87, Sweden, 2004.

[6] EN 1993-1-5: Eurocode 3: Design of steel structures – Part 1-5: Plated structural elements, 2019

[7] Veljkovic M, Johansson B. "Design for buckling of plates due to direct stress". Nordic Steel Construction Conference, Helsingfors. 2001, p. 729–36.

[8] Gogou E. "Use of High Strength Steel Grades for Economical Bridge Design" (Part 1 – Literature), 2012.

[9] EN 1993-1-1: Eurocode 3: Design of steel structures. Part 1.1 General rules and rules for buildings, 2005.

[10] Denis Cyrille, T. "Advanced structural problematics in steel bridges". Universita degli Studi di Padova, 2019.

[11] Kövesdi, B., Alcaine, J., Dunai, L. "Interaction behaviour of steel I-girders. Part I: Longitudinally unstiffened girders.", 2014.

[12] EN 1993-1-5: Eurocode 3: Design of steel structures – Part 1-5: Plated structural elements, 2006.

[13] Beg, D., Sinur, F. "Moment-shear interaction of longitudinally stiffened girders." Structural Stability Conference, 2012.

[14] Ghadami, A., Broujerdian, V. "Flexure shear interaction in hybrid steel I-girders at ambient and elevated temperatures." Advances in Structural Engineering, 2018.

[15] Kuhlmann, U., "COMBRI DESIGN MANUAL Part II: State-of-the-Art and Conceptual Design of Steel and Composite Bridges", Project partners, Stuttgart, Germany, 2008.

Annex list

Annex A – Code verification model

```
FINISH
/CLEAR,START
/NERR,0,99999999,,0

datnam = arg1    ! Name of the project

/FILNAME, %datnam%
/TITLE,   %datnam%

/PREP7

! This code was used to run the verifcation for both models:
! Code SP600: verification,'Sp600',2390*2,600,6,450,20,200,430,430
! Code SP1200: verification,'Sp1200',2390*2,1200,6,450,20,200,520,520
!                              1        2      3 4 5  6 7   8   9

! ==========
! Parameters
! ==========

! Stress paramaters
FYw = 383         ! Yield strength web ; 383 test
Fuw = 543         ! Ultimate yield strength web ; 543 test

FYf = 354         ! Yield strength flange ; 354 test
Fuf = 519         ! Ultimate yield strength flange ; 519 test

FYb = 354         ! Yield strength stiffeners ; 354 test
Fub = 519         ! Ultimate yield strength stiffeners ; 519 test

! Cross-section parameters
Length = arg2     ! Length of the panel [mm]
hw = arg3         ! Web height [mm]
tw = arg4         ! Web thickness [mm]
bf = arg5         ! Flange width [mm]
tf = arg6         ! Flange thickness [mm]

tv = 20           ! Thickness of the vertical stiffeners [mm] ; fixed

! Loading parameters
ss = arg7         ! Loading length [mm]
Ff = arg8         ! Applied load [kN]
Vv = arg9         ! Shear load [kN]

halo = 20         ! Mesh size, 20 mm

EX = 210000       ! Young's modulus

*AFUN,DEG


! =================================
! Element type and Material models
! =================================

ET,1,SHELL181

R,1,tw,tw,tw,tw, , ,
R,2,tf,tf,tf,tf, , ,
R,3,0,0,0,0, , ,
R,4,tv,tv,tv,tv, , ,

MPTEMP,,,,,,,,          ! Material model web
MPTEMP,1,0
MPDATA,EX,1,,EX
MPDATA,PRXY,1,,0.3         ! Poisson's ratio
MPDATA,DENS,1,,7.85e-9     ! Density steel

MPDATA,EX,2,,EX         ! Material model flanges
MPDATA,PRXY,2,,0.3         ! Poisson's ratio
MPDATA,DENS,2,,7.85e-9     ! Density steel

MPDATA,EX,3,,EX         ! Material model stiffener
MPDATA,PRXY,3,,0.3         ! Poisson's ratio
MPDATA,DENS,3,,7.85e-9     ! Density steel

MPDATA,EX,4,,EX         ! Material model stiffener
MPDATA,PRXY,4,,0.3         ! Poisson's ratio
MPDATA,DENS,4,,7.85e-9     ! Density steel
```

```
! ============================
! Geometry
! ============================

globimp = 0              !Global imperfection
locimp = hw/200          !Local imperfection web

kpszam=11
kmszam=11
*DIM,kmhely,ARRAY,kmszam,7

kmhely(1,1)=0.001,0,-Length/8,-Length/8*2,-Length/8*3,-Length/8*4
kmhely(7,1)=-Length/8*5,-Length/8*6,-Length/8*7,-Length,-Length-0.001

*DO,i,2,kmszam-1
     kmhely(i,2)=globimp*sin(180*(kmhely(i,1))/(-Length))
     kmhely(i,3)=locimp*sin(180*(kmhely(i,1))/(-Length/2))
*ENDDO


*DIM,szelvenyhely,ARRAY,5,1
szelvenyhely(1,1)=-bf/2,0,0,0,bf/2

*DO,j,1,kmszam
*DO,i,1,5
          K,1+(i-1)*100+(j-1)*1000, szelvenyhely(i,1),hw,kmhely(j,1)
          K,2+(i-1)*100+(j-1)*1000, szelvenyhely(i,1)+kmhely(j,2)/4+kmhely(j,3)*sin(180/hw*(hw/2)/5*1),hw/2+(hw/2)/5*4,kmhely(j,1)
          K,3+(i-1)*100+(j-1)*1000, szelvenyhely(i,1)+kmhely(j,2)/2+kmhely(j,3)*sin(180/hw*(hw/2)/5*2),hw/2+(hw/2)/5*3,kmhely(j,1)
          K,4+(i-1)*100+(j-1)*1000, szelvenyhely(i,1)+kmhely(j,2)/4+kmhely(j,3)*sin(180/hw*(hw/2)/5*3),hw/2+(hw/2)/5*2,kmhely(j,1)

          K,5+(i-1)*100+(j-1)*1000, szelvenyhely(i,1)+kmhely(j,2)+kmhely(j,3)*sin(180/hw*(hw/2)/5*4),hw/2+(hw/2)/5,kmhely(j,1)
          K,6+(i-1)*100+(j-1)*1000, szelvenyhely(i,1)+kmhely(j,2)+kmhely(j,3)*sin(180/hw*(hw/2)),hw/2,kmhely(j,1)
          K,7+(i-1)*100+(j-1)*1000, szelvenyhely(i,1)+kmhely(j,2)+kmhely(j,3)*sin(180/hw*(hw/2)/5*4),hw/2-(hw/2)/5,kmhely(j,1)

          K,8+(i-1)*100+(j-1)*1000, szelvenyhely(i,1)+kmhely(j,2)/4*3+kmhely(j,3)*sin(180/hw*(hw/2)/5*3),hw/2-(hw/2)/5*2,kmhely(j,1)
          K,9+(i-1)*100+(j-1)*1000, szelvenyhely(i,1)+kmhely(j,2)/2+kmhely(j,3)*sin(180/hw*(hw/2)/5*2),hw/2-(hw/2)/5*3,kmhely(j,1)
          K,10+(i-1)*100+(j-1)*1000, szelvenyhely(i,1)+kmhely(j,2)/4+kmhely(j,3)*sin(180/hw*(hw/2)/5*1),hw/2-(hw/2)/5*4,kmhely(j,1)
          K,11+(i-1)*100+(j-1)*1000, szelvenyhely(i,1),0,kmhely(j,1)
*ENDDO
*ENDDO


! ============================
! Definition of areas
! ============================
! ------
! Web
! ------

*DO,j,1,kmszam-1
*DO,i,1,kpszam-1
     A,200+i+(j-1)*1000,200+i+1+(j-1)*1000,1200+i+1+(j-1)*1000,1200+i+(j-1)*1000
*ENDDO
*ENDDO

AATT,1,1,1,
AESIZE,ALL,halo
AMESH,ALL
ALLSEL,ALL

! ------
! Flanges
! ------

*DO,j,1,kmszam-1
     A,1+(j-1)*1000,201+(j-1)*1000,201+(j)*1000,1+(j)*1000
     A,201+(j-1)*1000,401+(j-1)*1000,401+(j)*1000,201+(j)*1000
*ENDDO

*DO,j,1,kmszam-1
     A,kpszam+(j-1)*1000,200+kpszam+(j-1)*1000,200+kpszam+(j)*1000,kpszam+(j)*1000
     A,200+kpszam+(j-1)*1000,400+kpszam+(j-1)*1000,400+kpszam+(j)*1000,200+kpszam+(j)*1000
*ENDDO

AATT,2,2,1,
AESIZE,ALL,halo
AMESH,ALL
ALLSEL,ALL
```

```
! ==============================
! Stiffeners
! ==============================

  *DO,j,1,10
      A,1000+j,1200+j,1200+(j+1),1000+(j+1)
      A,1200+j,1400+j,1400+(j+1),1200+(j+1)
      A,9000+j,9200+j,9200+(j+1),9000+(j+1)
      A,9200+j,9400+j,9400+(j+1),9200+(j+1)
      A,5000+j,5200+j,5200+(j+1),5000+(j+1)
      A,5200+j,5400+j,5400+(j+1),5200+(j+1)
  *ENDDO

      AATT,4,4,1,
      AESIZE,ALL,halo
      AMESH,ALL
      ALLSEL,ALL

! ==============================
! Supports
! ==============================

NSEL,S,LOC,y,-1,1
NSEL,r,LOC,z,-1,1
D,ALL,UY
D,ALL,UX
D,ALL,UZ
ALLSEL,ALL


NSEL,S,LOC,y,-1,1
NSEL,r,LOC,z,-Length-1,-Length+1,
D,ALL,UY
D,ALL,UX
ALLSEL,ALL


NSEL,s,loc,z,0,-Length
NSEL,r,loc,y,hw-1,hw+1
NSEL,r,loc,x,-bf/2-1,-bf/2+1
D,ALL,UX
ALLSEL,ALL


! ==============================
! Definition of patch load
! ==============================

NSEL,S,LOC,Y,hw-1,hw+1
NSEL,R,LOC,z,-Length/(4/3)-ss/2,-Length/(4/3)+ss/2
NSEL,r,loc,x,-20,20
*GET,nodeszam,NODE,0,COUNT
F,ALL,FY,-Ff*1000/nodeszam
ALLSEL,ALL

NSEL,s,loc,y,hw-1,hw+1
NSEL,r,loc,x,-1,1
NSEL,r,loc,z,-Length/(4/3)-ss/2,-Length/(4/3)+ss/2
*GET,nodeszam,NODE,0,COUNT
CM,cpzendo,node
ALLSEL,ALL

*DO,i,1,nodeszam
      CMSEL,s,cpzendo,node
      *GET,minnode,NODE,0,NUM,MIN
      *GET,locz,NODE,minnode,LOC,Z
      NSEL,u,NODE,,minnode
      CM,cpzendo,node
      ALLSEL,ALL

      NSEL,s,loc,y,hw-1,hw+1
      NSEL,r,loc,z,locz-1,locz+1
      CERIG,minnode,ALL,ROTZ
*ENDDO

NSEL,s,loc,y,hw-1,hw+1
NSEL,r,loc,x,-1,1
NSEL,r,loc,z,-Length/(4/3)-ss/2,-Length/(4/3)+ss/2
D,ALL,ROTZ,0
D,ALL,UX,0
ALLSEL,ALL
```

```
! ==============================
! Definintion of shear force
! ==============================

NSEL,S,LOC,Y,hw-1,hw+1
NSEL,R,LOC,z,-Length/2,-Length/2

*GET,nodeszam,NODE,0,COUNT
F,ALL,FY,-Vv*1000/nodeszam
ALLSEL,ALL


!==============================
!Non-linear material model
!==============================

*DO,i,1,1                      ! Strain - stress curve web
      TB,MISO,i,1,4,
      TBTEMP,0
      TBPT,,0,0
      TBPT,,FYw/EX,FYw
      TBPT,,0.01,FYw+5
      TBPT,,0.15,Fuw
*ENDDO

*DO,i,2,2                      ! Strain - stress curve flanges
      TB,MISO,i,1,4,
      TBTEMP,0
      TBPT,,0,0
      TBPT,,FYf/EX,FYf
      TBPT,,0.01,FYf+5
      TBPT,,0.15,Fuf
*ENDDO

*DO,i,3,4                      ! Strain - stress curve stiffeners
      TB,MISO,i,1,4,
      TBTEMP,0
      TBPT,,0,0
      TBPT,,FYb/EX,FYb
      TBPT,,0.01,FYb+5
      TBPT,,0.15,Fub
*ENDDO

SAVE

/SOLU
  ALLSEL
  ANTYPE,STATIC
  PSTRES,ON
  NLGEOM,1
  DELTIM,0.05,0.001,0.1
  OUTRES,ALL, ALL
  OUTRES,ALL, ALL
  TIME,1
  SOLVE
  FINISH

evaluation        ! This is the macro which was used to perform the verification based on the middle node
/eof
```

Annex B – Code displacement middle node

```
/POST1
  INRES, all
  FILE, datnam

actnode1=NODE(0,hw,-Length/2)

  SET, last
  *GET, no_ds, active, 0, set, sbst
  *IF, no_ds, eq, 999999, then
    SET, previous
    *GET, no_ds, active, 0, set, sbst
  *ENDIF

! Definition Arrays

  *DIM, t_lis, array, no_ds                  ! Array for time
  *DIM, res_FU, array, no_ds, 3              ! Array for output

! Loop over all data sets

  *DO, loop0, 1, no_ds, 1
    SET, , , , , , , , loop0
    *GET, t_lis(loop0), active, 0, set, time
      res_FU(loop0,1) = t_lis(loop0)         ! Output in [kN]
      res_FU(loop0,2) = UY(actnode1)*(-1)    ! Enter node number
  *ENDDO

*CFOPEN,datnam,txt,,APPEND,
*VWRITE,res_FU(1,1),res_FU(1,2),,,,,,
(F10.2,F10.2)
*CFCLOS

/eof
```

Annex C – Results verification of SP 600 and SP 1200 model

The results regarding the verification (displacement and force) for the SP 600 model can be found in table 1:

Table 1: Results verification SP 600

$T\,[s]$	$u\,[mm]$	Effective total force [kN]
0.05	0.37	43
0.10	0.73	86
0.18	1.28	154,8
0.28	2.02	240.8
0.38	2.75	326.8
0.47	3.49	404.2
0.57	4.22	490.2
0.67	4.96	576.2
0.77	5.70	662.2
0.87	6.44	748.2
0.94	6.91	808.4
0.96	7.08	825.6
0.98	7.28	842.8
0.99	7.37	851.4
0.99	7.40	851.4
0.99	7.43	851.4

The results regarding the verification (displacement and force) for the SP 1200 model can be found in table 2:

Table 2: Results verification SP 1200

$T\,[s]$	$u\,[mm]$	Effective total force [kN]
0.05	0.16	52
0.10	0.31	104
0.18	0.54	187.2
0.28	0.86	291.2
0.38	1.18	395,2
0.47	1.52	488.8
0.57	1.87	592.8
0.67	2.25	696.8
0.77	2.65	800.8
0.87	3.11	904.8
0.91	3.27	946.4
0.94	3.49	977.6
0.94	3.50	977.6
0.94	3.52	977.6
0.94	3.54	977.6

Annex D – Code M-V interaction model

```
FINISH
/CLEAR,START
/NERR,0,99999999,,0

datnam = arg1    ! Name of the project

/FILNAME, %datnam%
/TITLE,   %datnam%

/PREP7

! Code SP600: interaction,'Sp600',1000,600,6,450,20,M,V
! Code SP1200: interaction,'Sp1200',2000,1200,6,450,20,M,V
!                           1      2    3 4 5 6  78

! Code simulations: the values of the yield strength and the ultimate strength have to be manually adjusted (or by adding six additional parameters)

! ===========
! Parameters
! ===========

! Stress paramaters
FYw = 460          ! Yield strength web ; 383 test ; adjust this value
Fuw = 540          ! Ultimate yield strength web ; 543 test ; adjust this value

FYf = 690          ! Yield strength flange ; 354 test ; adjust this value
Fuf = 770          ! Ultimate yield strength flange ; 519 test ; adjust this value

FYb = 460          ! Yield strength stiffeners ; 354 test ; adjust this value
Fub = 540          ! Ultimate yield strength stiffeners ; 519 test ; adjust this value

! Cross-section parameters
Length = arg2      ! Length of the panel [mm]
hw = arg3          ! Web height [mm]
tw = arg4          ! Web thickness [mm]
bf = arg5          ! Flange width [mm]
tf = arg6          ! Flange thickness [mm]

tv = 20            !Thickness of the vertical stiffeners [mm] ; fixed

! Loading parameters
M = arg7           ! Applied load to create bending moment [kN]
                   ! This force will be applied both on the top and on the bottom flange
                   ! The bending moment is equal to the force M * height of the web
V = arg8           ! Shear load [kN]

halo = 20          ! Mesh size, 20 mm

EX = 210000        ! Young's modulus

*AFUN,DEG
```

```
! ==================================
! Element type and Material models
! ==================================

ET,1,SHELL181

R,1,tw,tw,tw,tw, , ,
R,2,tf,tf,tf,tf, , ,
R,3,0,0,0,0, , ,
R,4,tv,tv,tv,tv, , ,

MPTEMP,,,,,,,,              ! Material model web
MPTEMP,1,0
MPDATA,EX,1,,EX
MPDATA,PRXY,1,,0.3          ! Poisson's ratio
MPDATA,DENS,1,,7.85e-9      ! Density steel

MPDATA,EX,2,,EX            ! Material model flanges
MPDATA,PRXY,2,,0.3          ! Poisson's ratio
MPDATA,DENS,2,,7.85e-9      ! Density steel

MPDATA,EX,3,,EX            ! Material model stiffener
MPDATA,PRXY,3,,0.3          ! Poisson's ratio
MPDATA,DENS,3,,7.85e-9      ! Density steel

MPDATA,EX,4,,EX            ! Material model stiffener
MPDATA,PRXY,4,,0.3          ! Poisson's ratio
MPDATA,DENS,4,,7.85e-9      ! Density steel
```

```
! ==============================
! Definition of areas
! ==============================
! ------
! Web
! ------

*DO,j,1,kmszam-1
*DO,i,1,kpszam-1
    A,200+i+(j-1)*1000,200+i+1+(j-1)*1000,1200+i+1+(j-1)*1000,1200+i+(j-1)*1000
*ENDDO
*ENDDO

AATT,1,1,1,
AESIZE,ALL,halo
AMESH,ALL
ALLSEL,ALL

! ------
! Flanges
! ------

*DO,j,1,kmszam-1
    A,1+(j-1)*1000,201+(j-1)*1000,201+(j)*1000,1+(j)*1000
    A,201+(j-1)*1000,401+(j-1)*1000,401+(j)*1000,201+(j)*1000
*ENDDO

*DO,j,1,kmszam-1
    A,kpszam+(j-1)*1000,200+kpszam+(j-1)*1000,200+kpszam+(j)*1000,kpszam+(j)*1000
    A,200+kpszam+(j-1)*1000,400+kpszam+(j-1)*1000,400+kpszam+(j)*1000,200+kpszam+(j)*1000
*ENDDO

AATT,2,2,1,
AESIZE,ALL,halo
AMESH,ALL
ALLSEL,ALL

! ==============================
! Geometry
! ==============================

globimp = 0              ! Global imperfection at longitudinal stiffener
locimp = hw/200          ! Local imperfection full panel

kpszam=11
kmszam=11
*DIM,kmhely,ARRAY,kmszam,7

kmhely(1,1)=0.001,0,-Length/8,-Length/8*1.5,-Length/8*2,-Length/8*3,-Length/8*4
kmhely(7,1)=-Length/8*5,-Length/8*6,-Length/8*7,-Length,-Length-0.001

*DO,i,2,kmszam-1
    kmhely(i,2)=globimp*sin(180*(kmhely(i,1))/(-Length))
    kmhely(i,3)=locimp*sin(180*(kmhely(i,1))/(-Length))
*ENDDO


*DIM,szelvenyhely,ARRAY,5,1
szelvenyhely(1,1)=-bf/2,0,0,0,bf/2

*DO,j,1,kmszam
*DO,i,1,5
        K,1+(i-1)*100+(j-1)*1000, szelvenyhely(i,1),hw,kmhely(j,1)
        K,2+(i-1)*100+(j-1)*1000, szelvenyhely(i,1)+kmhely(j,2)/4+kmhely(j,3)*sin(180/hw*(hw/2)/5*1),hw/2+(hw/2)/5*4,kmhely(j,1)
        K,3+(i-1)*100+(j-1)*1000, szelvenyhely(i,1)+kmhely(j,2)/2+kmhely(j,3)*sin(180/hw*(hw/2)/5*2),hw/2+(hw/2)/5*3,kmhely(j,1)
        K,4+(i-1)*100+(j-1)*1000, szelvenyhely(i,1)+kmhely(j,2)/4+kmhely(j,3)*sin(180/hw*(hw/2)/5*3),hw/2+(hw/2)/5*2,kmhely(j,1)

        K,5+(i-1)*100+(j-1)*1000, szelvenyhely(i,1)+kmhely(j,2)+kmhely(j,3)*sin(180/hw*(hw/2)/5*4),hw/2+(hw/2)/5,kmhely(j,1)
        K,6+(i-1)*100+(j-1)*1000, szelvenyhely(i,1)+kmhely(j,2)+kmhely(j,3)*sin(180/hw*(hw/2)),hw/2,kmhely(j,1)
        K,7+(i-1)*100+(j-1)*1000, szelvenyhely(i,1)+kmhely(j,2)+kmhely(j,3)*sin(180/hw*(hw/2)/5*4),hw/2-(hw/2)/5,kmhely(j,1)

        K,8+(i-1)*100+(j-1)*1000, szelvenyhely(i,1)+kmhely(j,2)/4*3+kmhely(j,3)*sin(180/hw*(hw/2)/5*3),hw/2-(hw/2)/5*2,kmhely(j,1)
        K,9+(i-1)*100+(j-1)*1000, szelvenyhely(i,1)+kmhely(j,2)/2+kmhely(j,3)*sin(180/hw*(hw/2)/5*2),hw/2-(hw/2)/5*3,kmhely(j,1)
        K,10+(i-1)*100+(j-1)*1000, szelvenyhely(i,1)+kmhely(j,2)/4+kmhely(j,3)*sin(180/hw*(hw/2)/5*1),hw/2-(hw/2)/5*4,kmhely(j,1)
        K,11+(i-1)*100+(j-1)*1000, szelvenyhely(i,1),0,kmhely(j,1)
*ENDDO
*ENDDO
```

```
! ==============================
! Stiffeners
! ==============================

  *DO,j,1,10
      A,1000+j,1200+j,1200+(j+1),1000+(j+1)
      A,1200+j,1400+j,1400+(j+1),1200+(j+1)
      A,2000+j,2200+j,2200+(j+1),2000+(j+1)
      A,2200+j,2400+j,2400+(j+1),2200+(j+1)
      A,9000+j,9200+j,9200+(j+1),9000+(j+1)
      A,9200+j,9400+j,9400+(j+1),9200+(j+1)
  *ENDDO

      AATT,4,4,1,
      AESIZE,ALL,halo
      AMESH,ALL
      ALLSEL,ALL


! ==============================
! Supports
! ==============================
! Support in x-direction along the flanges
NSEL,s,loc,z,0,-Length
NSEL,r,loc,y,hw-1,hw+1
NSEL,r,loc,x,-bf/2-1,-bf/2+1
D,ALL,UX
ALLSEL,ALL

NSEL,s,loc,z,0,-Length
NSEL,r,loc,y,-1,1
NSEL,r,loc,x,-bf/2-1,-bf/2+1
D,ALL,UX
ALLSEL,ALL

!Supports at the right hand side

NSEL,s,loc,z,-Length-1,-Length+1, ! Finding the middle point
NSEL,r,LOC,y,-1+hw/2,1+hw/2
NSEL,r,LOC,x,-1,1
*GET,midnode,NODE,0,NUM,MAX
CM,CM_1,NODE
ALLSEL,ALL


!Supports on the whole surface in longitudinal direction
NSEL,s,loc,z,-Length-1,-Length+1,
NSEL,r,loc,y,-1,1+hw
CM,CM_3,NODE

CERIG,midnode,ALL,ALL, , , ,
D,midnode,UZ
D,midnode,ROTX
ALLSEL,ALL

! Supports on the whole surface in tranversal direction
NSEL,s,loc,z,-Length-1,-Length+1,
NSEL,r,LOC,x,-1,1
CM,CM_2,NODE

CMSEL,s,CM_2
CERIG,midnode,ALL,ALL, , , ,
ALLSEL,ALL
D,midnode,UY
ALLSEL,ALL
```

```
! ===============================
! Definition of bending
! ===============================

NSEL,S,LOC,z,-1,1
NSEL,r,LOC,y,-1,1
*GET,nodeszam,NODE,0,COUNT
F,all,FZ,M*1000/nodeszam        ! Force in kN
ALLSEL,ALL


NSEL,S,LOC,z,-1,1
NSEL,r,LOC,y,hw-1,hw+1
*GET,nodeszam,NODE,0,COUNT
F,all,FZ,-M*1000/nodeszam       ! Force in kN
ALLSEL,ALL

! ===============================
! Definition of shear
! ===============================

NSEL,S,LOC,z,-Length/8-1,-Length/8+1
NSEL,r,LOC,y,-1,1
*GET,nodeszam3,NODE,0,COUNT
F,all,FY,V*1000/nodeszam3       ! Force in kN
ALLSEL,ALL


! ===============================
! Non-linear material model
! ===============================

*DO,i,1,1                       ! Strain - stress curve web
      TB,MISO,i,1,4,
      TBTEMP,0
      TBPT,,0,0
      TBPT,,FYw/EX,FYw
      TBPT,,0.01,FYw+5
      TBPT,,0.15,Fuw
*ENDDO

*DO,i,2,2                       ! Strain - stress curve flanges
      TB,MISO,i,1,4,
      TBTEMP,0
      TBPT,,0,0
      TBPT,,FYf/EX,FYf
      TBPT,,0.01,FYf+5
      TBPT,,0.15,Fuf
*ENDDO

*DO,i,3,4                       ! Strain - stress curve stiffeners
      TB,MISO,i,1,4,
      TBTEMP,0
      TBPT,,0,0
      TBPT,,FYb/EX,FYb
      TBPT,,0.01,FYb+5
      TBPT,,0.15,Fub
*ENDDO

SAVE

/SOLU
  ALLSEL
  ANTYPE,STATIC
  PSTRES,ON
  NLGEOM,1
  DELTIM,0.05,0.001,0.1
  OUTRES,ALL, ALL
  OUTRES,ALL, ALL
  TIME,1
  SOLVE
  FINISH

!evaluation
```

```
! ===============================
! Shear force at hw/2
! ===============================

!Finding the shear force at support and at hw/2

*GET, shearSupport, NODE, midnode, RF, FY
shearHw=shearSupport

! ===============================
! Maximum bending moment at hw/2
! ===============================

!Finding the bending moment at hw/2

*GET, bendingSupport, NODE, midnode, RF, MX
BendingMomentHW=shearSupport*hw/2+bendingSupport

/eof
```

Annex E – List of results numerical simulations and hand calculations

test	f_{yf} [MPa]	f_{yw} [MPa]	class	M_{Rk} [kNm]	M_{Ansys} [kNm]	$\dfrac{M_{Ansys}}{M_{Rk}}$	$V_{bw,Rk}$ [kN]	V_{Ansys} [kN]	$\dfrac{V_{Ansys}}{V_{bw,Rk}}$
1	355	355	3	170	170	1,00	191	241	1,26
2	355	355	4	260	299	1,15	227	298	1,32
3	355	355	1	185	195	1,06	299	266	0,89
4	355	355	2	185	191	1,03	191	208	1,09
5	355	355	3	233	232	0,99	191	244	1,28
6	355	355	4	352	403	1,14	227	307	1,35
7	460	355	3	177	214	1,21	191	241	1,26
8	460	355	4	281	352	1,25	227	298	1,32
9	460	355	1	317	291	0,92	299	284	0,95
10	460	355	2	311	283	0,91	191	194	1,01
11	460	355	3	298	364	1,22	191	245	1,28
12	460	355	4	456	534	1,17	227	309	1,36
13	690	355	3	225	307	1,37	191	243	1,27
14	690	355	4	350	453	1,29	227	306	1,35
15	690	355	1	538	387	0,72	299	294	0,98
16	690	355	2	532	357	0,67	191	215	1,12
17	690	355	3	348	420	1,21	191	246	1,29
18	690	355	4	528	630	1,19	227	312	1,38
19	960	355	3	249	337	1,35	191	244	1,28
20	960	355	4	385	491	1,28	227	307	1,35
21	960	355	1	845	437	0,52	299	355	1,19
22	960	355	2	839	390	0,46	191	350	1,83
23	960	355	3	400	466	1,17	191	248	1,30
24	960	355	4	601	656	1,09	227	314	1,39
25	460	460	3	179	177	0,99	218	264	1,21
26	460	460	4	285	296	1,04	251	334	1,33
27	460	460	1	289	292	1,01	340	343	1,01
28	460	460	2	345	353	1,02	340	400	1,18
29	460	460	3	294	285	0,97	218	268	1,23
30	460	460	4	458	451	0,98	251	346	1,38
31	690	460	3	241	263	1,09	218	265	1,22
32	690	460	4	371	385	1,04	251	340	1,35
33	690	460	1	546	372	0,68	340	362	1,06
34	690	460	2	658	451	0,68	340	408	1,20
35	690	460	3	379	360	0,95	218	272	1,25
36	690	460	4	566	548	0,97	251	348	1,39
37	960	460	3	268	296	1,10	218	267	1,23
38	960	460	4	409	429	1,05	251	343	1,37
39	960	460	1	853	432	0,51	340	360	1,06
40	960	460	2	1023	503	0,49	340	405	1,19
41	960	460	3	436	415	0,95	218	275	1,26

42	960	460	4	647	664	1,03	251	350	1,39
43	690	690	3	338	263	0,78	281	385	1,37
44	690	690	4	424	312	0,74	299	415	1,39
45	690	690	1	510	403	0,79	600	623	1,04
46	690	690	2	607	506	0,83	817	850	1,04
47	690	690	3	511	360	0,70	281	392	1,39
48	690	690	4	637	427	0,67	299	424	1,42
49	960	690	3	402	296	0,74	281	388	1,38
50	960	690	4	472	349	0,74	299	418	1,40
51	960	690	1	882	517	0,59	600	642	1,07
52	960	690	2	1079	630	0,58	817	860	1,05
53	960	690	3	654	438	0,67	281	394	1,40
54	960	690	4	759	515	0,68	299	427	1,43

Annex F – Data parametric study

Simulation 31	Bending [kNm]	Shear [kN]	Area [m^2]	bf [mm]	tf [mm]	% (Bending / Area)	Class 3 flange - Class 3 web
1	263,30095	264,7968	3,6	200	9	73,13915278	1
2	283,7796	266,5218	4	200	10	70,9449	0,969998931
3	326,04005	268,24	4,8	200	12	67,92501042	0,928709287
4	448,4255	269,95808	6	250	12	74,73758333	1,02185465
5	501,924975	273,63168	7	250	14	71,70356786	0,980371868
6	544,990625	283,77216	8	250	16	68,12382813	0,931427635

Simulation 32	Bending [kNm]	Shear [kN]	Area [m^2]	bf [mm]	tf [mm]	% (Bending / Area)	Class 1 flange - Class 1 web
one (ref)	385	339,7148	3,6	200	9	106,9444444	1
two	429,53616	342,5652	4	200	10	107,38404	1,004110504
three	505,78112	345,75	4,8	200	12	105,3710667	0,985287896
four	676,81876	348,28538	6	250	12	112,8031267	1,054782483
five	750,94272	350,78884	7	250	14	107,2775314	1,00311458
six	825	352,41725	8	250	16	103,125	0,964285714

Simulation 33	Bending [kNm]	Shear [kN]	Area [m^2]	bf [mm]	tf [mm]	% (Bending / Area)	Class 1 flange - Class 2 web
one (ref)	371,875	361,9648	5,6	200	14	66,40625	1
two	430,66395	360,4216	6,4	200	16	67,29124219	1,013326941
three	457,662975	389,7756	7,2	200	18	63,56430208	0,957203608
four	498,29615	441,38655	8	200	20	62,28701875	0,937969224
							0
five	626,4999	419,2465	9	250	18	69,6111	1,048261271
six	673,6995	479,406	10	250	20	67,36995	1,014512188

Simulation 34	Bending [kNm]	Shear [kN]	Area [m^2]	bf [mm]	tf [mm]	% (Bending / Area)	Class 3 flange - Class 3 web
one (ref)	450,73239	407,822	5,6	200	14	80,48792679	1
two	502,03125	405,5495	6,4	200	16	78,44238281	0,974585704
three	537,74142	409,093	7,2	200	18	74,68630833	0,927919395
four	585,70344	414,0365	8	200	20	73,21293	0,909613813
five	746,20884	411,929	9	250	18	82,91209333	1,030118387
six	790,986	419,358	10	250	20	79,0986	0,982738693

Simulation 35	Bending [kNm]	Shear [kN]	Area [m^2]	bf [mm]	tf [mm]	% (Bending / Area)	Class 1 flange - Class 3 web
one (ref)	359,6922	271,4436	5,6	200	14	64,23075	1
two	398,03175	275,7621	6,4	200	16	62,19246094	0,968266149
three	423,9375	280,54464	7,2	200	18	58,88020833	0,916698129
four	459,375	288,41004	8	200	20	57,421875	0,893993531
five	590,595625	285,0267	9	250	18	65,62173611	1,021656078
six	644,67765	409,382	10	250	20	64,467765	1,003690055

Simulation 36	Bending [kNm]	Shear [kN]	Area [m^2]	bf [mm]	tf [mm]	% (Bending / Area)	Class 1 flange - Class 4 web
one (ref)	547,50016	348,226	5,6	200	14	97,76788571	1
two	606,25024	350,8748	6,4	200	16	94,7266	0,968892794
three	675	352,38084	7,2	200	18	93,75	0,958903829
four	750	353,61102	8	200	20	93,75	0,958903829
five	920,898	354,28638	9	250	18	102,322	1,046580881
six	979,01352	355,53042	10	250	20	97,901352	1,001365134

The area (material surface) for the flanges was determined for both flanges due to the change of parameters for both flanges.